


國立交通大學

機械工程學系

碩士論文

創新建材在圓錐量熱儀、表面測試爐及
單材耐燃測試儀之火災試驗數據相關性
之研究



The Research for Testing Data Correlation
of New and Innovative Building Materials
between the Cone Calorimeter, the Surface
and SBI Tests

研究生：戴嘉鴻

指導教授：陳俊勳 教授

中華民國九十五年六月

創新建材在圓錐量熱儀、表面測試爐及單材耐燃測試儀之火災試驗數據
據相關性之研究

The Research for Testing Data Correlation of New and Innovative
Building Materials between the Cone Calorimeter, the Surface and SBI
Tests

研究生：戴嘉鴻

Student : Jia-Hong Dai

指導教授：陳俊勳

Advisor : Chiun-Hsun Chen



A Thesis

Submitted to Department of Mechanical Engineering
College of Engineering

National Chiao Tung University

In Partial Fulfillment of the Requirements

For the Degree of

Master of Science

In Mechanical Engineering

June 2006

Hsinchu, Taiwan, Republic of China

中華民國九十五年六月

創新建材在圓錐量熱儀、表面測試爐及單材耐燃測試儀之火災試驗數據相關性之研究

學生：戴嘉鴻

指導教授：陳俊勳

國立交通大學機械工程學系

摘要

本論文以十五種材料分別於圓錐量測儀以及表面測試爐上進行測試，其中圓錐量測儀測試結果依照日本現行防火材料等級分類標準進行分級，而表面測試爐測試結果則依照 CNS 6532 進行分級。在圓錐量測儀測試中，也同時探討樣品在水平測試與垂直測試結果的差異性，兩者比較發現在引燃時間和熱釋放率是有所差異，其中水平測試的引燃時間較垂直測試的短，且水平測試的平均 180 秒熱釋放率值以及總熱釋放率皆高於垂直測試，因此使用圓錐量熱儀水平測試之數據來分級是較為嚴苛的。另外亦從前述十五種測試材料中挑選其中的七種材料來進行單材耐燃測試儀(SBI) 測試，並依歐盟標準進行分級，另外並與圓錐量測儀以及表面測試爐之分級結果進行比對。結果發現歐盟在建築材料防火等級分類上並沒有材料破裂之限制，且歐盟與日本之防火等級分類中也沒有針對煙產生量作評量，這是他們與 CNS 6532 防火等級性能評估上之主要差異。在相關性分析中，由圓錐量測儀水平與垂直測試實驗中所得到的熱釋放率計算出的火災成長率進行相關性比對，發現圓錐量測儀在水平測試之數據與單材耐燃測試儀相關性較高；表面測試爐與單材耐燃測試儀之發熱性與發煙性相關係數均良好；表面測試與圓錐量測儀在水平與垂直測試之發熱性相關係數均良好；另外表面測試引燃時間與圓錐量測儀在垂直測試之引燃時間相關性良好。

The Research for Testing Data Correlation of New and Innovative
Building Materials between the Cone Calorimeter, the Surface and SBI
Tests

Student: Jia-Hong Dai

Advisor: Prof. Chiun-Hsun Chen

Department of Mechanical Engineering

National Chiao Tung University

Abstract

Fifteen building materials were selected and tested in the Cone Calorimeter and the surface test, respectively, and they were classified by Japanese classification and CNS 6532 accordingly. Tests in the Cone Calorimeter were performed in the horizontal and vertical directions, respectively, under a fixed incident heat flux 50kW/m^2 . The results from these two orientations show some differences existed in HRR and ignition time. For the flammable material, the measured average values of $\text{HRR}_{\text{av}_180\text{s}}$, and THR in the horizontal orientation are higher than those in vertical one. The ignition time in horizontal orientation is found shorter. Those indicate that the classification using Cone Calorimeter test in horizontal orientation is stringent. In addition, 7 materials from the previously mentioned 15 ones are selected to test in SBI and classified by EU classification. Correlation based on test results of these materials by using these three different standards are given and discussed. It is found that the smoke generation rate and crack appearance are not included in the performance evaluations in Japanese and EU classifications that causes the different ranks in different test methods. The obtained results

in SBI test are compared with the simulated FIGRA from Cone data. It is found that the correlation between SBI and cone calorimeter test in horizontal orientation is better than the corresponding one with the cone calorimeter test in vertical orientation. The correlation between $td\theta$ value of surface test and THR_{600s} of SBI test finds that the value of R^2 is 0.75. Correlation between the C_A value of surface test and maximum 60s mean value of SPR of SBI test gives the value of R^2 is 0.92, indicating that the correlation between the surface and SBI tests are relatively well. From the comparison between HRR_{av_180s} of Cone Calorimeter test in vertical orientation and $td\theta$ value of the surface test, R^2 for the correlation is 0.95. The correlated R^2 value between Cone Calorimeter test in horizontal orientation and the surface test is 0.96. Apparently, the correlation between the Cone Calorimeter and the surface tests is relatively well. The correlation for ignition time between cone calorimeter test in vertical direction and the one in surface test is relatively well as well.

誌謝

兩年碩士時光即將過去，回首其中包含了數不清的歡笑與辛勞、站在實驗室外的窗口無數次以及每天一杯黑咖啡等的珍貴回憶！感謝恩師 陳俊勳教授諄諄教誨，對於研究方法與態度、思考與做事觀念等之啟迪，另外在待人處世亦是或益良多，謹在此向老師致上無比的敬意和感謝。

感謝中台技術學院 徐一量教授與台灣警察專科學校 邱晨瑋教授於口試期間的耐心教導與指正，使得本論文更臻完善。

在燃燒防火實驗室的兩年碩士生涯裡，體會到各式各樣的研究生生活。感謝宋文義學長這兩年在實驗和論文上的幫忙。感謝大達、文奎、文耀以及小季學長幫忙解答諸多研究上的困惑。同學國華、靜慈、關恕有福同享，有難同當。以及學弟耀文、炳坤以及建宏在忙碌之虞所給予的幫忙，能在燃燒防火實驗室所一起生活的兩年將是我最美好的回憶。另外也感謝隔壁實驗室的純情堡、高個兒以及阿肥，在我最需要幫助時鼓勵我。

另外在工研院打工的一年多中，感謝洪大姐、瓊瑤、玟雅以及文濱對於實驗上以及論文上的指導與鼓勵，這一年多來學到很多東西。另外感謝小綠在我寫論文以及準備口試期間的鼓勵。

最後要感謝我親愛的父母和老姐，感謝你們長久的支持與關懷。在求學的各階段不斷的給予我鼓勵，你們的支持是我前進最大的力量。最後，僅以此論文獻給我摯愛的家人，謝謝你們。

CONTENTS

摘要.....	i
Abstract	ii
誌謝.....	iv
CONTENTS	v
LIST OF TABLES	x
LIST OF FIGURES	xii
Appendix	xiv
Nomenclature	xiv
Chapter One INTRODUCTION.....	1
1.1 Motivation.....	1
1.2 Literature review.....	4
1.3 Scope of present study.....	7
Chapter Two Test Apparatus and Evaluation Methods.....	9
2.1 Cone calorimeter.....	9
2.1.1 Introduction for cone calorimeter apparatus	9
2.1.1.1 Cone-shaped radiant electric heater	9
2.1.1.2 Load cell	10
2.1.1.3 Specimen holders.....	10
2.1.1.4 Exhaust gas system.....	11
2.1.1.5 Gas analyzer instrumentation	11
2.1.1.6 Smoke system.....	11
2.1.1.7 Heater flux meter	12
2.1.1.8 Calibration burner	12

2.1.1.9 Optical calibration filter.....	12
2.1.1.10 Ignition circuit.....	12
2.1.2 Specimen construction and preparation for cone calorimeter	13
2.1.2.1 Specimens.....	13
2.1.2.2 Conditioning of specimens.....	13
2.1.2.3 Preparation.....	13
2.1.3 Test procedure for cone calorimeter.....	13
2.1.4 Evaluation methods of cone calorimeter.....	16
2.1.4.1 The principle of Oxygen Consumption.....	16
2.1.4.2 Calibration Factor (C factor).....	17
2.1.4.3 Heat Release Rate.....	17
2.1.4.4 Mass Loss Rate of Specimen.....	18
2.1.4.5 Effective Heat of Combustion.....	19
2.1.4.6 Smoke.....	19
2.2 The surface and elementary material tests.....	20
2.2.1 Introduction for the surface test apparatus.....	20
2.2.1.1 Furnace.....	20
2.2.1.2 Smoke accumulation box.....	21
2.2.1.3 Optical density-measuring system.....	21
2.2.2 Specimen preparation for the surface test.....	21
2.2.2.1 Specimens.....	21
2.2.2.2 Conditioning of specimens.....	21
2.2.2.3 Preparation.....	22
2.2.3 Test procedure for surface test.....	22
2.2.4 Evaluation methods of the surface test.....	23

2.2.5 An elementary material test.....	24
2.3 SBI test.....	24
2.3.1 Introduction for SBI apparatus	25
2.3.1.1 Burners and propane supply system.....	25
2.3.1.2 Smoke Exhaust system.....	25
2.3.1.3 General measurement section equipment.....	26
2.3.1.4 Smoke measurement system	26
2.3.1.5 Data acquisition system.....	26
2.3.2 Specimen construction and preparation of SBI test	27
2.3.2.1 Specimens.....	27
2.3.2.2 Backing Boards	27
2.3.2.3 Condition of specimens	27
2.3.2.4 Preparation.....	28
2.3.3 Test procedure for SBI.....	28
2.3.4 Evaluation methods of SBI test.....	30
2.3.4.1 Calculation of heat release rate (HRR)	30
2.3.4.1.1 Total HRR of specimen and burner: HRR_{total}	30
2.3.4.1.2 HRR of the burner	31
2.3.4.1.3 HRR of the specimen	31
2.3.4.2 Calculation of THR(t) and THR_{600s}	32
2.3.4.3 Calculation of $FIGRA_{0.2MJ}$ and $FIGRA_{0.4MJ}$	32
2.3.4.4 Calculation of smoke production rate (SPR).....	33
2.3.4.4.1 Total SPR	33
2.3.4.4.2 SPR of the burner	33
2.3.4.4.3 SPR of the specimen	34
2.3.4.5 Calculation of TSP(t) and TSP_{600s}	34

2.3.4.6 Calculation of SMOGRA	35
Chapter Three UNCERTAINTY ANALYSIS	36
3.2 Uncertainty of cone calorimeter	38
3.2.1 Simplification of the heat release rate calculation.....	38
3.2.2 Uncertainty of heat release rate calculation.....	39
3.3 Uncertainty of surface test	42
3.4 Uncertainty of SBI	43
3.4.1 Uncertainty of HRR.....	44
3.4.2 Uncertainty of SPR.....	47
Chapter Four Results and Discussions.....	48
4.1 The test results of Cone Calorimeter	48
4.1.1 HRR of cone calorimeter tested in vertical orientation.....	48
4.1.2 HRR of cone calorimeter tested in horizontal orientation.....	50
4.1.3 Correlation between vertical and horizontal directions of cone calorimeter test.....	51
4.2 The results of surface test and elementary material test.....	52
4.3 The test results of SBI.....	55
4.3.1 THR_{600s} and FIGRA.....	55
4.3.2 TSP_{600s} and SMOGRA.....	56
4.4 Comparison between cone calorimeter, the surface and SBI tests	56
4.4.1 Comparison between cone calorimeter, the surface and SBI tests for classification.....	56
4.4.2 Comparison between Cone Calorimeter and SBI tests using regression line	58
4.4.3 Comparison between the surface and SBI tests using regression line	60

4.4.4 Comparison between the Cone Calorimeter and the surface tests using regression line	61
Chapter Five CONCLUSIONS	64
Reference	67



LIST OF TABLES

Table 1.1: The apparatus and criteria of classification.....	4
Table 2.1: Heats of combustion and heats of combustion per gram of oxygen consumed for typical organic liquids and gases	70
Table 2.2: Heats of combustion and heats of combustion per gram of oxygen consumed for typical synthetic polymers	70
Table 2.3: Heats of combustion and heats of combustion per gram of oxygen consumed for selected natural fuel	71
Table 3.1: The used parameters of uncertainty for cone calorimeter [29]	71
Table 3.2: The exhaust temperature of standard for CNS 6532 [6]	72
Table 3.3: Uncertainties in volume flow measurement in the SBI test [30]	72
Table 3.4: HRR uncertainty of SBI at the 35 kW level [30]	73
Table 3.5: HRR uncertainty of SBI at the 50 kW level [30]	74
Table 3.6: Summary of uncertainty for different levels of SPR [30]	74
Table 4.1: List of New and Innovative building materials.....	75
Table 4.2: Major compositions of materials.....	76
Table 4.3: The classification of Japanese cone calorimeter test.....	77
Table 4.4: Results of cone calorimeter tested in vertical orientation (average value)	78
Table 4.5: Results of cone calorimeter tested in horizontal orientation (average value)	79
Table 4.6: Classification according to CNS 6532.....	80
Table 4.7: Results of surface test (average value).....	81
Table 4.8: Results of elementary material test (average value).....	82
Table 4.9: Summary of classification criteria for SBI test	82

Table 4.10: EU classes for construction products excluding flooring83

Table 4.11: The summary results of SBI test (average value)84

Table 4.12: The classification of SBI test.....84

Table 4.13: The classification of Cone Calorimeter, the surface and85
SBI tests.....85

Table 4.14: FIGRA for Cone Calorimeter in vertical direction86

Table 4.15: FIGRA for Cone Calorimeter in horizontal direction86



LIST OF FIGURES

Figure 1.1: The Evolution of Fire Testing Methods	87
Figure 2.1: The picture of Cone Calorimeter (Cone2)	88
Figure 2.2: The schematic configuration of the Cone Calorimeter	88
Figure 2.3: Cone heater (Cone2)	89
Figure 2.4: Horizontal orientation (Cone2)	89
Figure 2.5: Vertical orientation (Cone2)	90
Figure 2.6: Gas analyzer instrumentation (Cone2).....	90
Figure 2.7: The surface test apparatus	91
Figure 2.8: The furnace of surface test	91
Figure 2.9: The average heat flux value of surface test [14]	92
Figure 2.10: The smoke accumulation box	92
Figure 2.11: Optical density-measuring system of surface test.....	93
Figure 2.12: Results and specification of surface test	93
Figure 2.13: An elementary material test apparatus	94
Figure 2.14: SBI test	94
Figure 2.15: Schematic picture of SBI	95
Figure 2.16: Trolley of SBI.....	95
Figure 2.17: Gas Control Box and Gas Analysis Rack of SBI.....	96
Figure 2.18: Exhaust hood and Ring of SBI.....	96
Figure 2.19: Exhaust system of SBI	97
Figure 3.1: HRR \pm absolute uncertainty and relative uncertainty histories form cone calorimeter results [29]	97
Figure 3.2: Component uncertainty histories from cone calorimeter results [29]	98
Figure 4.1: Correlation between vertical and horizontal directions of cone calorimeter tests using HRR_{av_180s}	99

Figure 4.2: The correlation between FIGRA of cone calorimeter in vertical direction and SBI tests.....	100
Figure 4.3: The correlation between FIGRA of cone calorimeter in horizontal direction and SBI tests.....	101
Figure 4.4: The correlation between THR_{600s} of SBI test and $td\theta$ of surface test	102
Figure 4.5: The correlation between the maximum SPR_{av_60s} of SBI test and C_A value of surface test.....	103
Figure 4.6: The correlation between 180s mean value of Cone Calorimeter test in vertical direction and $td\theta$ value of surface test.....	104
Figure 4.7: The correlation between 180s mean value of Cone Calorimeter test in horizontal direction and $td\theta$ value of surface test...	105
Figure 4.8: The correlation between 180s mean value of Cone Calorimeter test in vertical direction and $td\theta$ value of surface test without M12.....	106
Figure 4.9: The correlation between 180s mean value of Cone Calorimeter test in horizontal direction and $td\theta$ value of surface test without M12	107
Figure 4.10: The correlation between ignition time of cone calorimeter in vertical direction and t_c value of surface test	108
Figure 4.11: The correlation between ignition time of cone calorimeter in vertical direction and t_c value of surface test without M06	109
Figure 4.12: The correlation between ignition time of cone calorimeter in horizontal direction and t_c value of surface test	110
Figure 4.13: The correlation between ignition time of cone calorimeter in horizontal direction and t_c value of surface test without M06	111

Appendix

<u>Appendix A</u>	112
<u>Appendix B1</u>	113
<u>Appendix B2</u>	115
<u>Appendix C1</u>	117
<u>Appendix C2</u>	120
<u>Appendix D1</u>	121
<u>Appendix D2</u>	122



Nomenclature

Cone Calorimeter

As	Initially exposed surface area of the specimen	m ²
C	Calibration constant for oxygen consumption analysis	(m·kg·K) ^{1/2}
Δh_c	Net heat of combustion	kJ/g
$\Delta h_{c,eff}$	Effective net heat of combustion	kJ/g
I_0	Initial laser intensity	
I	Laser intensity measured	
K	Extinction Coefficient	1/m
m	Mass of the specimen	kg
mf	Mass of the specimen at the end of the test	kg
mi	Mass of the specimen at sustained flaming	kg
\dot{m}	Mass loss rate of the specimen	kg/s
\dot{m}_e	Mass flow rate in exhaust duct	kg/s
Δp	Orifice meter pressure differential	Pa
\dot{q}	Heat release rate	kW
\dot{q}''	Heat release rate per unit area	kW/m ²
\dot{q}''_{max}	Maximum value of the heat release rate	kW/m ²
\dot{q}''_{180}	The average heat release rate over the period starting at t_{ig} and ending 180s later	kW/m ²
\dot{q}''_{300}	The average heat release rate over the period starting at t_{ig} and ending 300s later	kW/m ²
\dot{q}''_{total}	The total heat released during the entire test	MJ/m ²
r_O	Stoichiometric oxygen/fuel mass ratio	
t	Time	s
t_d	Delay time of the oxygen analyser	s
t_{ig}	Time to ignition (sustained flaming)	s
Δt	Sampling time intervals	s
Te	Absolute temperature of gas at the orifice meter	K
\dot{V}	Volume flow of outlet	m ³ /s

χ_{O_2}	Oxygen analyzer reading, mole fraction of oxygen	
$\chi_{O_2}^0$	Initial value of oxygen analyzer reading	
$\chi_{O_2}^1$	Oxygen analyzer reading, before delay time correction	
σ_f	Specific extinction area	m^2/kg

Surface test

C_A	Smoke-generation coefficient	
$td\Theta$	the area under the test and the standard temperature curves	$^{\circ}C \cdot min$
t_1	time of sustained flaming after completion of the test	sec
C_k	cracking of the back surface	

SBI

A	Area of the exhaust duct at the general measurement section	m^2
c	$(2T_0 / \rho_0)^{0.5} = 22.4$	$K^{0.5} \cdot m^{1.5} \cdot kg^{-0.5}$
E	Heat release per unit volume of oxygen consumed at 298 K, $17200kJ/m^3$	
FIGRA	Fire growth rate index	W/s
H	Relative humidity	%
$HRR_{total}(t)$	Total heat release rate of the specimen and burner	kW
HRR_{av_burner}	Average heat release rate of the burner	kW

HRR(t)	Heat release of the specimen	kW
HRR _{av} (t)	Average heat release rate of the specimen	kW
I(t)	Signal from the light receiver	%
k_t	Flow profile factor	
k_ρ	Reynolds number correction for the bidirectional probe, taken as 1.08	
L	Length or diameter of the light path through the exhaust duct	m
max.[a(t)]	Maximum of a(t) within the given time period	
max.[a,b]	Maximum of the two values a and b	
$\Delta p(t)$	Pressure difference	Pa
p	Ambient pressure	Pa
SPR _{total} (t)	Total smoke production rate of specimen and burner	m ² /s
SPR _{av} (t)	Average of SPR(t)	m ² /s
SMOGRA	Smoke growth rate index	m ² /s ²
SPR(t)	Smoke production rate of the specimen	m ² /s
SPR _{av_burner}	The average smoke production rate of the burner, $0 \pm 0.1 \text{ m}^2 / \text{s}$	m ² /s
$T_{ms}(t)$	Temperature in general measurement section	K
THR(t)	Total heat release of the specimen	MJ
THR _{600s}	total heat release of specimen in the first 600s of the exposure period ($300s \leq t \leq 900s$)	MJ
TSP(t _a)	Total smoke production of the specimen within $300s \leq t \leq t_a$	m ²
$V(t)$	Volume flow in the exhaust duct	m ³ /s
V ₂₉₈ (t)	Volume flow of exhaust system, normalized at 298K	m ³ /s
$x_{O_2}(t)$	Oxygen concentration in mole fraction	

$x_{CO_2}(t)$	Carbon dioxide concentration in mole fraction	
$x_{a_{O_2}}$	Ambient mole fraction of oxygen including water vapor	
$\phi(t)$	Calculation of the oxygen depletion factor	



Chapter One

INTRODUCTION

1.1 Motivation

Mankind can feel different aspects of fire. It can provide beneficial ways of living, such as heating source for cooking, warming people and a source of energy for many mechanical devices. On the other hand, fire implies another kind of severe hazard to human being. As a room catches fire, it generates heat, and even toxic and corrosive substances that cause fatal and properties loss. Thus it initiates many scientists and engineers to work together for obtaining a systematic solution to alleviate the loss. Hence many fire testing methods and models have been developed for assessing the fire hazard. The evolution can be seen in Fig. 1.1.

In the very early days, the testing method basically was only used to evaluate the fire performance of material in a bench scale under an assigned environment. These bench scale tests usually were only provided result of pass or fail without any detailed information. However, they served as the baseline for the fire safety regulation. As the advance of material science and technology, many new materials are developed and the above-mentioned test method may not get along with the progress of technologies as expected. Therefore, a revolution testing methodology, termed as reaction-to-fire, was developed in the era of 1990. The Cone Calorimeter (ISO 5660) [1] was the representative testing apparatus. The reaction-to-fire properties of building materials include the flammability, combustibility, toxicity, heat release rate...etc. Among

them, heat release rate is an important parameter to characterize a fire. It describes the total energy release of a material, or upholstery furniture, or a confined space during burning. As pointed out by Thornton [2] and then Huggett [3], there exists a more or less an approximate constant of heat release per unit mass of oxygen consumed for a large number of organic matters. This constant is given as 13.1MJ/kg of O₂. Therefore heat release rate can be measured by using Oxygen Depletion Method (or Oxygen Consumption Method), which is a well-known method and widely adopted for both bench-scale and large-scale experiments in many fire laboratories all over the world.

The general goal of fire safety regulations is to provide life safety and sufficient property protection in case of fire. In order to achieve this goal, combustibility of materials, fire protection of structures, evacuation arrangements, and relative locations of buildings are set to define how buildings should be designed and constructed for their respective use. Traditionally, fire testing and classification systems are developed individually in different countries, each with its different background and circumstances. A wide variety of requirements has thus been drawn up. However, as a result of the development of transportation facilities and international trade, the harmonization of standards and fire classification systems has become an issue of increasing importance. Canada adopted the cone calorimeter (ASTM 1354) [4] to make classification for the fire performance of building materials in 1992. In the Building Standard Law (BSL) of Japanese, it has already adopted the heat release rate obtained from the cone calorimeter (ISO 5660) [1] as the test criteria to replace the

original JIS A 1321 [5], equivalent to Taiwan CNS 6532 [6]; Method of Test for Incombustibility of Interior Finish Material of Buildings. In the European Union (EU), the development of the Euroclass system, EN 13823 [7], was completed in 2002. It defines the fire performance classification of building productions and building components by using the single burning item (SBI) test.

Since 1990s, EU planed to adopt the cone calorimeter test (ISO 5660) [1] for the small-scale test and the room corner test (ISO 9705) [8] for large-scale one. However, it was difficult to obtain the satisfactory correlation between the test results obtained from cone calorimeter and room corner tests respectively, after several years of research. Of course, the room corner test could show the real reaction-to-fire behaviors of materials in a fire, but it cost a lot of time and resource. On the other hand, the small scale fire test of cone calorimeter cannot exhibit the reaction-to-fire properties in the situation of a real fire. Therefore the EU developed a medium-scale test, called single burning item test (EN 13823 [7]), to make a compromise. It was carried out since 2002, and now the building materials, which are intended to be sold in EU, must comply with the proper standard of the SBI test except the fire door of buildings. In addition, for harmonization of fire standards for trains the EU wanted to develop a standard, called prEN 45545-2 [9], to replace all national corresponding standards. According to prEN 45545-2 [9], the burning behaviors of passenger seats for railway vehicles should be tested by including the complete passenger seat, upholstery and head rest, seat shell and arm rest. Test methods consists of ISO 9705(Furniture Calorimeter)

[8], ISO 5660 (Cone Calorimeter) [1] and ISO 5659-2(Smoke chamber with FTIR) [10]. The FTIR (Fourier Transformation InfraRed spectroscopy) is used for analyzing toxic components. However, this proposed standard is not perfect enough to carry out yet.

As becoming a member of WTO, the corresponding testing standards and classifications of Taiwan inevitably must harmonize with the ones that are popular adopted by the other countries. Although the cone calorimeter test method (CNS 14705) [11] has not become the legal criteria of classification yet in Taiwan, it is expected to be adopted like Japan in the near future. Table 1.1 lists the criteria of classification of the cone calorimeter [1], the surface [6] and single burning item tests [7], and the room corner test (ISO 9705) [8] are also included.

Table 1.1: The apparatus and criteria of classification

Test apparatus	Criteria of classification
Cone calorimeter test	Canada: CAN/ULC S 135-1992 Taiwan: CNS 14705 Japanese: NO.5 Article 1, NO.6 Article 1 and NO.9 Article 2of the Building Standard Law EU: prEN45545-2(Draft)
Surface test	Taiwan: CNS 6532
Single burning item test	EU: EN13823 Taiwan: CNS protocol
Room corner test	EU: ISO 9705 Norway: NS 3919

1.2 Literature review

The first application of Oxygen Depletion Method in research was

done by Parker [12] on the ASTM E-84 tunnel test. Later, it was applied to a room fire test [13]. During the late of 70's and early in 80's this principle was refined at the National Institute of Standards and Technology (NIST). The first version of test standard of cone calorimeter (ASTM E1354) [4] was announced in 1990. ISO also announced the cone calorimeter test as ISO 5660 [1] and room corner test as ISO 9705 [8]. For ISO 5660 and 9705, the measurements and calculations of the heat release rate are similar, whereas the major difference is the magnitude of heat release rate which sustained.

Chen et al. [14] tested eighteen different wall-covering materials according to Chinese National Standard (CNS) 6532, equivalent to Japanese Industry Standard (JIS) A1321, and ASTM E1354 (Cone Calorimeter). A comparison of test results was presented, and a qualitative relationship was developed between the performances in the two methods.

Tsantaridis and Ostman [15] tested 30 products separately by cone calorimeter, SBI and room corner test. They found that the occurring times of the first peak of heat release rates for these three tests are in the good correlation. The comparisons of FIGRA (Fire Growth Rate) indices, defined in Chapter Two, of 30 products showed that the R^2 of correlation between cone calorimeter and SBI is about 0.85, SBI and room corner test is about 0.92, and cone calorimeter and room corner test is about 0.76. The burning situation of materials in SBI was found very similar to that of Cone Calorimeter.

Heskestad and Hovde [16] used the experimental data of 17 products,

which are obtained from the full- and bench-scale tests, to consider the influence of the combustion conditions on the full scale smoke production. All these materials caused the occurrences of flashover within 10 min in the ISO Room Corner Fire Test. The smoke to heat ratio S_Q (m^2/MJ) was used to compare smoke generation rates between these two tests. Plastics did produce more smoke yields than wood-based materials in both tests. However, no simple correlations were found between full scale and bench scale for smoke yield. An accurate empirical smoke prediction model by using bench scale fire parameters was presented to predict the full-scale smoke production rate at a heat release rate of 400kW.

Messerschmidt and Hees [17] studied the SBI tested data, which are obtained from fifteen laboratories of EU. They found that the test results for some materials tested in different laboratories show very different behaviors with each other. The reason discussed was the sensitivity of oxygen analysis instrument, indicating that the operation of oxygen analysis instrument must be careful in order to avoid the error.

Hakkarainen and Kokkala [18] developed a one-dimensional thermal flame spread model, which was used to predict the rate of heat release in the SBI test on the basis of the cone calorimeter data. The features of the measured and calculated heat release rate curves were compared for 33 building products. The fire growth rate indices (FIGRA) were calculated to predict the classification in the forthcoming Euroclass system. Although the model used cone calorimeter data could not simulate the heat release rate of SBI perfectly, the model still can provide the correct classification for 90% of the products studied.

Hees et al. [19] developed a prediction software tool by using the test data obtained from cone calorimeter (ISO 5660). The user-friendly software package, called cone-tools, allows users to predict the major classification parameters of HRR and FIGRA in the SBI and room corner tests. The results showed that the predictions are satisfactory, implying that the tool will be powerful for the product development by industry. Comparison between the SBI test results and data of cone-tools, it was shown that cone-tools could predict the accurate classification of EU up to 90%. Comparing with the room corner test results, the correction of prediction for the classification of EU was about 85%.

Axelsson and Hees [20] tested the sandwich panels, which were already tested from the previous Nordtest project. In that project, it was shown that the correlation between the SBI test method (EN 13823) and both the ISO 9705 and ISO 13784 part1 was insufficient. New data, tested by Axelsson and Hees on sandwich panels, were generated by using the European product standard prEN 14509. They were compared with ones from Nortest project. It showed that the correlation between the data from the full-scale test and SBI was not satisfactory. In addition, the SBI test method for sandwich panels would give irreproducible results so that the classifications could not reflect the real fire behaviors of the panels.

1.3 Scope of present study

This thesis intends to find the correlation among the fire performance tested data for the selected materials, which are measured from the Cone Calorimeter (in both vertical and horizontal positions),

Surface and Single Burning Item (SBI) tests. These measured data are analyzed in advance and then tried to correlate. Finally, the proper suggestions will be made for the fire performance criteria of classification for Taiwan according to these results.



Chapter Two

TEST APPARATUS AND EVALUATION

METHODS

This chapter will introduce four kinds of apparatus, which are the cone calorimeter, surface test, elementary materials test and SBI test, respectively, and their test procedures. The calculation methods for the Cone calorimeter and SBI tests are presented as well. Those fire parameters obtained from Cone calorimeter are especially crucial for the application of fire modeling.

2.1 Cone calorimeter

The ISO 5660[1] for cone calorimeter test is a bench-scale fire test method for assessing the contribution that the product tested can measure the rate of evolution of heat during its involvement in fire. The main parts of the apparatus are a cone-shaped radiant electrical heater with a temperature controller, spark igniter, weighing cell, holder of specimen, gas analyzer instrumentation, calibration equipment, smoke system and exhaust gas system. The picture and a schematic configuration of the cone calorimeter are presented in Figs. 2.1 and 2.2, respectively.

2.1.1 Introduction for cone calorimeter apparatus

2.1.1.1 Cone-shaped radiant electric heater

The electric heater is able to be of capable of horizontal or vertical orientation. The active element of the heater shall consist of an electrical heater rod, rated at 5kW at 240V, tightly wound into the shape of a

truncated cone (see Fig. 2.3). The heater is encased on the outside with a double-well stainless steel cone, packed with a refractory fiber material of approximately 100kg/m^3 density. The irradiance from the heater is capable of being held at preset level by means of a temperature controller and three, type K, stainless steel sheathed thermocouples. The heater is capable of producing irradiances on the surface of the specimen of up to 100kW/m^2 . The irradiance is uniform within the central $50\text{mm} \times 50\text{mm}$ area of the specimen, to within $\pm 2\%$ in the horizontal orientation and to within $\pm 10\%$ in the vertical orientation.

2.1.1.2 Load cell

The load cell for measuring specimen mass loss has an accuracy of 0.1g and it preferably has a measuring range of 500 g and a mechanical tare adjustment range of 3.5 kg.

2.1.1.3 Specimen holders

There are two kinds of specimen holders, horizontal and vertical orientations, showed in Figs. 2.4 and 2.5. The bottom of the holder is lined with a layer of density (nominal density 65kg/m^3) refractory fiber blanket with a thickness of at least 13 mm. When testing on the horizontal orientation, the distance between the bottom surface of the cone heater and the top of the specimen is adjusted to 25 mm by using the sliding cone height adjustment. In the vertical orientation, the cone heater height is set so the centre lines up with the specimen centre. A retainer frame and wire grid are used when testing intumescent specimens in the horizontal orientation and can also be used to reduce unrepresentative edge burning of composite specimens and for retaining specimens prone

to delamination.

2.1.1.4 Exhaust gas system

The exhaust gas system with flow measuring instrumentation consists of a high temperature centrifugal exhaust fan, a hood, intake and exhaust ducts for the fan and an orifice plate flow meter. The exhaust system is capable of developing flows from 0.012m³/s to 0.035 m³/s. A restrictive orifice with an internal diameter of 57mm is located between the hood and the duct to promote mixing. A ring sampler is located in the fan intake duct for gas sampling, 685mm from the hood. The flow rate is determined by measuring the differential pressure across a sharp edge orifice (internal diameter 57mm) in the exhaust stack, at least 350mm downstream from the fan.

2.1.1.5 Gas analyzer instrumentation

The instrumentation incorporates a pump, a filter to prevent entry of soot, a cold trap to remove most of the moisture, a by-pass system set to divert all flow except that required for the oxygen analyzer and a further moisture trap. The detail part of instrumentation is shown in Fig. 2.6.

2.1.1.6 Smoke system

The smoke detection and measurement system employs a 0.5mW Helium-Neon laser operating at 632.8 nanometers. The laser system provides a means of obtaining the extinction coefficient based upon the degree of visual obscuration caused by suspended particulates in the exhaust stream.

2.1.1.7 Heater flux meter

The heater flux meter is the Gardon (foil) or Schmidt-Boelter (thermopiles) type with a design range of about 100kW/m². The target receiving radiation, and possibly to a small extent convection, shall be flat, circular, of approximately 12.5 mm in diameter and coated with a durable matt black finish. The target shall be water-cooled. The instrument shall have an accuracy of within $\pm 3\%$ and the repeatability within 0.5%. It is positioned at a location equivalent to the centre of the specimen face in either orientation during this calibration.

2.1.1.8 Calibration burner

The burner is constructed from a square-section brass tube with a square orifice covered with wire gauze through which the methane diffuses. The tube is packed with ceramic fiber to improve uniformity of flow. The calibration burner is suitably connected to a metered supply of methane of at least 99.5% purity.

2.1.1.9 Optical calibration filter

Calibration of the smoke system is by operator insertion of pre-calibrated neutral density filters. Two high-quality optical filters of approximately 0.3 O.D. (Optical Density) and 0.8 O.D. are provided with precision fabricated keyed positioning holders. The manufacturer's optical density curve is provided with each filter.

2.1.1.10 Ignition circuit

External ignition is accomplished by a spark plug powered from a 10 kV transformer. The spark electrode position is 13mm above the center of

the specimen in the horizontal orientation and 5mm above the top of the holder in the specimen plane in the vertical orientation.

2.1.2 Specimen construction and preparation for cone calorimeter

2.1.2.1 Specimens

Unless otherwise specified, three specimens shall be tested at each level of irradiance selected and for each different exposed surface.

The test specimen has an area of 100 mm × 100 mm and a maximum thickness of 50 mm. For products with normal thickness of greater than 50 mm, the requisite specimens shall be obtained by cutting away the unexposed face to reduce the thickness to 50 ± 3 mm.

2.1.2.2 Conditioning of specimens

Before the test, specimens shall be conditioned to constant mass at a temperature of $23 \pm 2^\circ\text{C}$, and a relative humidity of $50 \pm 5\%$ in accordance with ISO 554.

2.1.2.3 Preparation

A conditioned specimen is wrapped in a single layer of aluminum foil, of 0.03 mm to 0.05 mm thickness, with the shiny side towards the specimen, covering the unexposed surfaces. Composite specimens are exposed in a manner typical of the end-use condition. They are tested with the retainer frame and also prepared so that the sides are enveloped with the outer layer(s) or otherwise protected. If using retainer frame and wire grid, they shall be specified in the test report.

2.1.3 Test procedure for cone calorimeter

- 1) Check the CO₂ trap and the final moisture trap. Replace the sorbents

if necessary. Drain any accumulated water in the cold trap separation chamber. Adjust the distance between the bottom of cone heater and surface of specimen. This distance shall be 25mm.

- 2) Turn ON the computer and type CONE2A. The Calibrate & Test Specimens option allows operator to start the AutoCal cycle for complete system calibration prior to performing tests.
- 3) Turn ON all calibration gas, air, water and methane supplies. N₂ gas always shall be opened.
- 4) Change the Drierite, Ascarite and new 9cm filter if needed.
- 5) The computer program requests that all external exhaust blowers be turned off so a static pressure reading can be taken.
- 6) Turn ON external exhaust fans. The operator enters the desired Exhaust Flow Rate in m³/sec. Here we use 0.024m³/sec. When the reading is stable at the desired flow rate for 15 seconds, the AutoCal system will continue.
- 7) Choose YES or NO to use the last C factor. Select YES to use the last C factor. AutoCal will proceed to Heat Flux Calibration. Select NO to determine a new C factor. AutoCal will proceed to calibrate gas analyzers, smoke and weigh system to determining the new C factor.
- 8) For determining the new C factor, we first calibrate the laser system. Insert the 0.8 O.D. filter and wait to read it completely. Repeat the procedure for the 0.3 O.D. filter.
- 9) For weigh cell calibration, operator is requested to place the

specimen holder, without specimen, onto the weigh cell platform.

- 10) Enter the weight of the specimen holder and adjust the mechanical tare for 0.00 ± 0.2 g.
- 11) With the specimen holder on the weigh cell, add a 500 gram mass. AutoCal will detect the mass and take a Span reading. Don't remove the specimen holder. Remove the 500 gram mass.
- 12) The CONE2 will display this screen until the cold trap temperature reading is below 9°C before proceeding with the analyzer Span.
- 13) Remove the specimen holder and insert the calibration burner. Enter the desired Methane Flame Energy in the range of 3.5kW to 10kW. AutoCal will take a baseline oxygen reading and insert the spark igniter in preparation for methane flow. The nominal value of C factor should range from approximately 0.042 to 0.046.
- 14) Put the Heat Flux Transducer in place. Enter the desired heat flux level (0 to $100\text{kW}/\text{m}^2$) and the orientation for the test specimens.
- 15) Enter test information.
- 16) Start test. Insert the holder with specimen on the weigh cell platform and then press the START TEST button on the handset control.
- 17) When full flame ignition is observed, press and hold the FLAME VERIFICATION button on the handset. After the flame verification time has elapsed, the button will light up. Release the button and press SPARK OFF button to retract the spark.
- 18) Collect all data until 2 min after flaming or other signs of combustion

cease and the average mass loss over a 1 min period has dropped below 150 g/m². Press END TEST button.

2.1.4 Evaluation methods of cone calorimeter

2.1.4.1 The principle of Oxygen Consumption

During 70's to 80's, a technique known as Oxygen Consumption Method was developed. It is a simple, versatile and powerful tool for estimating the rate of total heat release in fire tests. As early as 1917, Thornton [2] pointed out that the heats of combustion per unit mass of oxygen consumed for organic gases and liquids were approximately the same. Huggett [3] has examined a wide variety of fuels and concluded that $\Delta h_c / r_0 = 13.1$ MJ/kg O₂ represents a value typical of most combustibles, including gases, liquids, and solids. To implement this principle it would be necessary only to measure the total mass flow of oxygen in the combustion products and to compare that to the initial inflow, that is

$$\dot{q} = \frac{\Delta h_c}{r_0} (\dot{m}_{O_2, \infty} - \dot{m}_{O_2}) \quad (2.1)$$

where the subscript ∞ denotes baseline ambient condition prior to start of test. From the form of this expression it can be seen that it does not matter at what speed the products are exhausted or how much excess air is pulled through. It is as if we were interested only in counting oxygen

“holes” . Some of the typical values of heat of combustion per unit mass of oxygen consumed are listed in the Table 2.1 to 2.3.

2.1.4.2 Calibration Factor (C factor)

The methane calibration shall be performed daily to check for the proper operation of the instrument and to compensate for minor changes in determination of mass flow.

$$C = \frac{10.0}{(12.54 \times 10^3)(1.10)} \sqrt{\frac{T_e}{\Delta p}} \frac{1.105 - 1.5\chi_{O_2}}{\chi_{O_2}^0 - \chi_{O_2}} \quad (2.2)$$

The calibration constant C, is calculated using equation (2.2), where 10.0kW methane supplied, $12.54 \times 10^3 \text{ KJ/Kg}$ value of heat of combustion per unit mass of methane consumed and 1.10 is the ratio of the molecular weights of oxygen and air.

2.1.4.3 Heat Release Rate

Prior to performing other calculations, calculate the oxygen analyzer time shift, t_d , using the following equation:

$$\chi_{O_2}(t) = \chi_{O_2}^1(t + t_d) \quad (2.3)$$

Calculate the heat release rate, $\dot{q}(t)$:

$$\dot{q}(t) = \left(\frac{\Delta h_c}{r_0} \right) (1.10) C \sqrt{\frac{\Delta p}{T_e}} \frac{\chi_{O_2}^0 - \chi_{O_2}(t)}{1.105 - 1.5\chi_{O_2}(t)} \quad (2.4)$$

Heat release rate per unit area can then be obtained:

$$\dot{q}''(t) = \dot{q}(t) / A_s \quad (2.5)$$

Total heat release rate:

$$q'' = \sum_i \dot{q}_i''(t) \Delta t \quad (2.6)$$

where $\frac{\Delta h_c}{r_0}$ is 13.1kJ/kg, value of heat of combustion per unit mass of oxygen consumed.

2.1.4.4 Mass Loss Rate of Specimen

Evaluation of mass loss rate of testing specimen is necessary for providing information like critical mass loss rates for ignition and extinction, yielding of gaseous products and effective heat of combustion. The mass loss rate is calculated numerically by a five-point approximation method with a given Δt time interval.

For the first scan $i = 0$,

$$-\left[\frac{dm}{dt} \right]_{i=0} = \frac{25m_0 - 48m_1 + 36m_2 - 16m_3 + 3m_4}{12\Delta t} \quad (2.7)$$

For the second scan $i = 1$,

$$-\left[\frac{dm}{dt} \right]_{i=1} = \frac{10m_0 + 3m_1 - 18m_2 + 6m_3 - m_4}{12\Delta t} \quad (2.8)$$

For scan $i = 1 < i < i = n - 1$,

$$-\left[\frac{dm}{dt} \right]_i = \frac{-m_{i-2} + 8m_{i-1} - 8m_{i+1} + m_{i+2}}{12\Delta t} \quad (2.9)$$

For scan $i = n - 1$,

$$-\left[\frac{dm}{dt}\right]_{i=n-1} = \frac{-10m_n - 3m_{n-1} + 18m_{n-2} - 6m_{n-3} + m_{n-4}}{12\Delta t} \quad (2.10)$$

For last scan $i = n$,

$$-\left[\frac{dm}{dt}\right]_{i=n} = \frac{-25m_n + 48m_{n-1} - 36m_{n-2} + 16m_{n-3} - 3m_{n-4}}{12\Delta t} \quad (2.11)$$

2.1.4.5 Effective Heat of Combustion

The averaged effective heat of combustion can be determined as

$$\Delta h_{c,eff} = \frac{\sum_i \dot{q}(t)\Delta t}{m_i - m_f} \quad (2.12)$$

$$\Rightarrow \Delta h_{c,eff}(t) = \frac{\dot{q}_i(t)\Delta t}{-\left(\frac{dm}{dt}\right)} \quad (2.13)$$

where $m_{initial}$ and m_{final} are mass of specimen at ignition and extinction, respectively.

2.1.4.6 Smoke

Extinction Coefficient K [1/m] is determined by laser intensity.

$$K = \left(\frac{1}{L}\right) \ln \frac{I_0}{I} \quad (2.14)$$

$$\sigma_{f(avg)} = \frac{\sum_i \dot{V}_i \dot{K}_i \Delta t_i}{m_i - m_f} \quad (2.15)$$

2.2 The surface and elementary material tests

The Chinese National Standard (CNS) 6532, assigned in the building code for Taiwan, is a bench-scale test for interior finish materials. It includes two test procedures: a surface test, which is compulsory, and an elementary material test. Whether the latter has to be performed depends on the result of the surface test. The apparatus for the surface test mainly consists of a smoke accumulation box, a furnace and an optical density-measuring system; see Fig. 2.7.

2.2.1 Introduction for the surface test apparatus

2.2.1.1 Furnace

The furnace is shown in Fig. 2.8. There are two quartz lamps, a propane burner, a thermocouple to measure back-face temperature of specimen and two thermocouples to get exhaust temperature of specimen in the furnace. In the furnace, heat is provided by a T-shaped propane burner, with a flow rate of 0.35 l/min for the first 3 mins, subsequently, an additional heat is supplied by two quartz lamps (total output is 1.5kW). The history of average value of heat flux is shown in Fig. 2.9, which is adopted from [14]. In the first 3 mins, the average value of heat flux is 0.49kW/m² and at the 10 mins it is 13.71kW/m². As to the theoretical value, it is 14.15kW/m² for the first 3 mins.. After that, the theoretical value of total heat flux is 60.45kW/m². The detailed calculation of theoretical value of heat flux is given in Appendix A. The tremendous discrepancy between the theoretical value and measurement is attributed to the neglected convectional effect, which is existed in the experiment, on the theoretical computation. The total heating time for fire-retardant

materials is 6 mins. For non-combustible and semi-combustible materials, it is 10 mins.

2.2.1.2 Smoke accumulation box

The smoke accumulation box (see Fig. 2.10) measures 1.41 m x 1.41 m x 1.0 m (Width x length x height) and is equipped with a stirrer to make the smoke homogenous distributed.

2.2.1.3 Optical density-measuring system

The capacity of smoke flow is about 1.5L/min. The light source is a halogen light. The device is shown in Fig. 2.11.

2.2.2 Specimen preparation for the surface test

2.2.2.1 Specimens

The test specimen must be the same as the one in end-use. Six specimens are provided and three of them are randomly chosen to test. The area of specimen is 220 mm × 220 mm and its thickness is the same as the original one. The heating zone is 180 mm × 180 mm. For the standard-testing material (Pearlite board), its dimension is 220 mm × 220 mm × 10 mm.

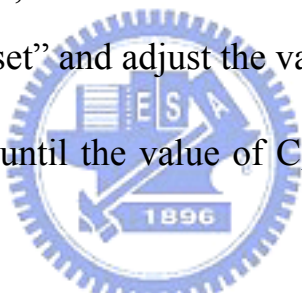
2.2.2.2 Conditioning of specimens

The testing specimens should be put in the ventilated room for more than one month. Just before the test, specimens shall be dried more than 24 hours in an oven and then they are put it into a dry box more than 24 hours. The temperature of oven is about $40 \pm 5^{\circ}\text{C}$. In addition, the perlite board shall be dried in the oven for more than 72 hours and then putd it into dry box for more than 24 hours.

2.2.2.3 Preparation

The surface lining material is installed into the furnace and the backboard with a thermocouple is put tightly behind the specimen.

2.2.3 Test procedure for surface test

- 1) Turn on all power sources, which included Logarithmic Converter, smoke agitator and computer. Wait for over 30 mins to stabilize. The smoke agitator shall be always opened.
- 2) On the Logarithmic Converter, choose the “OFF” and set the value of C_A as zero.
- 3) On the same Converter, choose the “MEAS” and zero the value of C_A . Then choose the “ C_A set” and adjust the value of C_A to 240.
- 4) Repeat the third step until the value of C_A becomes steady and then choose the “MEAS”. 
- 5) Adjust the flow of propane to about 0.35 L/min.
- 6) Preheat two quartz lamps. First heat them for 15 mins by using 1.0 kW and then turn off the power for 10 mins. After that, heat them for 10 mins by using 1.5 kW and then turn off the heater to complete the preheating.
- 7) The exhaust valve of smoke shall be closed during the test.
- 8) Wait the exhaust temperature to drop to the atmosphere value.
- 9) Pearlite board shall be tested first to get the reference curve. The error of temperature per min is tolerated up to about $\pm 20^\circ\text{C}$.

- 10) Key the information data of specimen into the computer and start the test.
- 11) Observe the sustained flaming and cracks in the back surface after completion of the test. And then open exhaust valve of smoke.

2.2.4 Evaluation methods of the surface test

Typical temperature and smoke-generation curves, together with the standard curves are shown in Fig. 2.12. The standard temperature curve is obtained by adding 50°C to the calibration curve. One of the results from each test is the $td\Theta$ value, which is a measurement of increase in temperature. The $td\Theta$ value is equal to the area under the test and the standard temperature curves. If the former is always below the latter during the heating period, $td\Theta$ is equal to zero. The time when the two curves intersect, t_c , must always be greater than 3 mins. If this is not the case, the material fails and is unclassified according to CNS 6532.

The coefficient of smoke generation, C_A , is calculated by measuring the intensity of the light transmitted through the smoke flow before the test, I_0 , and during the test, I . When these values are obtained, C_A value is calculated using the following expression:

$$C_A = 240 \cdot \log \frac{I_0}{I} \quad (2.16)$$

where I_0 = Intensity of the light before the test (LUX)

I = Intensity of the light during the test (LUX)

2.2.5 An elementary material test

The elementary material test apparatus is almost similar to the ISO test apparatus, see Fig. 2.13. The test is only used when the requirements in the surface test for a non-combustible material are met. The test apparatus can provide a high temperature environment, equivalent to the fully developed fire, to estimate the fire protection of entire specimen.

The specimens are piled up to $(40 \pm 2 \text{ mm}) \times (40 \pm 2 \text{ mm}) \times (50 \pm 2 \text{ mm})$, which are cut from building material. Three specimens shall be prepared. The conditioning process is the same as that for surface test.

Test procedure for the elementary material test is described as follows. It must be preheated at first. During preheating procedure a firebrick shall be suspended in the furnace all the time. Total preheated time is about 3 hours that the resultant hot environment inside the furnace is 750°C . Specimens are subjected to a 750°C furnace environment for 20 min when the furnace maintains 750°C for 20 mins in advance. The temperature difference shall be observing during the test.

2.3 SBI test

The SBI test is an intermediate scale test which consists of a compartment surmounted by a small calorimeter hood, which is connected to a calorimeter duct via a mixing box and baffles. The pictures are shown in Figs. 2.14 and 2.15. The specimen is a corner section and is positioned on a trolley (see Fig. 2.16) that can insert into the compartment. The compartment is positioned within a $3 \text{ m} \times 3 \text{ m} \times$

2.6 m test room.

2.3.1 Introduction for SBI apparatus

2.3.1.1 Burners and propane supply system

The SBI apparatus contains two identical sandbox burners, one in the bottom plate of the trolley (the main burner), one fixed to a post of the frame (the auxiliary burner). The main burner is mounted in the tray and connected to the U-profile at the bottom of the specimen position. The top edge of the main burner is at 10 mm above the trolley floor level. The auxiliary burner is fixed to the post of the frame opposite to the specimen corner, with the top of the burner at a height of 1450 mm from the floor.

The specimens are protected from the heat flux of the flames of the auxiliary burner by a shield of rectangular shape, width 350 ± 5 mm, height 550 ± 5 mm, made of calcium silicate board (backing boards).

The burners are equipped with an ignition glow plug. There is a solenoid valve for immediate and automatic cut-off of the gas supply in case of extinction of the main or auxiliary burners which is detected via two UV detectors. The propane controller is housed in the Gas Diverter (see Fig. 2.14) on the outside of the room. The switch used to supply propane to one of both burners is operated by Gas Control Box (see Fig. 2.17).

2.3.1.2 Smoke Exhaust system

Under test conditions, the smoke exhaust is capable of continuously extracting a volume flow, normalized at 298 K, of $0.5 - 0.65 \text{ m}^3/\text{s}$. The system are shown in Figs. 2.18 and 2.19.

2.3.1.3 General measurement section equipment

The general measurement section of the exhaust tube contains, among others, three thermocouples, a bi-directional probe, a gas sampling probe, and a light attenuation measurement system.

Three thermocouples, all of the K-type in accordance with EN 60584-1, diameter 0.5mm sheathed and insulated.

The bi-directional probe is connected to a pressure transducer with a range of 0-100Pa and an accuracy of ± 2 Pa. The pressure transducer, primary filter and air flow meter for the smoke measurement system are located on the Filter Panel, situated next to the Measurement Section.

The gas sampling is connected to a gas conditioning unit and gas analyzers for O₂ and CO₂ housed in the FTT Gas Analysis Rack. The O₂ analyzer is of the paramagnetic type, and meets the specification of EN 13823, with a range of 0% - 21% oxygen, an absolute accuracy of 0.05% (V_{O_2}/V_{air}). The CO₂ analyzer is of the IR type, with a range of 0% - 10% carbon dioxide, with an absolute accuracy of 0.1% (V_{CO_2}/V_{air}).

2.3.1.4 Smoke measurement system

The smoke measurement system consists of lamp, lens system and detector. A lamp is incandescent filament type and operating at a color temperature of 2900 ± 100 K. A lens system to align the light is a parallel beam.

2.3.1.5 Data acquisition system

The signals are collected using a HP Data Acquisition / Switch Unit. A screen based software package enables simple data acquisition and

analysis to determine the various parameters needed for heat release determination. It generates files that integrate with the current TNO spreadsheet, (which are also supplied) so that the Fire Growth Rate Index (FIGRA) and Smoke Growth Rate Index (SMOGRA) can be calculated.

2.3.2 Specimen construction and preparation of SBI test

2.3.2.1 Specimens

The corner specimen consists of two wings, designated the short and long wings respectively. The dimensions of the short wing are (495 ± 5) mm \times (1500 ± 5) mm. The dimensions of the long wing are (1000 ± 5) mm \times (1500 ± 5) mm. The maximum thickness of a specimen is 200mm. Specimens with a thickness of more than 200mm shall be reduced to a thickness of 200mm by cutting away the unexposed surface.

2.3.2.2 Backing Boards

The backing boards is calcium silicate boards with a density of (800 ± 150) kg/m³ and a thickness of (12 ± 3) mm. The dimensions of the short wing shall be (at least 570mm + width of specimen) mm \times (1500 ± 5) mm. The long wing shall be (1000 ± 5) mm \times (1500 ± 5) mm. Three specimens (three sets of long plus short wing) are needed.

2.3.2.3 Condition of specimens

The parts that compose a specimen may be conditioned separately or fixed together. However, specimens that tested glued to a substrate shall be glued before conditioning. The entire procedure is carried out within 2h of removal of the specimen from the conditioning environment.

2.3.2.4 Preparation

The specimen wings are placed in the trolley. First the short wing specimen and backing board are placed on the trolley, with the bottom edge of the specimen against the short U-profile on the trolley floor. Next the long wing specimen and backing board are placed on the trolley. Both wings are wedged at the top and the bottom. Be sure that the corner line of the backing boards does not widen during the test.

2.3.3 Test procedure for SBI

- 1) Check trolley shall be installed into the test room. Connect two lines of Gas Diverter and open two valves. Replace the sorbents if necessary. Close the door of test room. Open the propane gas.
- 2) Push the Analyzers button of Gas Analysis Rack and Power On button of Gas Control Box.
- 3) Push the Cold Trap button of Gas Analysis Rack. Open the computer and run the software of SBICalc.
- 4) There are 9 buttons displayed across the button of the screen. Choose the Calibrations and All transducers.
- 5) Zero DPT and SMOKE (No light, 0%) on software.
- 6) Push the Smoke button of Gas Analysis Rack.
- 7) Open an exhaust fan. Under ambient conditions, the volume flow shall be normalized about $0.6\text{m}^3/\text{s}$.
- 8) Push the Gas On button of the Gas Control Box. The Interlocks Made on the Gas Control Box shall be green light.

- 9) Zero MFM and push the OK button to save the settings.
- 10) Open N₂ gas and turn two valves of the Rack to Nitrogen. Wait for five minutes.
- 11) Zero O₂ on analyzers. (Password : 4000)
- 12) Zero O₂ on software and push the OK button to save settings.
- 13) Zero CO₂ on analyzers. Zero CO₂ on software.
- 14) Zero CO on analyzers. Zero CO on software and push the OK button to save settings.
- 15) Close the N₂ gas. Open the CO/CO₂ gas and turn two valves of the Rack to Air and CO/CO₂. Wait for five minutes.
- 16) Span CO₂ on analyzers and Span CO₂ on software.
- 17) Span CO SPAN CO on analyzers and Span CO on software.
- 18) Close CO/CO₂ gas. Turn two valves of the Rack to Air and Sample gas.
- 19) Push the Pump button and wait for 5-10 minutes.
- 20) Span O₂ on analyzers and Span O₂ on the software.
- 21) Span Smoke (Light, 100%) on software and save settings.
- 22) Enter test information, included humidity.
- 23) Start the test. When $t = (120 \pm 5)$ s, auxiliary burner shall be ignited. Adjust the propane mass flow m_{gas} to (647 ± 5) mg/s. The time period $210 \text{ s} < t < 270 \text{ s}$ is used to measure the base line for the rate

of heat release.

- 24) When $t = (300 \pm 5)$ s, the propane supply from the auxiliary burner to the main burner shall be switched.
- 25) Observe the burning behavior of the specimen for a period of 1260 s and record the data on the record sheet. The nominal exposure period of the specimen to the flames of the main burner is 1260 s. The performance is evaluated over a period of 1200 s.
- 26) After $t = 1560$ s, the end of test conditions on the record sheet at least 1 min shall be recorded, without the influence of remaining combustion. If the specimen is difficult to extinguish totally, the trolley may need to be removed.

2.3.4 Evaluation methods of SBI test

2.3.4.1 Calculation of heat release rate (HRR)

2.3.4.1.1 Total HRR of specimen and burner: HRR_{total}

- a) Calculation of the volume flow of exhaust system, normalized at 298 K, $V_{298}(t)$:

$$V_{298}(t) = cA \frac{k_t}{k_\rho} \sqrt{\frac{\Delta p(t)}{T_{ms}(t)}} \quad (2.17)$$

- b) Calculation of the oxygen depletion factor $\phi(t)$:

$$\phi(t) = \frac{\bar{x}O_2(30s...90s)\{1 - xCO_2(t)\} - xO_2(t)\{1 - \bar{x}CO_2(30s...90s)\}}{\bar{x}O_2(30s...90s)\{1 - xCO_2(t)\} - xO_2(t)} \quad (2.18)$$

- c) Calculation of $x_{a_O_2}$:

$$x_{a_{-}O_2} = \bar{x}_{O_2}(30s...90s) \left[1 - \frac{H}{100p} \exp \left\{ 23.2 - \frac{3816}{\bar{T}_{ms}(30s...90s) - 46} \right\} \right] \quad (2.19)$$

d) Calculation of $HRR_{total}(t)$ [kW]:

$$HRR_{total}(t) = EV_{298}(t) x_{a_{-}O_2} \left(\frac{\phi(t)}{1 + 0.105\phi(t)} \right) \quad (2.20)$$

2.3.4.1.2 HRR of the burner

The $HRR_{burner}(t)$ is equal to $HRR_{total}(t)$ during the base line period.

The average HRR of the burner is calculated as the average $HRR_{total}(t)$ during the base line period ($210s \leq t \leq 270s$):

$$HRR_{av_burner} = \overline{HRR_{total}(210s...270s)} \quad (2.21)$$

where HRR_{av_burner} is the average heat release rate of the burner [kW].

The criteria of HRR_{av_burner} shall meet the value, $30.7 \pm 2.0kW$.

2.3.4.1.3 HRR of the specimen

In general, the heat release rate of the specimen is taken as the total heat release rate $HRR_{total}(t)$ minus the average heat release rate of the burner HRR_{av_burner} :

$$\text{For } t > 312s, \quad HRR(t) = HRR_{total}(t) - HRR_{av_burner} \quad (2.22)$$

where $HRR(t)$ is the heat release of the specimen [kW].

During the switch from the auxiliary to the main burner at the start

of the exposure period, the total heat output of the two burners is less than HRR_{av_burner} .

For $t = 300s$, $HRR(300s) = 0 \text{ kW}$

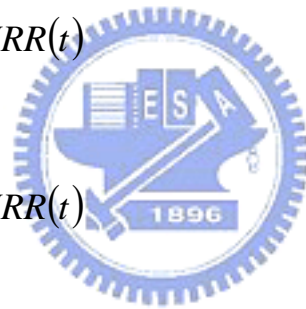
$$\text{For } 300s < t \leq 312s, \quad HRR(t) = \max.\{0, HRR_{total}(t) - HRR_{av_burner}\} \quad (2.23)$$

2.3.4.2 Calculation of THR(t) and THR_{600s}

The total heat release of the specimen THR(t) [MJ] and the total heat release of specimen in the first 600s of the exposure period ($300s \leq t \leq 900s$), THR_{600s}, are calculated as follows:

$$THR(t_a) = \frac{3}{1000} \sum_{300s}^{t_a} HRR(t) \quad (2.24)$$

$$THR_{600s} = \frac{3}{1000} \sum_{300s}^{900s} HRR(t) \quad (2.25)$$



where the factor 3 is introduced since only one data point is available every three seconds.

2.3.4.3 Calculation of FIGRA_{0.2MJ} and FIGRA_{0.4MJ}

The FIGRA (fire growth rate indices) [W/s] are defined as the maximum of the quotient $HRR_{av}(t)/(t-300)$, multiplied by 1000. The quotient is calculated only for that part of the exposure period in which the threshold levels for HRR_{av} and THR have been exceeded. If one or both threshold values of a FIGRA index are not exceeded during the exposure period, that FIGRA index is equal to zero. Two different

THR-threshold values are used, resulting in $FIGRA_{0.2MJ}$ and $FIGRA_{0.4MJ}$.

a) Calculate $FIGRA_{0.2MJ}$ for all t where:

$$(HRR_{av}(t) > 3 \text{ kW}) \text{ and } (THR(t) > 0.2 \text{ MJ}) \text{ and } 300s < t \leq 1500s ;$$

b) Calculate $FIGRA_{0.4MJ}$ for all t where:

$$(HRR_{av}(t) > 3 \text{ kW}) \text{ and } (THR(t) > 0.4 \text{ MJ}) \text{ and } 300s < t \leq 1500s ;$$

Both using:

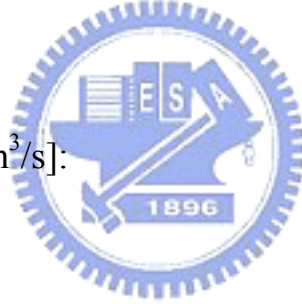
$$FIGRA = 1000 \times \max \left(\frac{HRR_{av}(t)}{t - 300} \right) \quad (2.26)$$

2.3.4.4 Calculation of smoke production rate (SPR)

2.3.4.4.1 Total SPR

a) Calculation of $V(t)$ [m^3/s]:

$$V(t) = V_{298}(t) \frac{T_{ms}(t)}{298} \quad (2.27)$$



b) Calculation of $SPR_{total}(t)$ [m^2/s]:

$$SPR_{total}(t) = \frac{V(t)}{L} \ln \left[\frac{\bar{I}(30s...90s)}{I(t)} \right] \quad (2.28)$$

2.3.4.4.2 SPR of the burner

The smoke production rate of the burner is equal to $SPR_{total}(t)$ [m^2/s] during the base line period. The average SPR of the burner is calculated as the average $SPR_{total}(t)$ during the base line period ($210s \leq t \leq 270s$) :

$$SPR_{av_burner} = \overline{SPR_{total}}(210s...270s) \quad (2.29)$$

The average smoke production rate of the burner SPR_{av_burner} [m^2/s] shall meet the value, $0 \pm 0.1m^2 / s$.

2.3.4.4.3 SPR of the specimen

In general, the smoke production rate of the specimen $SPR(t)$ [m^2/s] is taken as the total smoke production rate $SPR_{total}(t)$, minus the average SPR of the burner, SPR_{av_burner} .

$$\text{For } t > 312s, \quad SPR(t) = SPR_{total}(t) - SPR_{av_burner} \quad (2.30)$$

During the switch from auxiliary to main burner at the start of the exposure period, the total smoke production of the two burners might be less than SPR_{av_burner} .

$$\text{For } t = 300s, \quad SPR(300) = 0 \text{ m}^2/s$$

$$\text{For } 300s < t \leq 312s, \quad SPR(t) = \max.[0, SPR_{total}(t) - SPR_{av_burner}] \quad (2.31)$$

2.3.4.5 Calculation of TSP(t) and TSP_{600s}

The total smoke production of the specimen $TSP(t)$ [m^2] and the total smoke production of the specimen in the first 600s of the exposure period ($300s \leq t \leq 900s$), TSP_{600s} , are calculated as follows:

$$TSP(t_a) = 3 \sum_{300s}^{t_a} (\max.[SPR(t), 0]) \quad (2.32)$$

$$TSP_{600s} = 3 \sum_{300s}^{900s} (\max.[SPR(t), 0]) \quad (2.33)$$

2.3.4.6 Calculation of SMOGRA

The smoke growth rate index (SMOGRA) [m^2/s^2] is defined as the maximum of the quotient $SPR_{av}(t)/(t - 300)$, multiplied by 10000. The quotient is calculated only for that part of the exposure period in which the threshold levels for SPR_{av} and TSP have been exceeded. If one or both threshold values are not exceeded during the exposure period, SMOGRA is equal to zero. Calculation SMOGRA for all t where :

$$\left(SPR_{av(t)} > 0.1m^2 / s \right) \text{ and } \left(TSP(t) > 6m^2 \right) \text{ and } (300s < t \leq 1500s)$$

$$SMOGRA = 10000 \times \max \left(\frac{SPR_{av}(t)}{t - 300} \right) \quad (2.34)$$



Chapter Three

UNCERTAINTY ANALYSIS

All of the data from experimental results may not be equally good to adopt. Their accuracy should be confirmed before the analyses of experimental results are carried out. Uncertainty analysis (or error analysis) is a procedure used to quantify data validity and accuracy [21]. Errors always are presented in experimental measuring. Experimental errors can be categorized into the fixed (systematic) error and random (non-repeatability) error, respectively [21]. Fixed error is the same for each reading and can be removed by proper calibration and correction. Random error is different for every reading and hence cannot be removed. The objective of uncertainty analysis is to estimate the probable random error in experimental results.

From the viewpoint of reliable estimation, it can be categorized into single-sample and multi-sample experiments. If experiments could be repeated enough times by enough observers and diverse instruments, then the reliability of the results could be assured by the use of statistics [22]. Like such, repetitive experiments would be called multi-sample ones. Experiments of the type, in which uncertainties are not found by repetition because of time and costs, would be called single-sample experiments.

3.1 Analyses of the Propagation of Uncertainty in Calculations

Uncertainty analysis is carried out here to estimate the uncertainty levels in the experiment. Formulas for evaluating the uncertainty levels in the experiment can be found in many papers [22, 23] and textbooks [21, 24, 25]. They are presented as follows:

Suppose that there are n independent variables, x_1, x_2, \dots, x_n , of experimental measurements, and the relative uncertainty of each independently measured quantity is estimated as u_i . The measurements are used to calculate some experimental result, R , which is a function of independent variables, x_1, x_2, \dots, x_n ; $R = R(x_1, x_2, \dots, x_n)$.

An individual x_i , which affects error of R , can be estimated by the deviation of a function. A variation, δx_i , in x_i would cause R to vary according to

$$\delta R_i = \frac{\partial R}{\partial x_i} \delta x_i. \quad (3.1)$$

Normalize above equation by dividing R to obtain

$$\frac{\delta R_i}{R} = \frac{1}{R} \frac{\partial R}{\partial x_i} \delta x_i = \frac{x_i}{R} \frac{\partial R}{\partial x_i} \frac{\delta x_i}{x_i} \quad (3.2)$$

Equation (3.2) can be used to estimate the uncertainty interval in the result due to the variation in x_i . Substitute the uncertainty interval for x_i ,

$$u_{R_i} = \frac{x_i}{R} \frac{\partial R}{\partial x_i} u_{x_i} \quad (3.3)$$

To estimate the uncertainty in R due to the combined effects of uncertainty intervals in all the x_i 's, it can be shown that the best

representation for the uncertainty interval of the result is [23]

$$u_R = \pm \left[\left(\frac{x_1}{R} \frac{\partial R}{\partial x_1} u_1 \right)^2 + \left(\frac{x_2}{R} \frac{\partial R}{\partial x_2} u_2 \right)^2 + \dots + \left(\frac{x_n}{R} \frac{\partial R}{\partial x_n} u_n \right)^2 \right]^{1/2} \quad (3.4)$$

The sensitivity coefficient equals the partial derivative of the final result with respect to the measured quantity. Equation 3.4 transforms to

$$u_R = k \sqrt{c_{r,1}^2 (u_1)^2 + c_{r,2}^2 (u_2)^2 + \dots} \quad (3.5)$$

where $c_{r,i}$ is the relative sensitivity coefficients and k is the coverage factor. When using the coverage factor of 2 the confidence level is approximately 95%.

3.2 Uncertainty of cone calorimeter

3.2.1 Simplification of the heat release rate calculation

Equation (2.4) in Chapter Two is a simplification of the general equations developed by Parker [26] and elaborated by Janssens [27]. Consider Equation 2.4 beside the more detailed, general equation for this gas analysis configuration, Equation 3.6.

$$\dot{q}(t) = \left(\frac{\Delta h_c}{r_o} \right) \left(\frac{M_{O_2}}{M_a} \right) C \sqrt{\frac{\Delta p}{T_e}} \left(\frac{\chi_{O_2}^o - \chi_{O_2}}{[1 + (\beta - 1)\chi_{O_2}^o] - \beta \chi_{O_2}} \right) \quad (3.6)$$

where $\dot{q}(t)$ is the heat release rate, Δh_c is the net heat of combustion, r_o is the stoichiometric oxygen to fuel mass ratio, M_{O_2} is the molecular weight of oxygen, M_a is the molecular weight of air, C is the calibration constant, Δp is the orifice flow meter pressure differential, T_e is the

absolute temperature of gas at the orifice flow meter, $\chi_{O_2}^o$ is the initial (ambient) value of oxygen analyzer reading (normally the dry-air oxygen concentration is 0.2095), χ_{O_2} is the oxygen analyzer reading, and β is a stoichiometric factor described in Babrauskas [28] as the ratio of the number of moles of products to moles of oxygen consumed. The $\frac{M_{O_2}}{M_a}$ is calculated as following:

$$\frac{M_{O_2}}{M_a} = \frac{32}{28.97} \approx 1.10 \quad (3.7)$$

where M_a is the molecular weight of dry air assumed. And Equation 3.6 becomes Equation 3.8.

$$\dot{q}(t) = \left(\frac{\Delta h_c}{r_0} \right) (1.10) C \sqrt{\frac{\Delta p}{T_e} \left(\frac{\chi_{O_2}^o - \chi_{O_2}}{[1 + (\beta - 1)\chi_{O_2}^o] - \beta\chi_{O_2}} \right)} \quad (3.8)$$

The value of β depends on the C to H to O ratio of the fuel, and it varies from $\beta=1.0$ for pure carbon to $\beta=2.0$ for pure hydrogen. Equation 2.4 assumes that $\chi_{O_2}^o = 0.2095$ and $\beta=1.5$ (correct for Methane and PMMA).

3.2.2 Uncertainty of heat release rate calculation

Equation 3.7, which includes the combustion expansion effect due to the fuel-dependent stoichiometric factor, β , and an assumed value of 0.2095 for $\chi_{O_2}^o$. Equation 3.8 assumes that the uncertainty of $\chi_{O_2}^o$ is negligible.

$$\begin{aligned}\dot{q}(t) &= f\left(\frac{\Delta h_c}{r_0}, C, \Delta p, T_e, \chi_{O_2}, \beta\right) \\ &= \left(\frac{\Delta h_c}{r_0}\right)(1.10)C \sqrt{\frac{\Delta p}{T_e}} \left(\frac{\chi_{O_2}^o - \chi_{O_2}}{[1 + (\beta - 1)\chi_{O_2}^o] - \beta\chi_{O_2}}\right)\end{aligned}\quad (3.9)$$

The general expression for absolute uncertainty of HRR from this functional relationship is:

$$\begin{aligned}\delta\dot{q}(t) &= \left\{ \left(\frac{\partial\dot{q}(t)}{\partial\left(\frac{\Delta h_c}{r_0}\right)} \delta\left(\frac{\Delta h_c}{r_0}\right) \right)^2 + \left(\frac{\partial\dot{q}(t)}{\partial C} \delta C \right)^2 + \left(\frac{\partial\dot{q}(t)}{\partial\Delta p} \delta(\Delta p) \right)^2 \right. \\ &\quad \left. + \left(\frac{\partial\dot{q}(t)}{\partial T_e} \delta T_e \right)^2 + \left(\frac{\partial\dot{q}(t)}{\partial\chi_{O_2}} \delta\chi_{O_2} \right)^2 + \left(\frac{\partial\dot{q}(t)}{\partial\beta} \delta\beta \right)^2 \right\}\end{aligned}\quad (3.10)$$

The partial derivatives follow. These are referred to as the sensitivity coefficients, since the product of these coefficients and an individual component's uncertainty gives the individual component's contribution to the overall uncertainty.

$$\frac{\partial}{\partial\left(\frac{\Delta h_c}{r_0}\right)} \dot{q}(t) = (1.10)C \sqrt{\frac{\Delta p}{T_e}} \left(\frac{0.2095 - \chi_{O_2}}{[1 + 0.2095(\beta - 1)] - \beta\chi_{O_2}}\right)\quad (3.11)$$

$$\frac{\partial}{\partial C} \dot{q}(t) = \left(\frac{\Delta h_c}{r_0}\right)(1.10) \sqrt{\frac{\Delta p}{T_e}} \left(\frac{0.2095 - \chi_{O_2}}{[1 + 0.2095(\beta - 1)] - \beta\chi_{O_2}}\right)\quad (3.12)$$

$$\frac{\partial}{\partial(\Delta p)} \dot{q}(t) = \frac{1}{2} \left(\frac{\Delta h_c}{r_o} \right) (1.10) C \sqrt{\frac{1}{\Delta p \cdot T_e}} \left(\frac{0.2095 - \chi_{O_2}}{[1 + 0.2095(\beta - 1)] - \beta \chi_{O_2}} \right) \quad (3.13)$$

$$\frac{\partial}{\partial T_e} \dot{q}(t) = -\frac{1}{2} \left(\frac{\Delta h_c}{r_o} \right) (1.10) C \sqrt{\frac{\Delta p}{T_e^3}} \left(\frac{0.2095 - \chi_{O_2}}{[1 + 0.2095(\beta - 1)] - \beta \chi_{O_2}} \right) \quad (3.14)$$

$$\frac{\partial}{\partial \chi_{O_2}} \dot{q}(t) = -\left(\frac{\Delta h_c}{r_o} \right) (1.10) C \sqrt{\frac{\Delta p}{T_e}} \left(\frac{0.7905}{([1 + 0.2095(\beta - 1)] - \beta \chi_{O_2})^2} \right) \quad (3.15)$$

$$\frac{\partial}{\partial \beta} \dot{q}(t) = -\left(\frac{\Delta h_c}{r_o} \right) (1.10) C \sqrt{\frac{\Delta p}{T_e}} \left(\frac{(0.2095 - \chi_{O_2})^2}{([1 + 0.2095(\beta - 1)] - \beta \chi_{O_2})^2} \right) \quad (3.16)$$

The partial differential equations must be independent for an analysis to be mathematically valid. For the calculation of uncertainty by using Eqs. (3.10) to (3.16), Enright and Fleischmann [29] considered the following test using data from cone calorimeter tests. The tested sample was an upholstered furniture composite. The assumed effective heat of combustion term may vary $\pm 5\%$ from its value of 13100 kJ/kg (± 655 kJ/kg). The assumed β value of 1.5 may vary by ± 0.5 . The corresponding details of test are shown as Table 3.1.

Figures 3.1 and 3.2 demonstrate that at low HRR, the uncertainty is very high. The total relative uncertainty is the root mean squares of the individual components. For the expansion factor and assumed effective heat of combustion term, uncertainties can be reduced if the composition of the fuel is known. With respect to oxygen analyzer uncertainty at low HRR, using a suppressed zero measuring range or otherwise measuring the oxygen difference directly, may reduce this uncertainty.

3.3 Uncertainty of surface test

According to CNS 6532, the perlite board shall be tested first to get the reference curve. The error of temperature per min is tolerated up to about $\pm 20^\circ\text{C}$. The measured temperatures per min are shown in Table 3.2. The calculated errors are as follows:

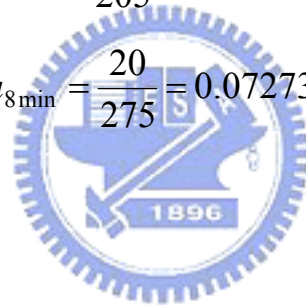
$$u_R = \pm \left[(u_{1\min})^2 + (u_{2\min})^2 + \dots + (u_{10\min})^2 \right]^{1/2} = \pm 0.4972 = \pm 49.72\%$$

$$\left(u_{1\min} = \frac{20}{70} = 0.28571, u_{2\min} = \frac{20}{80} = 0.25, u_{3\min} = \frac{20}{90} = 0.22222, \right.$$

$$u_{4\min} = \frac{20}{155} = 0.12903, u_{5\min} = \frac{20}{205} = 0.09756, u_{6\min} = \frac{20}{235} = 0.08511,$$

$$u_{7\min} = \frac{20}{260} = 0.07692, u_{8\min} = \frac{20}{275} = 0.07273, u_{9\min} = \frac{20}{290} = 0.06897,$$

$$u_{10\min} = \frac{20}{305} = 0.06557 \left. \right)$$



The uncertainty of exhaust temperature for perlite board is very high. The standard temperature curve is obtained by adding 50°C to the calibration curve. The $td\Theta$ value is equal to the area under the test and the standard temperature curves, and the time, t_c , is obtained when the two curves intersect. Therefore, the $td\Theta$ value and t_c used for classification of CNS 6532 are subjected to the influence of uncertainty. For the classification of CNS 6532, t_c must be greater than 3 mins and the uncertainty of exhaust temperature for 3 mins will affect if the material can be classified consequently. If the error of exhaust temperature per min is close to $\pm 20^\circ\text{C}$, it can be improved by replacing a new perlite

board. In addition, the examination of the total output of two quartz lamps to be 1.5 kW and the valve of exhaust being closed are very crucial.

For the coefficient of smoke generation, C_A , it is calculated as follows:

$$C_A = \frac{V}{LA} \cdot \log \frac{I_0}{I} = 240 \cdot \log \frac{I_0}{I} \quad (3.17)$$

where V = Volume of smoke accumulation box

L = Length of light path

A = Heating area of specimen

$$V = l \times w \times h = 1.41 \times 1.41 \times 1 = 1.9881(m^3), \quad A = 0.18 \times 0.18 = 0.0324(m^2),$$

$$L = 25cm = 0.25m, \text{ so } \frac{V}{LA} = \frac{1.9881}{0.25 \times 0.0324} = 245.44444$$

$$Error = \frac{245.44444 - 240}{240} = 0.022685 = 2.27\%$$

The volume value of 240 used by CNS 6532 has a small deviation about 2.27%. The reason is given as follows. The smoke accumulation box includes agitator, smoke sampling tube and exhaust device of furnace. The volume of smoke accumulation box should extract the ones occupied by these instruments. In addition, the smoke accumulation box should be cleaned frequently to reduce the errors of C_A calculation.

3.4 Uncertainty of SBI

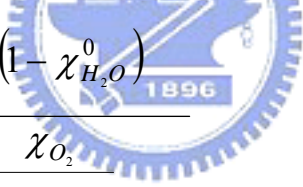
The SBI and the room corner test are both part of the Euroclass

system. Rather complicated measurements are included in the methods for measuring the HRR and SPR. These data are then transformed into the FIGRA and SMOGRA values which are crucial for the classification of the product according to the Euroclass system. The details of test methods are described in Chapter Two.

Axelsson et al. [30] analyzed the individual sources of errors from the HRR and the SPR calculations in the SBI and room corner tests. For the uncertainty of SBI, it is described as follows.

3.4.1 Uncertainty of HRR

Equation (3.17) normally used for calculating the HRR during a fire test using oxygen consumption principle is:



$$\dot{Q} = \frac{E \cdot \dot{m} \cdot \frac{M_{O_2}}{M_{air}} \cdot (1 - \chi_{H_2O}^0)}{1 - \frac{\chi_{O_2}}{\alpha - 1} + \frac{\chi_{O_2}^0}{\chi_{O_2}^0 - \frac{\chi_{O_2} \cdot (1 - \chi_{CO_2}^0)}{1 - \chi_{CO_2}}}} \quad (3.17)$$

where

\dot{Q} = heat release rate [kW]

E = amount of energy developed per consumed kilogram of oxygen
[kJ/kg]

\dot{m} = mass flow in exhaust duct [kg/s]

M_{O_2} =molecular weight for oxygen [g/mol]

M_{air} =molecular weight of air [g/mol]

α =ratio between the number of moles of combustion products including nitrogen and the number of moles of reactants including nitrogen (expansion factor)

$\chi_{O_2}^0$ =mole fraction for O₂ in the ambient air, measured on dry gases

$\chi_{CO_2}^0$ =mole fraction for CO₂ in the ambient air, measured on dry gases

$\chi_{H_2O}^0$ =mole fraction for H₂O in the ambient air

χ_{O_2} = mole fraction for O₂ in the flue gases, measured on dry gases

χ_{CO_2} = mole fraction for CO₂ in the flue gases, measured on dry gases

The volume flow, in the exhaust duct expressed in cubic metres per second, related to atmospheric pressure and an ambient temperature of 25°C, is given by the Equation 3.18.

$$\dot{V}_{298} = A \frac{k_t}{k_p} \frac{1}{\rho_{298}} \sqrt{2\Delta p T_0 \rho_0 / T_s} = 22.4 \left(A \cdot k_t / k_p \right) \sqrt{\Delta p / T_s} \quad (3.18)$$

where T_s is the gas temperature in the exhaust duct expressed in Kelvin (K). A is the cross section area, Δp is the pressure difference measured by the bi-directional probe (Pa), k_t is the ratio of the average volume flow per unit area to volume flow per unit area in the centre of the

exhaust duct and k_p is the Reynolds number correction for the bi-directional probe. The factor “22.4” involves the factor 2, T_0 (273.15K) and the density of the gas at 0 °C, ρ_0 and at 298 k, ρ_{298} . The mass flow, \dot{m} , is obtained by

$$\dot{m} = \frac{k_t}{k_p} \cdot A \cdot \sqrt{2 \cdot \Delta p \cdot \rho_{298} \cdot \frac{298}{T_s}} \quad (3.19)$$

The summary with the total uncertainty of volume flow for SBI is given in Table 3.3. The combined expanded relative standard uncertainty for the flow measurement in the SBI was determined as $\pm 3.3 \%$.

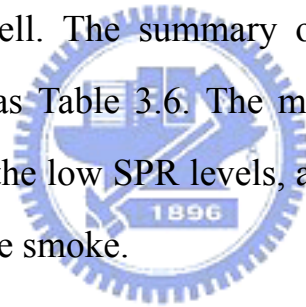
The combined uncertainty in heat release measurements for the SBI is presented in Table 3.4 and Table 3.5. The uncertainties were calculated for two different levels of HRR, which were 35kW and 50kW. The tables for the SBI show quite a high HRR uncertainty, mainly due to the O_2 uncertainty. At the 35 kW level, 13.5 % means ± 4.7 kW for a single value. This is, however, a conservative value as the calculation in the SBI standard requires 30 sec averaged values and measurements are made every third second. In the SBI, 30 sec averages are studied which reduces the uncertainty by a factor $\sqrt{10}$. The combined expanded relative standard uncertainty for the 30 sec averages is 4.3 % ($13.5\% / \sqrt{10}$) for the 35 kW level and 3.2 % for the 50 kW level.

For the uncertainty of HRR, the oxygen concentration contributes most followed by the E-factor and the mass flow. If the fuel used is known then the uncertainty of E-factor decreases. The uncertainty in the

velocity profile in the duct and the bi-directional probe constant are the most important for the mass flow. The uncertainty in the velocity profile can be decreased by designing the duct correctly and determining the velocity profile more precisely.

3.4.2 Uncertainty of SPR

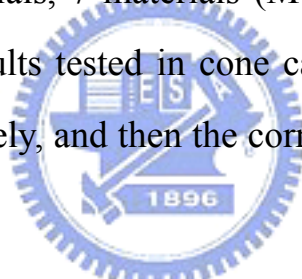
The sources of uncertainty in smoke production rate includes the mass flow in duct and gas temperature, soot accumulation on lenses, filter calibration, noise and drift, temperature influence and length of extinction beam. For the SPR the most important factors are the calibration of the filters used for calibrating the equipment together with the temperature sensitivity of the photocell. The summary of uncertainty for different levels of SPR is shown as Table 3.6. The most interesting result is the very high uncertainty on the low SPR levels, a fact that should be noticed that products produce little smoke.



Chapter Four

RESULTS AND DISCUSSIONS

15 building materials were selected and tested in the Cone Calorimeter and the surface test. Tests in the Cone Calorimeter were performed in the horizontal and vertical directions, respectively, under a fixed incident heat flux 50kW/m^2 . These materials are listed in Table 4.1, which includes green building (M01 and M02), nanocomposite (M03, M08 and M09), composite (M04, M05, M06, M07, M10 and M11) and flooring (M12~M15) materials. Their major compositions are shown in Table 4.2. In these materials, 7 materials (M01~M07) are tested in SBI test additionally. The results tested in cone calorimeter, surface test and SBI are presented separately, and then the corresponding comparisons are followed



4.1 The test results of Cone Calorimeter

The Japanese standard and classification of cone calorimeter test are shown in Table 4.3. The incident heat flux is set at 50kW/m^2 and heating time in the test is determined according to the classification level of each material. For class 1, the noncombustible material shall be tested for twenty minutes, for class 2, the semi noncombustible material for ten minutes, and for class 3, the fire retardant material for five minutes.

4.1.1 HRR of cone calorimeter tested in vertical orientation

The results of cone calorimeter tested in vertical orientation are summarized in Tables 4.4 and values are the average of three test results.

All detailed quantities can be referred Appendix B1. It finds that M06, M07, M12, M13, M14 and M15 were able to be ignited. Note that the ignited time of M06 was over 600s and it was marked “N.I.” in the Table 4.4. The reason is discussed in Section 4.1.2. Among these materials, M06 and M07 were added flame retardants of Phosphorus by using the way of soak. As they were subjected to the heat flux of 50kW/m^2 , their HRR increased slowly because of adding of flame retardants. After a period of heating, the flame retardants were decomposed and volatilized to become inert gases, which dilute the flammable gases. According to the chemical reaction, it would control the burning process of wood. Therefore, the THR average value of M06 could be controlled less than 8MJ/m^2 , about 5.12 MJ/m^2 . So M06 was classified as the rank of class 2. On the other hand, M07 was not qualified as class 2, even if class 3, since its average value of total heat release rate was 10.96 MJ/m^2 in 300 seconds. There are two major reasons: one is the thickness of material and the other is the content of flame retardants. The thicknesses of M06 and M07 were 14.5mm and 3.6mm, respectively. M07 was thinner such that its quantity of flame retardants was less. Therefore, the peak values of heat release rate of M07 were higher than that of M06.

M12, M13, M14 and M15 were flooring materials and had no flame retardants. M12 and M14 were solid wood flooring materials and M13 and M15 were laminate ones. Because the peak values of heat release rate and total heat release rates of these flooring materials were higher than required standard of Japanese classification, they could not possess any classification.

Other materials, such as M01, M02, M03, M04, M05, M08, M09, M10 and M11, responded with low values of heat release rate. The reasons are attributed to their main compositions. The main compositions for M01, M02, M04, M10 and M11 are mineral, fibers and adhesives. The latter two can generate low values of heat release rate. M03, M08 and M09 are ceramic board, composed of clay, so that they are noncombustible without generating any heat release. The compositions of M05 included farina and pulp, consequently it has higher heat release rate. According to the Japanese standard, they are classified as class 1, the noncombustible materials.

4.1.2 HRR of cone calorimeter tested in horizontal orientation

The corresponding results of cone calorimeter tested in horizontal orientation are shown in Table 4.5 and they are the average of three test results. All detailed ones are given in Appendix B2. Similarly, M01, M02, M03, M04, M05, M08, M09, M10 and M11 have low heat release rate values so that they were still ranked as class 1. M07, M12, M13, M14 and M15 could not be qualified for the classification. The major difference was that the rank of M06 was lowered to class 3 in horizontal orientation, whereas it was qualified as class 2 in vertical orientation. The total heat release rate average value of M06 tested in 300 seconds was 6.11 MJ/m^2 . However, the corresponding values tested in 600 seconds were over the limit of class 2. Apparently, the reason can be attributed to orientation effect. When the sample is tested in vertical direction, the flammable gas is not able to accumulate easily but discharged quickly by exhaust system. On the other hand, the sample placed in horizontal orientation has a

heater on the top. The flammable gas can be concentrated on the top of sample and ignited easier than that in vertical orientation. Such situation can also be observed in the tests of the flooring materials. Their ignition times tested in vertical orientation are longer than that in the horizontal one. Besides, the average values of HRR_{av_180s} and THR obtained in the horizontal orientation are higher than those in vertical one. It shows the classification using Cone Calorimeter test in horizontal orientation is more stringent.

In addition, the FR (flame retardants) materials have some arguments about their values of content, which can affect the ignition time and heat release. For an example, M06 tested in Cone Calorimeter showed some unusual behaviors. After being ignited, the sparker should be removed according to ISO 5660. However, the flame was extinguished within 60s after ignition. Then, the sparker should be installed once more and M06 was ignited again. The reason is mainly attributed to the flame retardants contained. The flame retardants of Phosphorus added in M06 used the way of soaking onto the plywood, layered by lauan. The flame retardants of Phosphorus was layered onto it and led to such phenomenon. According to ISO 5660, this situation is ranked as the failed result. Therefore, the sparker for the similar materials as M06 tested in Cone Calorimeter shall not removed during the test.

4.1.3 Correlation between vertical and horizontal directions of cone calorimeter test

According to ISO 5660[1], the mean heat release rate readings within 180 seconds should be compared each other for three specimens of

the same material. This parameter is selected to discuss the correlation. The results are demonstrated in Fig. 4.1. The correlation appears relatively good and the corresponding value of R^2 is about 0.95. Therefore, it can be concluded that there still have small difference for the test results between the vertical and horizontal orientation for the same material in Cone Calorimeter.

4.2 The results of surface test and elementary material test

The materials listed in Table 4.6 were classified according to CNS 6532. The test results of CNS 6532, included the surface test and elementary material test if needed based on the surface test results, are shown in Tables 4.7 and 4.8. As previous, these data are the average of three test results except the one of M06. The tested quantity of M06 in Table 4.7 is average value of five tests. All the detailed results are given in Appendixes C1 and C2.

M01 and M02 consist of inorganic substances. Therefore, they have no $td\theta$ value and their C_A values are very small, about 0.7. In the elementary material test, the maximum values of temperature are 766.5 °C for M01 and 752.4 °C for M02, which both are under the 810 °C. So they are ranked as Class 1 (non-combustible).

Although M03, M08 and M09 consist of inorganic substances, their back surfaces appeared the cracking situations, even broke entirely. The reason is that their major compositions are brittle clay, which cannot sustain with the thermal stress, therefore, they generate the cracking situations during the first three minutes in the test. Consequently, they do

not pass the CNS 6532 standard.

Constituents of M04 are MgO, MgCl₂, which are inorganic substances, wood and fiber. Although it contained wood, its $td\theta$ value is zero and C_A value is small, about 0.7. It shows that the wood in M04 does not affect its fire protection performance. In the elementary material test, the maximum value of temperature for M04 is 725.6 °C, in other words, its temperature is dropped rather than raised. It is because that MgO in the board absorbed heat during the heating so that its temperature was lower than 750 °C after test. Since the temperature does over the initial temperature 750 °C yet after 20 mins, M04 is ranked as Class 1. For M05, its $td\theta$ value is zero and C_A value is also small. But in the elementary material test, the maximum temperature for M05 reached 810.7 °C. The reason is that M05 contained pulp, which is combustible, so that it led to a temperature rise. According to CNS 6532, M05 is classified as class 2, the semi non-combustible material.

M06 and M07 are plywood and they are added flame retardants of Phosphorus. From Table 4.7, it can be seen that M06 is classified as Class 3, fire-retardant material, whereas M07 is failed. There are two major reasons: one is the thickness of material and the other is the content of flame retardants. M07 was thinner such that its amount of flame retardants was expected to be less. It was burnt-through after test in 6 mins. Note that t_1 values of M06 in five tests varied tremendously as shown in Appendix C1. It is believed that the distribution uniformity of flame retardants would affect t_1 , the time of sustained flaming after completion of the test.

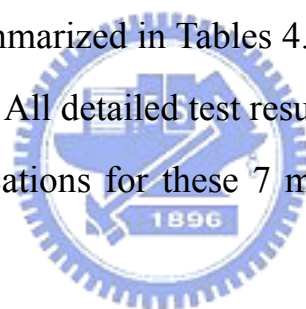
M10 is the glass fiber board and its compositions contained glass fiber and adhesives. In the 10 mins., the $td\theta$ value is zero and value C_A is 36.8. Therefore, its compositions, glass fiber and adhesives, can produce some smoke that affects C_A . Because the C_A is greater than 30, the upper limit value of Class 1, M10 is classified as Class 2.

M11 is the gypsum board and its compositions are inorganic materials and fiber. Note that M11 used in this study has no wallpaper covering. Tested for 10 mins, the back surface of M11 was found showing cracks, whose width was in excess of one tenth of the thickness, 0.7mm, with zero of $td\theta$ and 0.6 of C_A . Therefore, it needs to downgrade. Cracks in the back surface of M11 tested for 6 mins was smaller than the previous one for 10 mins, therefore, it was classified as Class 3.

M12, M13, M14, and M15 were flooring materials without containing flame retardants, so the combustible situations were very apparent. As a consequence, they could not possess any classification. In addition, different from M12~ M15, the glue was used in M12*~ M15*. From Table 4.7, it can be seen that the values of $td\theta$ except for M14, the values of C_A except for M15 and the values of t_1 of M12*~ M15* are higher than those of M12~ M15. Since the glue was the organic material, it could support combustion. As to the reasons for $td\theta$ of M14 and C_A of M15, which show no such features, it could be attributed to the uniform quality of materials and content of glue. M12*~ M15* can not pass the classification, either.

4.3 The test results of SBI

The classification parameters of the SBI test include the fire growth rate index (FIGRA), the lateral flame spread (LFS) and the total heat release (THR_{600s}). Additional classifications are defined for smoke production in terms of smoke growth rate index (SMOGRA) and total smoke production (TSP_{600s}), and for flaming droplets and particles according to their occurrence and burning time during the first 600s of the test. The first 600s is the exposure period ($300s \leq t \leq 900s$). The classification of European Union for SBI test is shown as Table 4.9. Those definitions of test results have been described in Chapter Two. The test results of SBI are summarized in Tables 4.11 and they are the average value of three test results. All detailed test results are given in Appendixes D1 and D2. The classifications for these 7 materials are summarized in Table 4.12.



4.3.1 THR_{600s} and FIGRA

The values of THR_{600s} for 7 materials (M01~M07) are 0.33MJ, 0.23MJ, 0.13MJ, 0.13MJ, 2.40MJ, 3.83MJ and 5.17MJ, respectively, which are lower than 7.5MJ required by class A2/B. The FIGRA's of 7 materials (M01~M07) are lower 120W/s for class A2/B except the one of M07. The FIGRA values of M07 are 127.7MJ, 130.3MJ and 173.4MJ. The classification of M07 is taken as class C. It shows that M01, M02 and M04 are comprised of inorganic substances so their values of THR_{600s} are low and not enough to calculate the FIGRA. M03 is the ceramic board, also consisting of inorganic substances, but its mean value of FIGRA is 1

W/s. From Appendix D1, it only has one test result reaching calculation of FIGRA among the three tests. The reason is that if the materials tested in SBI have cracked generated, then the main burner can heat the backing board, calcium silicate panel. In addition, FIGRA of M05 is 26.7 W/s, implying that its pulp and adhesives were combustible. Because of adding the flame retardants of Phosphorus, THR_{600s} value of M07 is lower than the limits of Class A2/B, but its FIGRA value higher than the limit of Class A2/B. The reasons are still attributed to the thickness and content of flame retardants.

4.3.2 TSP_{600s} and SMOGRA

The corresponding results of TSP_{600s} and SMOGRA are shown in Tables 4.11, respectively. The SMOGRA values of M06 and M07 are lower than $30m^2/s^2$ of Class s1. The mean TSP_{600s} value of M07 tested in three samples is $73.5m^2$ and it is higher than $50m^2$ of Class s1. Therefore M07 is ranked as Class s2. It indicates that organic material can produce more smoke.

4.4 Comparison between cone calorimeter, the surface and SBI tests

4.4.1 Comparison between cone calorimeter, the surface and SBI tests for classification

The classifications of three kinds of test results are summarized in Table 4.13. M01, M02 and M04 are classified as the highest level of three kinds of tests. Their Combustibility is quite low. The classifications of M03, M08 and M09, which are ceramic boards, tested in Cone Calorimeter in horizontal and vertical orientations are the same level,

Class 1. M03 also possesses the highest level in the SBI test. However, M03, M08 and M09 do not pass the classification of the surface test because of the appearance of cracks in the back of specimens.

At first, the cracks situations in three test methods are now discussed. The Japanese standard for Cone Calorimeter test mentions that no cracks or holes on test specimen at end of the heating are allowed for the qualification. The CNS 6532 also requires that to the no cracks in excess of one tenth of the thickness in the back surface can be allowed. The test software of SBI will ask if the specimen condition shows the crack or breakage after completion of the test. However, in the EU classification, it only notes the flaming droplets/particles and has no any regulation concerning on crack. From the viewpoint of fire protection, cracks of building material should be concerned and regulated. Therefore EU classification may consider the suggestion for inclusion of such issue. In addition, the dimensions of specimen also can affect the cracks. The dimension of specimen for Cone Calorimeter is 10 cm x 10 cm, for the surface test 220 mm x 220 mm, for SBI 1 m x 1.5 m and 0.5 m x 1.5 m. The specimen of Cone Calorimeter is so small that it is not easy let the cracks generate. As expected, because of cracks, M11 is classified as Class 3 in the surface test, whereas it is classified as Class 1 in Cone Calorimeter test.

M05 tested in Cone Calorimeter in horizontal and vertical orientations are ranked as the same level, Class 1, and it is also classified as the highest one in SBI test. However, in the surface test, its classification is Class 2 because of its failure in the elementary material

test. As mentioned previously, CNS 6532 adds the elementary material test for ensuring the highest level.

In Table 4.10, there are 7 classes so that M05 in EU class may be tested by other test methods. M06 and M07 tested in Cone Calorimeter in horizontal and vertical orientations have been discussed before (Sec. 4.1.2). M06 can pass the third (lowest) class in Cone Calorimeter (horizontal orientation) and the surface test, but in SBI test it is classified as A2/B. Therefore, for plywood with the flame retardants, the Cone Calorimeter and the surface tests are more stringent. For M07 with the flame retardants, its thickness was thinner that it responds to the lower classes in three test methods.

M10 is classified as Class 1 in Cone Calorimeter test but Class 2 in the surface test. It is because CNS 6532 has smoke classification (see Table 4.6), but Japanese classification by using Cone Calorimeter does not have such evaluation. Besides, in Tables 4.9 and 4.10, EU classification has additional classification for smoke production (s1, s2 and s3), but it does not really use as the classification criteria for construction products. The benchmarks of smoke hazard for safety levels may not be found [16]. M12, M13, M14 and M15 do not pass the classification in the Cone Calorimeter and surface tests.

4.4.2 Comparison between Cone Calorimeter and SBI tests using regression line

Tsantaridis and Ostman [15] carried out the cone calorimeter tests in

horizontal orientation under a heat flux of 50kW/m^2 . The index of FIGRA for the Cone Calorimeter was calculated as the peak value of heat release by the time from the beginning of test to the one at which this peak occurred. Here this work adopts the same way to calculate FIGRA and it also applies to the data tested in vertical orientation. These resultant FIGRA values both orientations are shown as Table 4.14 and Table 4.15, respectively.

The values of FIGRA from two test methods, Cone Calorimeter in vertical direction and SBI, are compared in Fig. 4.2. The correlation is relatively good and the value of R^2 is 0.77. The one for M06 (14.5mm plywood) seems to deviate from the correlation apparently. In the same way, the results of comparison between Cone Calorimeter in horizontal direction and SBI are shown in Fig. 4.3. The correlations are relatively good and the value of R^2 is 0.98. Comparing with the Cone results in the vertical direction, it can be found that the correlation between SBI results and cone calorimeter ones in horizontal direction are higher than that of the cone data in vertical direction. The reason inherently has been discussed in Sec. 4.1.2. The Cone Calorimeter test in horizontal direction shows the true reaction-to-fire behaviors because of orientation effect. The main burner using propane gas in the SBI test provides a heat output of 30 kW directly on the specimen. In other words, the effective amount of heating flux received by the specimen determines the effectiveness of the correlation.

4.4.3 Comparison between the surface and SBI tests using regression line

For combustibility, the comparisons between $td\theta$ value of surface test and THR_{600s} of SBI test are shown in Fig. 4.4. Because the $td\theta$ value in surface test is somewhat similar to the total heat release, it is chosen to compare here. The correlation is relatively good and the value of R^2 is 0.75. The one for M05 (rock wool board) seems to deviate from the correlation apparently. The reason for the deviation of M05 is attributed to the determination of standard curve in surface test, which is obtained by adding 50°C to the calibration curve. The measured exhaust temperatures per min of M05 do not exceed the standard curve after completion of the test so $td\theta$ value is zero. But it still can exhibit the reaction-to-fire feature since it is fail to meet the upper temperature limit in the elementary material test. In other words, its heat release rate is not null and has a THR value of about 2.4 MJ. Therefore it causes M05 deviating from the correlation between the surface and SBI tests.

For smoke generation, the C_A of surface test is usually the measured value at the end of test (maximum value). The 60s mean value of SPR in SBI test, which is chosen to be the maximum value, is compared with C_A . The results of comparison are shown in Fig. 4.5. The correlation is relatively well and the value of R^2 is 0.92.

4.4.4 Comparison between the Cone Calorimeter and the surface tests using regression line

Due to inconsistency of heating time, the 180s mean value of heat release rates of Cone Calorimeter for both orientations are chosen to compare with $td\theta$ value of surface test. The comparison between Cone Calorimeter test in vertical orientation and the surface test is shown in Fig. 4.6. The value of R^2 is 0.67. The one between Cone Calorimeter test in horizontal orientation and the surface test are shown in Fig. 4.7. The value of R^2 is 0.58. The behaviors of M12 (padauk of South America) in Figs.4.6 and 4.7 appear to deviate from the correlation apparently. It is because the density of M12 is about 1000 kg/m^3 , much higher than those of the other flooring materials. It is not easily to be ignited in the surface test due to the relatively high thermal inertia, therefore the $td\theta$ value of M12 is relatively low and in Figs.4.6 and 4.7. If the tested data of M12 are removed from the correlation in Fig.4.6, then R^2 can be improved from 0.67 to 0.95; see Fig.4.8. Also, if the data of M12 are removed from the correlation in Fig.4.7, then R^2 can be improved from 0.58 to 0.96; see Fig.4.9. Now, the correlation between the Cone Calorimeter and surface tests for combustibility becomes relatively well.

The t_c value in the surface test somewhat can be regarded as the time, at which the surface of specimen is ignited. The ignition times of Cone Calorimeter for both orientations are chosen to compare with t_c value of surface test that the comparison is given in Fig. 4.10. The value of R^2 is 0.4. The deviation is resulted from that the ignition time of M06 tested in Cone Calorimeter for vertical orientation is zero but its t_c value is 224.2

sec. If the tested data of M06 are removed from the correlation in Fig. 4.10, then R^2 can be improved from 0.4 to 0.89; see Fig. 4.11. The one between Cone Calorimeter test in horizontal orientation and the surface test is shown in Fig. 4.12, where the value of R^2 is 0.63. Similarly, if the tested data of M06 are removed from the correlation in Fig. 4.12, then R^2 can be improved from 0.63 to 0.67; see Fig. 4.13. It can be found that the correlation for ignition time between surface test and cone calorimeter ones in vertical horizontal direction is better than that of the cone data in horizontal direction. In addition, as indicated Figs. 4.10 and 4.12, the ignition times of Cone Calorimeter for both orientations are lower than t_c value of surface test.

In order to further investigate the features of ignition time mentioned above, the heat sources for both apparatuses are presented as follows. In the surface test, the T-shaped propane burner, with a flow rate of 0.35 l/min of propane, is used for the first 3 mins, and its average value of heat flux is 0.49 kW/m² [14]. The incident heat flux of Cone Calorimeter is set at 50kW/m² and the spark plug is used to ignite specimen. Since the exhaust system of Cone Calorimeter is provided by a forced flow of 0.024m³/s, the flammable gas is discharged easily by exhaust system. It still has a higher heat flux to heat the specimen. However, the furnace room of surface test is much smaller than the one in Cone Calorimeter. In the surface test, the air supply and exhaust gas adopt the way of natural convection so that the preheat effect in the furnace is relative intensive. However, the average value of heat flux for the first 3 mins is still much lower than Cone Calorimeter. Therefore, the ignition times of Cone

Calorimeter for both orientations are shorter than t_c value of surface test. In addition, the correlation for ignition time between surface test and cone calorimeter in vertical horizontal direction are better than that of the cone data in horizontal direction. The reason can be attributed to orientation effect; see Sec. 4.1.2. Because the ignition time of cone calorimeter test in vertical orientation are longer than that in horizontal orientation, the correlation for ignition time between cone calorimeter test in vertical direction and surface test is expected to be better.



Chapter Five

CONCLUSIONS

In this thesis work, 15 building materials were chosen and tested in the Cone Calorimeter and surface tests. Among them, 7 materials (M01~M07) are selected and tested in SBI test additionally. There are two goals in this study. One is to discuss the reaction-to-fire performance for each material in the three different test methods, and the other is to evaluate the potential use of the Cone Calorimeter and SBI as the test standards to replace the traditional CNS 6532, which is sole used by Taiwan building Code in the world. The following conclusions are drawn.

- 1) The FR (flame retardants) materials have some arguments about their values of content, which can affect the ignition time and heat release. Therefore, the specimen, similar to M06, tested in Cone Calorimeter shall not remove the sparker during the test.
- 2) For the flammable material in cone calorimeter test, the heat release rate and ignition time can be affected by the sample orientation. The measured average values of HRR_{av_180s} and THR in the horizontal orientation are higher than those in vertical one. The ignition time in horizontal orientation is found shorter than that in vertical one. It shows that the classification using Cone Calorimeter test in horizontal orientation is stringent.
- 3) Using the mean heat release rate within 180 seconds, HRR_{av_180s} , to compare the cone calorimeter test results in vertical and horizontal

directions, the correlation is relatively good and the value of R^2 is about 0.95.

- 4) The cracks situations in three test methods are discussed. However, in EU classification, it only notes the flaming droplets/particles and has no any regulation for the appearance of cracks. Therefore EU classification is suggested to add this to improve this shortcoming.
- 5) According to CNS 6532, the classification of Rock wool board is ranked as Class 2 because of its failure in the elementary material test. However, such material in EU class may need the other test methods for classify it to a higher rank.
- 6) The FR materials (M06) can pass the third (lowest) class in Cone Calorimeter (horizontal orientation) and the surface test, but it is classified as A2/B in SBI test. Therefore, for plywood which added the flame retardants, the Cone Calorimeter and the surface tests are more stringent than SBI.
- 7) CNS 6532 has the smoke classification but Japanese classification using Cone Calorimeter does not have such evaluation. EU standard has the additional classification for smoke production (s1, s2 and s3), but it does not really use as the classification criteria for construction products. The benchmarks of smoke hazard for safety levels might not be found at the present time.
- 8) For flooring materials without the addition of flame retardants, they can be qualified for any classification in Cone Calorimeter and the surface tests.

- 9) The correlation between the values from FIGRA of cone calorimeter in vertical direction and the SBI shows that the value of R^2 is about 0.77. The value of R^2 for the corresponding correlation between cone in horizontal direction and SBI is about 0.98. Apparently, the correlation between SBI and cone calorimeter test in horizontal direction is better.
- 10) The correlation between $td\theta$ value of surface test and THR_{600s} of SBI test finds that the value of R^2 is 0.75. Correlation between C_A value of surface test and maximum 60s mean value of SPR of SBI test gives the value of R^2 is 0.92.
- 11) From comparison between 180s mean value of heat release rate of Cone Calorimeter test in vertical orientation and $td\theta$ value of the surface test, the value of R^2 is 0.67. The correlated R^2 value between Cone Calorimeter test in horizontal orientation and the surface test is 0.58. If the tested data of M12 are removed from the correlation in Fig.4.6, then R^2 can be improved from 0.67 to 0.95; see Fig.4.8. Also, if the data of M12 are removed from the correlation in Fig.4.7, then R^2 can be improved from 0.58 to 0.96; see Fig.4.9. Now, the correlation between the Cone Calorimeter and surface tests for combustibility becomes relatively well.
- 12) The ignition times of Cone Calorimeter for both orientations are shorter than t_c value of surface test. The correlation for ignition time between cone calorimeter test in vertical direction and surface test is expected to be better.

Reference

- [1] ISO 5660-1. “Rate of Heat Release from Building Products (Cone Calorimeters),” International Organization for Standardization, 2002.
- [2] Thornton W. “The Relation of Oxygen to the Heat of Combustion of Organic Compounds”, Philosophical Magazine and J. of Science, Vol. 33, No. 196, 1917.
- [3] Hugget C. “Estimation of Heat Release by Means of Oxygen Consumption Measurement”, Fire and Materials Vol. 4, No. 2, 1980.
- [4] ASTM E1354. “Standard Test Method for Heat and Visible Smoke Release Rates for Materials and Products Using an Oxygen Consumption Calorimeter,” ASTM Fire Test Standards, 2004.
- [5] JIS A 1321. “Testing method for incombustibility of internal finish material and procedure of buildings,” Japanese Industrial Standards, 1994.
- [6] CNS 6532. “Method of Test for Incombustibility of Internal Finish Material of Building,” Chinese National Standard, 2003.
- [7] SBI (Single Burning Item), EN 13823. “Reaction to fire tests for building products - Building products excluding floorings exposed to the thermal attack by a single burning item” European Committee for Standardization, 2002.
- [8] ISO 9705. “Room Fire Test in Full Scale for Surface Products”, International Organization for Standardization, 1993.
- [9] prEN 45545-2. “Fire protection on railway vehicles-Part2, requirements for fire behavior of materials and components”, 2004.
- [10] ISO 5659-2. “Plastics-Smoke generation-Part 2, determination of optical density by a single-chamber test” International Organization for Standardization, 1994.
- [11] CNS 14705. “Method of test for heat release rate for building materials-cone calorimeter method,” Chinese National Standard, 2003.

- [12] Parker W. "An investigation of the Fire Environment in the ASTM E-84 Tunnel Test," NBS Technical Note 945, 1977.
- [13] Sensenig D. "An Oxygen Consumption Technique for Determining the Construction of Interior Wall Finishes to Room Fires," NBS Technical Note 1182, 1980.
- [14] Chen, C. H., Jang, L. S., Lei, M. Y., Chou, S. "A comparative study of combustibility and surface flammability of building materials," Fire and Materials, Vol.21, 1997.
- [15] Tsantaridis L., Ostman B., "Cone Calorimeter Data and Comparisons for the SBI RR Products," NTIS Report 9812090, 1999.
- [16] William Heskestad A, Jostein Hovde P. "Empirical Prediction of Smoke Production in the ISO Room Corner Fire Test by Use of ISO Cone Calorimeter Fire Test Data," Fire and Materials, Vol.23, 1999.
- [17] Messerschmidt B., Van Hees P., "Influence of delay times and response times on heat release measurements," Fire and Materials, Vol.24, 2000.
- [18] Hakkarainen T., Kokkala M. A., "Application of a One-dimensional Thermal Flame Spread Model on Predicting the Rate of Heat Release in the SBI test," Fire and Materials, Vol.25, 2001.
- [19] Van Hees P., Hertzberg T, Steen Hansen A. "Development of a Screening Method for the SBI and Room Corner using the Cone Calorimeter," SP REPORT, 2002:11.
- [20] Axelsson J., Van Hees P. "New data for sandwich panels on the correlation between the SBI test method and the room corner reference scenario," Fire and Materials, Vol.29, 2005.
- [21] Fox R. W. and McDonald A. T., John Wiley and Sons, "Introduction to Fluid Mechanics" Canada, 1994
- [22] Kline S. J., and McClintock F., "Describing Uncertainties in Single-Sample Experiments," Mechanical Engineering, vol.104, pp250-260,1982.
- [23] Moffat R. J., "Contributions to the Theory of Single-Sample Uncertainty Analysis," *Journal of Fluid Engineering*, vol. 104, pp. 250-260, 1982

- [24] Figliola R. S., and Beasley D. E., "Theory and Design for Mechanical Measurements," 2nd Ed., John Wiley and Sons, Canada, 1995.
- [25] Holman J. P., "Experimental Methods for Engineers", 5th Ed., McGraw-Hill, New York, 1989
- [26] Parker, W. J. "Calculation of the Heat Release Rate by Oxygen Consumption for Various Applications," NBSIR 81-2427, National Bureau of Standards, Gaithersburg, Md., 1982.
- [27] Janssens, M. L. "Measuring Heat Release Rate by Oxygen Consumption," Fire Technology, Vol.27, 1991.
- [28] Babrauskas, V. "Development of the Cone Calorimeter-A Bench-scale Heat Release Rate Apparatus based on Oxygen Consumption," NBSIR 82-2611, National Institute of Standards and Technology, Gaithersburg, MD, 1982.
- [29] Enright P. A. and Fleischmann C. M. "Uncertainty of Heat Release Rate Calculation of the ISO 5660-1 Cone Calorimeter Standard Test Method" Fire Technology, Vol. 35, NO.2, 1999.
- [30] Axelsson J., Andersson P., Lonnermark A., Hees P. V., Wetterlund I., "Uncertainties in measuring heat and smoke release rates in the Room/Corner Test and the SBI," SP REPORT, 2001:04.

Table 2.1: Heats of combustion and heats of combustion per gram of oxygen consumed for typical organic liquids and gases

Fuel	Formula	Heats of combustion kJ g ⁻¹	Heats of combustion kJ g ⁻¹ O ₂
Methane (g)	CH ₄	-50.01	-12.54
Ethane (g)	C ₂ H ₆	-47.48	-12.75
n-Butane (g)	C ₄ H ₁₀	-45.72	-12.78
n-Octane (g)	C ₈ H ₁₈	-44.42	-12.69
1-Butanol (l)	C ₄ H ₁₀ O	-33.13	-12.79

Table 2.2: Heats of combustion and heats of combustion per gram of oxygen consumed for typical synthetic polymers

Fuel	Formula	Heats of combustion kJ g ⁻¹	Heats of combustion kJ g ⁻¹ O ₂
Polyethylene	(-C ₂ H ₄ -) _n	-43.28	-12.65
Polypropylene	(-C ₃ H ₆ -) _n	-43.31	-12.66
Polyisobutylene	(-C ₄ H ₈ -) _n	-43.71	-12.77
Polycarbonate	(-C ₁₆ H ₁₄ O ₄ -) _n	-29.72	-13.12
Nylon	(-C ₆ H ₁₁ O ₄ -) _n	-29.58	-12.67

Table 2.3: Heats of combustion and heats of combustion per gram of oxygen consumed for selected natural fuel

Fuel	Heats of combustion kJ g ⁻¹	Heats of combustion kJ g ⁻¹ O ₂
Cellulose	-16.09	-13.59
Cotton	-15.56	-13.61
Newsprint	-18.4	-13.4
Lignite	-24.78	-13.12
Leaves, hardwood	-17.76	-12.51

Table 3.1: The used parameters of uncertainty for cone calorimeter [29]

Assumption	$\frac{\Delta h_c}{r_o} = 13,100 \text{ (kJ/kg)}$ $\beta = 1.5$	$\delta \frac{\Delta h_c}{r_o} = 655 \text{ (kJ/kg)}$ $\delta \beta = 0.5$
Calculation	$C = 0.0404$	$\delta C = 0.0404$
Measurement	$T_e = \text{variable (K)}$	$\delta T_e = 2.2 \text{ (K)}$
	$\Delta p = \text{variable (Pa)}$	$\delta \Delta p = 0.8 \text{ (Pa)}$
	$\chi_{O_2} = \text{variable by volume}$	$\delta \chi_{O_2} = 0.0001 \text{ by volume}$

Table 3.2: The exhaust temperature of standard for CNS 6532 [6]

Time (min)	1	2	3	4	5	6	7	8	9	10
T _{exhaust} (°C)	70	80	90	155	205	235	260	275	290	305

Table 3.3: Uncertainties in volume flow measurement in the SBI test [30]

Quantity x_i	Relative error (%)	Relative standard uncertainty $u(x_i)/x_i$ (%)	Relative sensitivity coefficient, $c_{r,i}$	Contribution to combined relative uncertainty of flow measurement $c_{r,i} \cdot u(x_i) / x_i = u_f(y)$ (%)
A (Area)	negligible		1	
Factor “22.4”	0.3	0.3	1	0.3
k_t		1.0	1	1.0
Δp	1.7	0.96	0.5	0.48
T_s	0.5	0.29	0.5	0.15
k_p	2.0	1.2	1	1.2
Combined expanded relative standard uncertainty				3.3 %

Table 3.4: HRR uncertainty of SBI at the 35 kW level [30]

Quantity x_i	Relative error (%)	Relative standard uncertainty $u(x_i)/x_i$ (%)	Relative sensitivity coefficient, $c_{r,i}$	Contribution to combined relative uncertainty of HRR measurement $c_{r,i} \cdot u(x_i) / x_i = u_i(y)$ (%)
Mass flow in duct		1.7	1	1.7
O ₂		0.078	-81	6.3
CO ₂	2	0.82	-0.18	0.15
E-factor	5	2.0	1	2.0
α	10	5.8	-0.017	0.1
Humidity	150	61.2	-0.0038	0.2
Molecular weight of gas species	1	0.58	1	0.6
Ambient pressure				negligible (included in O ₂ error)
Combined expanded relative standard uncertainty				13.5 %



Table 3.5: HRR uncertainty of SBI at the 50 kW level [30]

Quantity x_i	Relative error (%)	Relative standard uncertainty $u(x_i)/x_i$ (%)	Relative sensitivity coefficient, $c_{r,i}$	Contribution to combined relative uncertainty of HRR measurement $c_{r,i} \cdot u(x_i) / x_i = u_i(y)$ (%)
Mass flow in duct		1.7	1	1.7
O ₂		0.08	-53	4.2
CO ₂	2	0.82	-0.18	0.15
E-factor	5	2.0	1	2.0
α	10	5.8	-0.025	0.1
Humidity	150	61.2	-0.0038	0.2
Molecular weight of gas species	1	0.58	1	0.6
Ambient pressure				negligible (included in O ₂ error)
Combined expanded relative standard uncertainty				10.0 %

Table 3.6: Summary of uncertainty for different levels of SPR [30]

SPR level (m ² /s)	Combined expanded relative standard uncertainty (%)
0.1	103
0.3	35.0
0.5	21.5
1.0	11.6
5.0	6.2
10.0	4.9

Table 4.1: List of New and Innovative building materials

Code	Material name	Density(kg/m ³)	Thickness(mm)
M01	Fiber cement board	1200	12
M02	Calcium silicate panel	950	18
M03	Ceramic board coating Nano-TiO ₂	2000	4.2
M04	MgO board	1100	9
M05	Rock wool board	400	12
M06	14.5mm plywood	690	14.5
M07	3.6mm plywood	670	3.6
M08	Ceramic board coating far infrared rays	2000	4.2
M09	Ceramic board coating anion	2000	4.2
M10	Glass fiber board	400	25
M11	Gypsum board	970	7
M12	Padauk of South America	1000	18
M13	South America padauk of Island	470	12
M14	Teak of Myanmar	650	18
M15	Myanmar Teak of Island	540	12

Table 4.2: Major compositions of materials

Code	Material name	Compositions
M01	Fiber cement board	Cement, Silicon sand, Celluloid fiber, Strengthened fiber
M02	Calcium silicate panel	Lime, Silicate, Celluloid fiber
M03	Ceramic board coating Nano-TiO ₂	Clay, Nano-TiO ₂
M04	MgO board	MgO, MgCl ₂ , Wood, Fiber
M05	Rock wool board	Rock wool, Farina, Pulp, Adhesives
M06	14.5mm plywood	Lauan, Flame retardants of Phosphorus
M07	3.6mm plywood	Lauan, Flame retardants of Phosphorus
M08	Ceramic board coating far infrared rays	Clay, Far infrared rays of Nano
M09	Ceramic board coating anion	Clay, Nano-anion
M10	Glass fiber board	Glass fiber, Adhesives
M11	Gypsum board	Gypsum, Strengthened fiber
M12	Padauk of South America	Padauk
M13	South America padauk of Island	Padauk, Pine, Poplar, Lauan
M14	Teak of Myanmar	Teak
M15	Myanmar Teak of Island	Teak, Pine, Poplar, Lauan

Table 4.3: The classification of Japanese cone calorimeter test

Class	Heat flux	Heating time in the test	Maximum of HRR	Total HRR
1	50kW/m ²	20 min	≤ 200 kW/m ²	≤ 8 MJ/m ²
2	50kW/m ²	10 min	≤ 200 kW/m ²	≤ 8 MJ/m ²
3	50kW/m ²	5 min	≤ 200 kW/m ²	≤ 8 MJ/m ²

Annotation: There must not be any cracks or holes on test specimen at end of the heating.



Table 4.4: Results of cone calorimeter tested in vertical orientation
(average value)

Code	Class	Test time (s)	Ignition time(s)	Peak of HRR (kW/m ²)	HRR _{av_180s} (kW/m ²)	THR (MJ/m ²)
M01	1	1200	N.I.	5.86	1.13	3.06
M02	1	1200	N.I.	5.94	2.13	2.32
M03	1	1200	N.I.	0.69	0	0
M04	1	1200	N.I.	3.63	0.26	1
M05	1	1200	N.I.	10.5	6.86	4.28
M06	2	600	N.I.	14.49	3.91	5.12
M07	F	300	75.8	161.66	47.47	10.96
M08	1	1200	N.I.	0.59	0	0
M09	1	1200	N.I.	1.57	0	0.03
M10	1	1200	N.I.	8.51	5.94	1.76
M11	1	1200	N.I.	7.75	0.34	0.22
M12	F	300	93.65	198.25	135.26	29.92
M13	F	300	49.23	290.34	82.28	20.98
M14	F	300	60.55	228.45	97.4	24.54
M15	F	300	41.03	301.50	81.27	22.88

F: failure

N.I.: no sustained flaming

Table 4.5: Results of cone calorimeter tested in horizontal orientation
(average value)

Code	Class	Test time (s)	Ignition time(s)	Peak of HRR (kW/m ²)	HRR _{av_180s} (kW/m ²)	THR (MJ/m ²)
M01	1	1200	N.I.	3.73	1.81	1.42
M02	1	1200	N.I.	3.56	1.68	0.52
M03	1	1200	N.I.	0.38	0	0
M04	1	1200	N.I.	4.47	0.34	0.65
M05	1	1200	N.I.	13.79	9.34	3.44
M06	3	300	26	82.88	18.72	6.11
M07	F	300	27.23	293.57	88.03	24.7
M08	1	1200	N.I.	2.43	0	0.00
M09	1	1200	N.I.	1.78	0	0.00
M10	1	1200	N.I.	5.64	2.54	0.73
M11	1	1200	N.I.	1.07	0	0
M12	F	300	30.81	292.48	183.22	47.65
M13	F	300	35.26	369.47	83.93	22.99
M14	F	300	31.47	220.71	97.93	25.91
M15	F	300	18.26	401.26	94.02	24.74

F: failure

NI: no sustained flaming

Table 4.6: Classification according to CNS 6532

Test	Classification		
	1	2	3
Elementary material test	$T_{\max} < 810^{\circ}\text{C}$ [20min]	No test	No test
Surface test	$td\theta = 0^{\circ}\text{C}\cdot\text{min}$ $C_A < 30$ And (a),(b),(c),(d1) [10min]	$td\theta = 100^{\circ}\text{C}\cdot\text{min}$ $C_A < 60$ And (a),(b),(c),(d2) [10min]	$td\theta = 350^{\circ}\text{C}\cdot\text{min}$ $C_A < 120$ And (a),(b),(c),(d2) [6min]

Class 1: non-combustible material

Class 2: semi non-combustible material

Class 3: fire-retardant material

T_{\max} : maximum of temperature

(a): No penetration due to melting over the entire thickness

(b): No cracks in the back surface in excess of one tenth of the thickness

(c): No sustained flaming for more than 30 seconds after completion of the test

(d1): The curve of the exhaust gas temperature shall not exceed the standard temperature curve during the test

(d2): The curve of the exhaust gas temperature shall not exceed the standard temperature curve during the first three minutes of test

Table 4.7: Results of surface test (average value)

Code	Class	Test time (min)	t_c (s)	$td\theta$ ($^{\circ}\text{C}\cdot\text{min}$)	C_A	t_1 (s)	C_k
M01	1	10	N.I.	0	0.7	--	+
M02	1	10	N.I.	0	0.7	--	+
M03	F	6	N.I.	0	0.6	--	-
M04	1	10	N.I.	0	0.7	--	+
M05	2	10	N.I.	0	1.8	--	+
M06	3	6	224.2	110.8	8.5	26.4	+
M07	F	6	91	313.5	24.5	10	-
M08	F	6	N.I.	0	0.5	--	-
M09	F	6	N.I.	0	0.7	--	-
M10	2	10	N.I.	0	36.8	--	+
M11	3	6	N.I.	0	0.6	--	+
M12	F	6	224	190.3	110.3	340	+
M13	F	6	59.7	457.4	100.3	218.7	+
M14	F	6	90	421.3	160	223.3	+
M15	F	6	80.3	371.9	120.7	450	+
M12*	F	6	196	192	187.1	400	+
M13*	F	6	86	517.4	137.9	283.7	+
M14*	F	6	98	419.8	201.5	299.3	+
M15*	F	6	57.3	595.2	120.5	480.3	+

F: failure

N.I.: no intersect

--: no occur

t_1 : time of sustained flaming after completion of the test

C_k : cracking of the back surface (+ =pass, - =fail)

Table 4.8: Results of elementary material test (average value)

Code	T _{max} (°C)	T _{initial} (°C)	ΔT (°C)	Mass loss (g)	Class
M01	766.5	748.7	17.9	15	Pass
M02	752.4	747.7	4.8	12.9	Pass
M04	725.6	749.3	-23.8	32.5	Pass
M05	810.7	748	62.7	4.9	Fail

T_{max}: Maximum of temperature

T_{initial}: Initial temperature

ΔT: Temperature difference

Table 4.9: Summary of classification criteria for SBI test

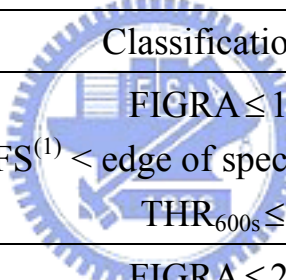
Class	Classification criteria
A2/B	 FIGRA ≤ 120Ws ⁻¹ LFS ⁽¹⁾ < edge of specimen (large wing) THR _{600s} ≤ 7.5MJ
C	FIGRA ≤ 250Ws ⁻¹ LFS < edge of specimen (large wing) THR _{600s} ≤ 15MJ
D	FIGRA ≤ 750Ws ⁻¹
Additional classification for smoke production: s1 = SMOGRA ≤ 30m ² s ⁻² and TSP _{600s} ≤ 50m ² ; s2 = SMOGRA ≤ 180m ² s ⁻² and TSP _{600s} ≤ 200m ² ; s3 = not s1 and s2. Additional classification for flaming droplets/particles: d0 = no flaming droplets/particles within 600 s; d1 = no flaming droplets/particles persisting longer than 10 s within 600s; d2 = not d0 or d1. (1) Lateral flame spread	

Table 4.10: EU classes for construction products excluding flooring

Class	Test method(s)	Classification criteria	Additional classification
A1	EN ISO 1182 (1); And	$\Delta T \leq 30^{\circ}\text{C}$; and $\Delta m \leq 50\%$; and $t_f = 0$ (i.e. no sustained flaming)	-
	EN ISO 1716	$\text{PCS} \leq 2.0 \text{ MJ.kg}^{-1}$ (1); and $\text{PCS} \leq 2.0 \text{ MJ.kg}^{-1}$ (2) (2a); and $\text{PCS} \leq 1.4 \text{ MJ.m}^{-2}$ (3); and $\text{PCS} \leq 2.0 \text{ MJ.kg}^{-1}$ (4)	-
A2	EN ISO 1182 (1); Or	$\Delta T \leq 50^{\circ}\text{C}$; and $\Delta m \leq 50\%$; and $t_f \leq 20\text{s}$	-
	EN ISO 1716; and	$\text{PCS} \leq 3.0 \text{ MJ.kg}^{-1}$ (1); and $\text{PCS} \leq 4.0 \text{ MJ.m}^{-2}$ (2); and $\text{PCS} \leq 4.0 \text{ MJ.m}^{-2}$ (3); and $\text{PCS} \leq 3.0 \text{ MJ.kg}^{-1}$ (4)	-
	EN 13823 (SBI)	$\text{FIGRA} \leq 120 \text{ W.s}^{-1}$; and LFS < edge of specimen; and $\text{THR}_{600\text{s}} \leq 7.5 \text{ MJ}$	Smoke production(5); and Flaming droplets/ particles (6)
B	EN 13823 (SBI); And	$\text{FIGRA} \leq 120 \text{ W.s}^{-1}$; and LFS < edge of specimen; and $\text{THR}_{600\text{s}} \leq 7.5 \text{ MJ}$	Smoke production(5); and Flaming droplets/ particles (6)
	EN ISO 11925-2(8); Exposure = 30s	$F_s \leq 150\text{mm}$ within 60s	
C	EN 13823 (SBI); And	$\text{FIGRA} \leq 250 \text{ W.s}^{-1}$; and LFS < edge of specimen; and $\text{THR}_{600\text{s}} \leq 15 \text{ MJ}$	Smoke production(5); and Flaming droplets/ particles (6)
	EN ISO 11925-2(8); Exposure = 30s	$F_s \leq 150\text{mm}$ within 60s	
D	EN 13823 (SBI); And	$\text{FIGRA} \leq 750 \text{ W.s}^{-1}$	Smoke production(5); and Flaming droplets/ particles (6)
	EN ISO 11925-2(8); Exposure = 30s	$F_s \leq 150\text{mm}$ within 60s	
E	EN ISO 11925-2(8); Exposure = 15s	$F_s \leq 150\text{mm}$ within 20s	Flaming droplets/ particles (7)
F	No performance determined		

(*) The treatment of some families of products, e.g. linear products (pipes, ducts, cables etc.), is still under review and may necessitate an amendment to this decision.

(1) For homogeneous products and substantial components of non-homogeneous products.

(2) For any external non-substantial component of non-homogeneous products.

(2a) Alternatively, any external non-substantial component having a $\text{PCS} \leq 2.0 \text{ MJ.m}^{-2}$, provided that the product satisfies the following criteria of EN 13823(SBI) : $\text{FIGRA} \leq 20 \text{ W.s}^{-1}$; and LFS < edge of specimen; and $\text{THR}_{600\text{s}} \leq 4.0 \text{ MJ}$; and s1; and d0.

(3) For any internal non-substantial component of non-homogeneous products.

(4) For the product as a whole.

(5) s1 = $\text{SMOGR}_{600\text{s}} \leq 30\text{m}^2.\text{s}^{-2}$ and $\text{TSP}_{600\text{s}} \leq 50\text{m}^2$; s2 = $\text{SMOGR}_{600\text{s}} \leq 180\text{m}^2.\text{s}^{-2}$ and $\text{TSP}_{600\text{s}} \leq 200\text{m}^2$; s3 = not s1 or s2.

(6) d0 = No flaming droplets/ particles in EN13823 (SBI) within 600s; d1 = No flaming droplets/ particles persisting longer than 10s in EN13823 (SBI) within 600s; d2 = not d0 or d1; Ignition of the paper in EN ISO 11925-2 results in a d2 classification.

(7) Pass = no ignition of the paper (no classification); Fail = ignition of the paper (d2 classification).

(8) Under conditions of surface flame attack and, if appropriate to end-use application of product, edge flame attack.

Table 4.11: The summary results of SBI test (average value)

Code	FIGRA _{0.2MJ} (W/s)	FIGRA _{0.4MJ} (W/s)	THR _{600s} (MJ)	SMOGRA (m ² /s ²)	TSP _{600s} (m ²)	SPR _{av_60s(max)} (m ² /s)
M01	--	--	0.33	--	10.03	0.0400
M02	--	--	0.23	--	13.80	0.0510
M03	1	1	0.13	--	0.70	0.0400
M04	--	--	0.13	--	13.33	0.0970
M05	26.7	22.37	2.40	--	16.37	0.0450
M06	71.23	48.37	3.83	1.47	25.0	0.1680
M07	143.8	143.8	5.17	11.23	73.53	0.2570

Table 4.12: The classification of SBI test

Code	Class	Smoke production	Flaming droplets/particles
M01	A2/B	s1	d0
M02	A2/B	s1	d0
M03	A2/B	s1	d0
M04	A2/B	s1	d0
M05	A2/B	s1	d0
M06	A2/B	s1	d0
M07	C	s2	d1

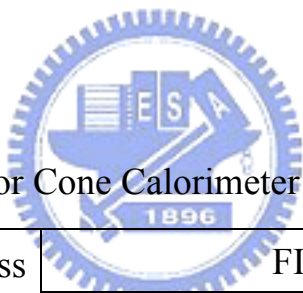
Table 4.13: The classification of Cone Calorimeter, the surface and SBI tests

Code	Material name	Cone Calorimeter (V)	Cone Calorimeter (H)	Surface test	SBI
M01	Fiber cement board	1	1	1	A2/B(s1,d0)
M02	Calcium silicate panel	1	1	1	A2/B(s1,d0)
M03	Ceramic board coating Nano-TiO ₂	1	1	F	A2/B(s1,d0)
M04	MgO board	1	1	1	A2/B(s1,d0)
M05	Rock wool board	1	1	2	A2/B(s1,d0)
M06	14.5mm plywood	2	3	3	A2/B(s1,d0)
M07	3.6mm plywood	F	F	F	C(s2,d1)
M08	Ceramic board coating far infrared rays	1	1	F	
M09	Ceramic board coating anion	1	1	F	
M10	Glass fiber board	1	1	2	
M11	Gypsum board	1	1	3	
M12	Paduk of South America	F	F	F	
M13	South America paduk of Island	F	F	F	
M14	Teak of Myanmar	F	F	F	
M15	Myanmar Teak of Island	F	F	F	

Table 4.14: FIGRA for Cone Calorimeter in vertical direction

Code	Thickness (mm)	FIGRA(W/s)			
		1	2	3	Avg.
M01	12	0.109	0.094	0.027	0.077
M02	18	0.172	0.5	0.087	0.253
M03	4.2	0	0.010	0.008	0.006
M04	9	0.064	1.756	0.070	0.63
M05	12	3.031	3.304	0.464	2.266
M06	14.5	0.227	0.243	0.276	0.249
M07	3.6	6.508	23.914	7.016	12.479

Table 4.15: FIGRA for Cone Calorimeter in horizontal direction



Code	Thickness (mm)	FIGRA(W/s)			
		1	2	3	Avg.
M01	12	0.212	0.267	0.131	0.203
M02	18	0.537	0.465	0.204	0.402
M03	4.2	0.431	0.081	0.271	0.261
M04	9	0.061	0.104	0.124	0.096
M05	12	5.483	0.693	9.935	5.371
M06	14.5	11.106	36.62	25.494	24.41
M07	3.6	75.726	63.953	63.222	67.63

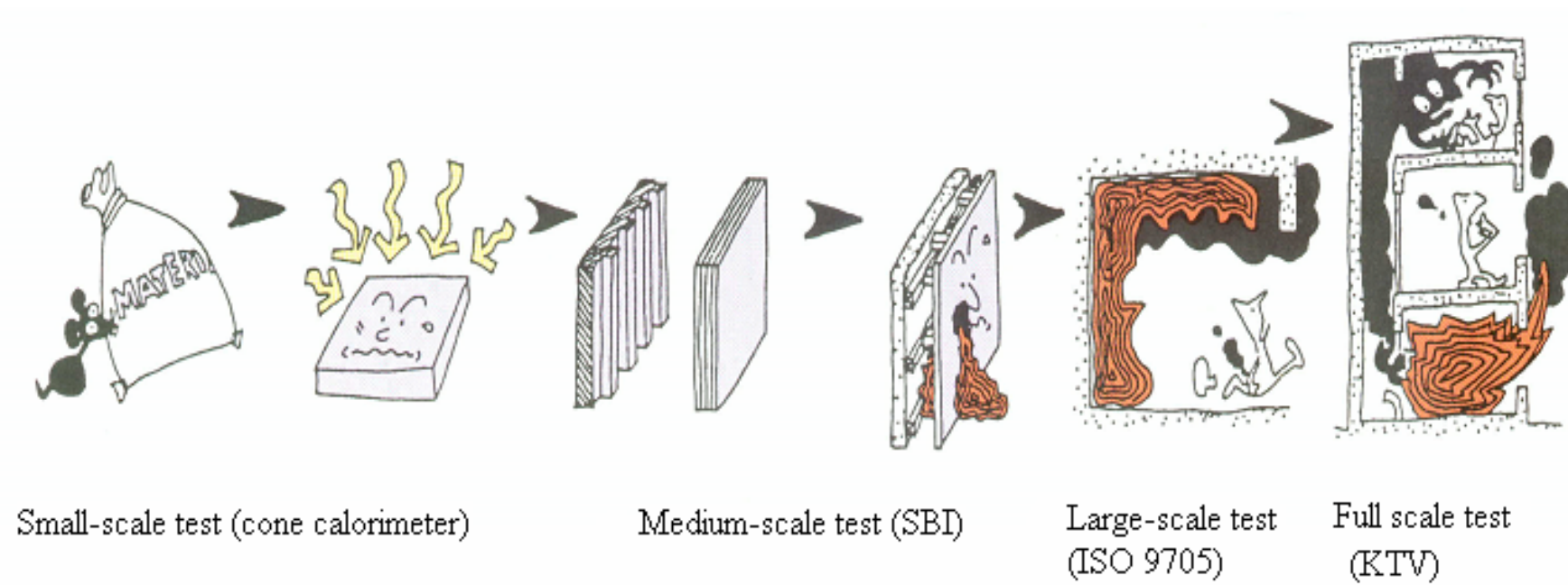


Figure 1.1: The Evolution of Fire Testing Methods



Figure 2.1: The picture of Cone Calorimeter (Cone2)

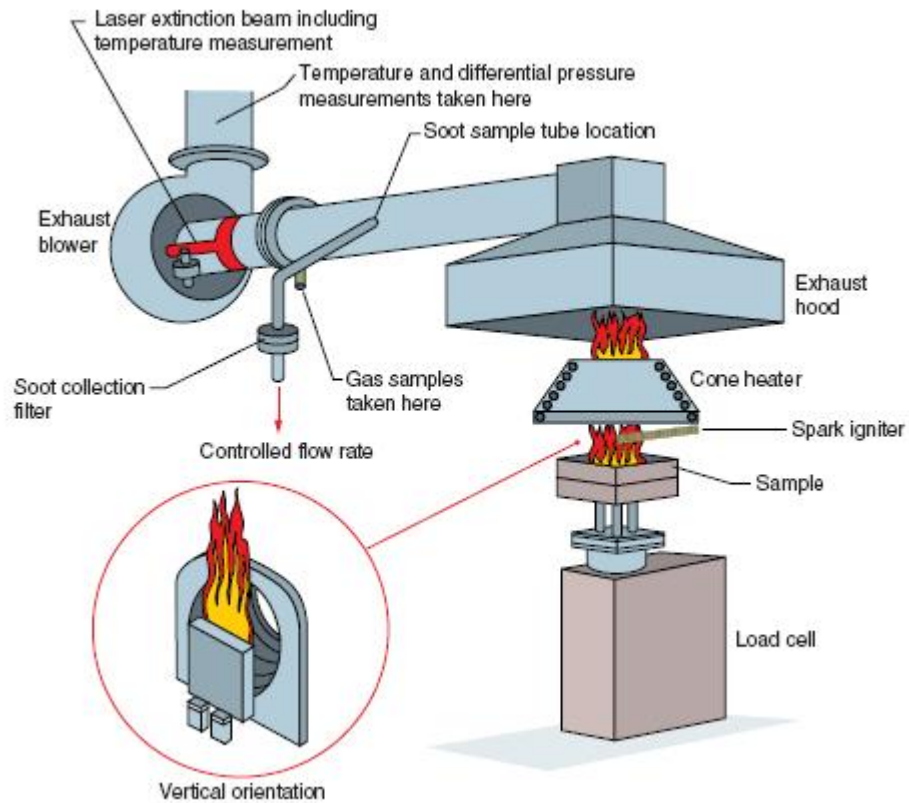


Figure 2.2: The schematic configuration of the Cone Calorimeter

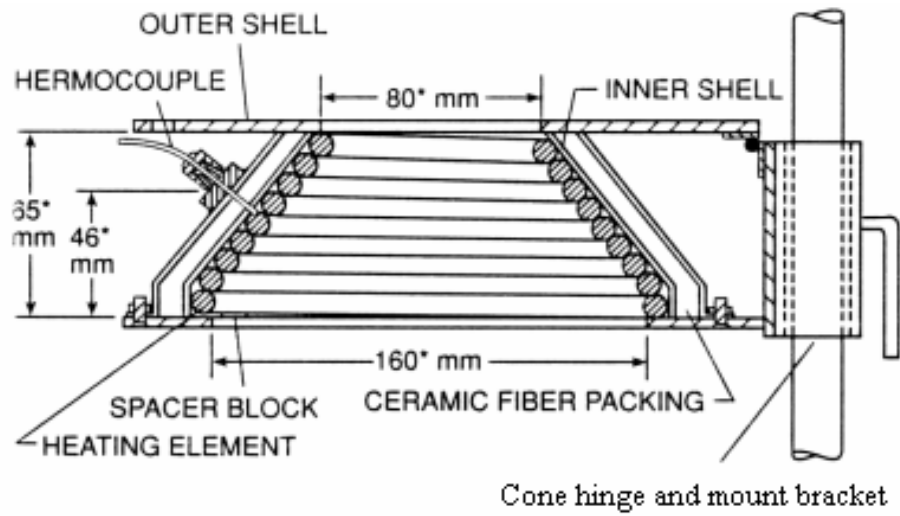


Figure 2.3: Cone heater (Cone2)

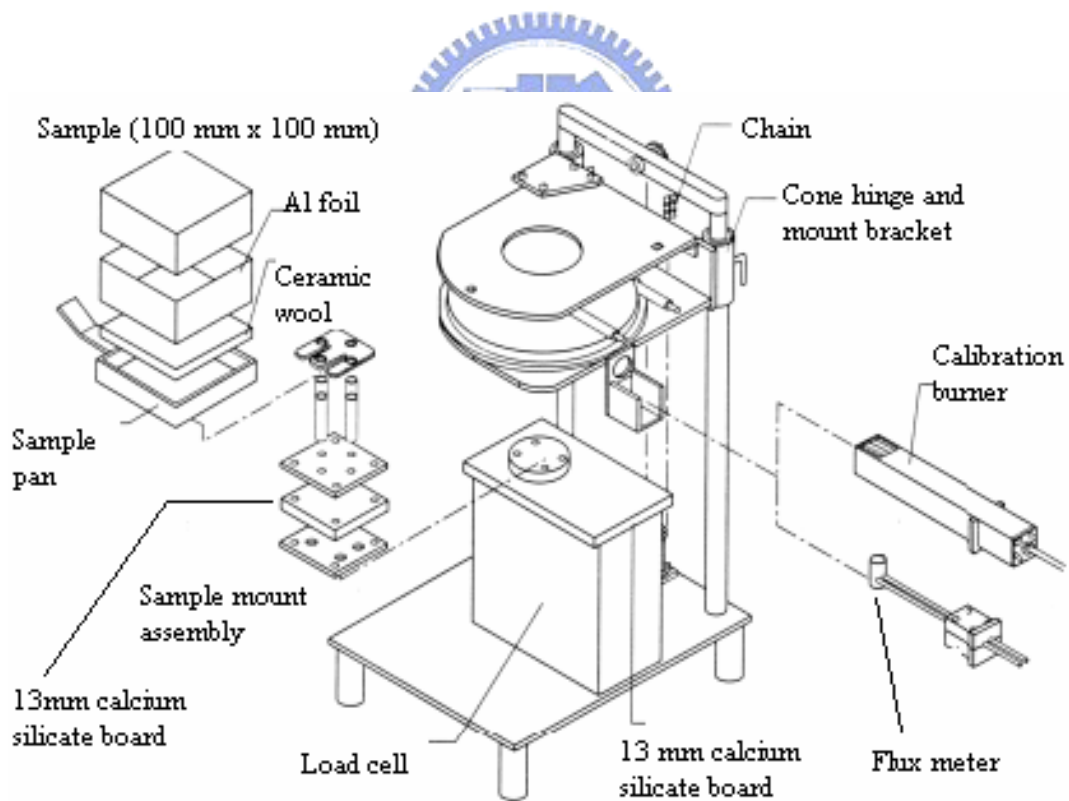


Figure 2.4: Horizontal orientation (Cone2)

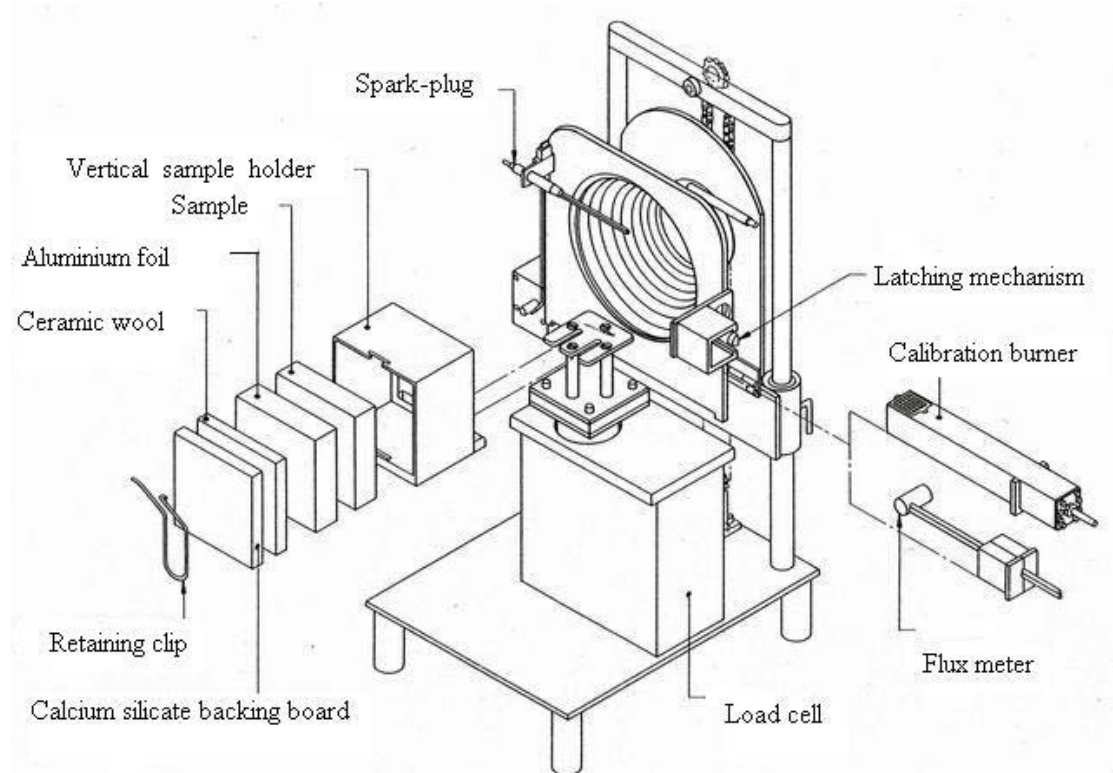


Figure 2.5: Vertical orientation (Cone2)

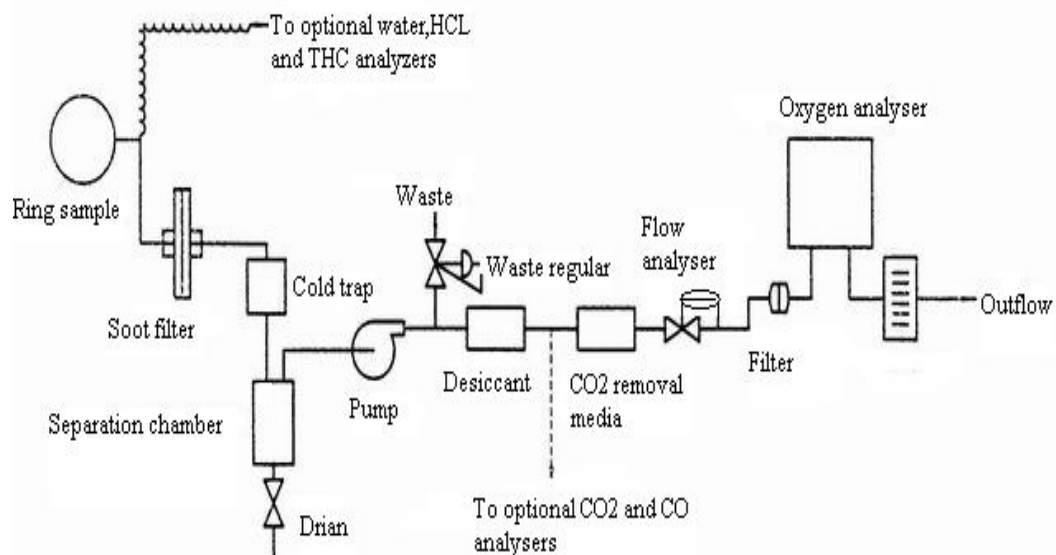


Figure 2.6: Gas analyzer instrumentation (Cone2)

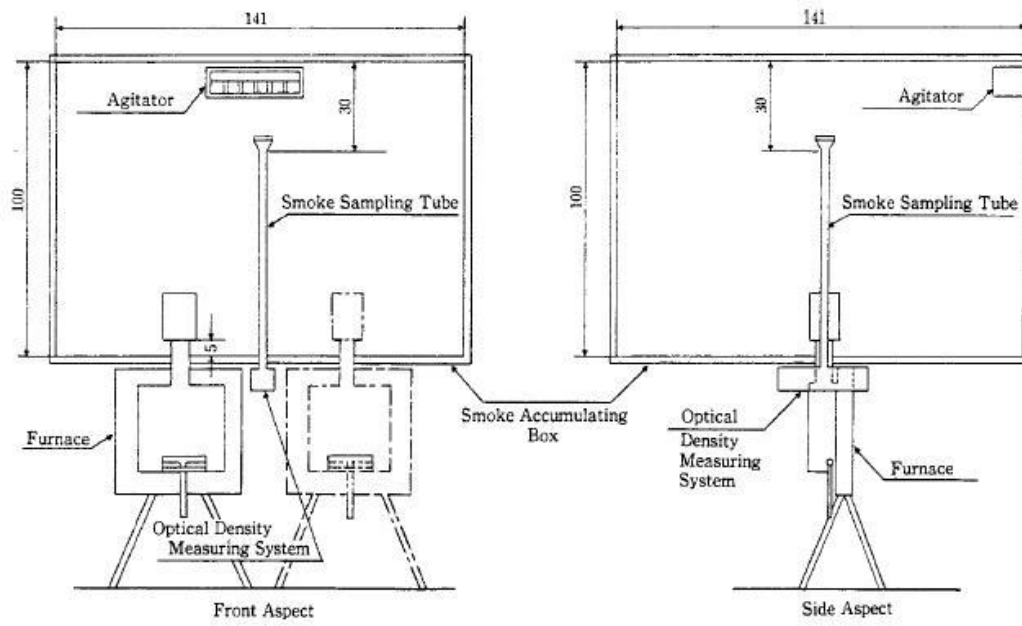


Figure 2.7: The surface test apparatus



Figure 2.8: The furnace of surface test

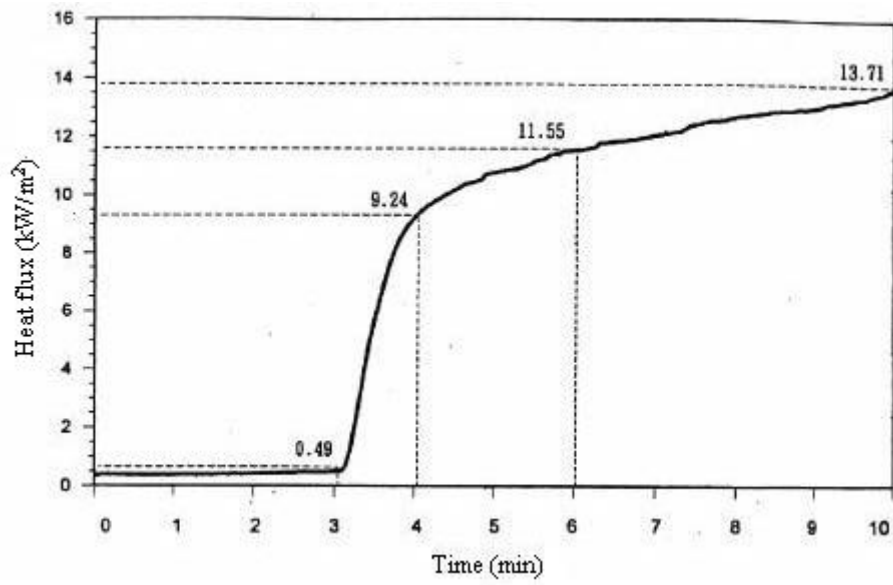


Figure 2.9: The average heat flux value of surface test [14]



Figure 2.10: The smoke accumulation box

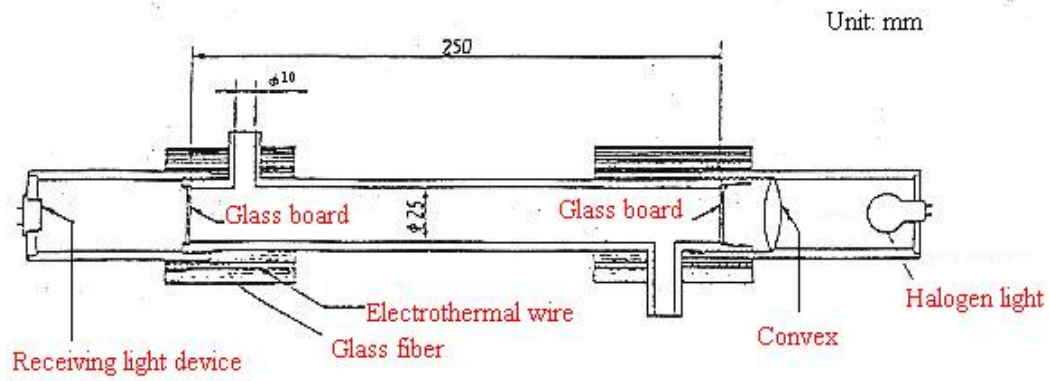


Figure 2.11: Optical density-measuring system of surface test

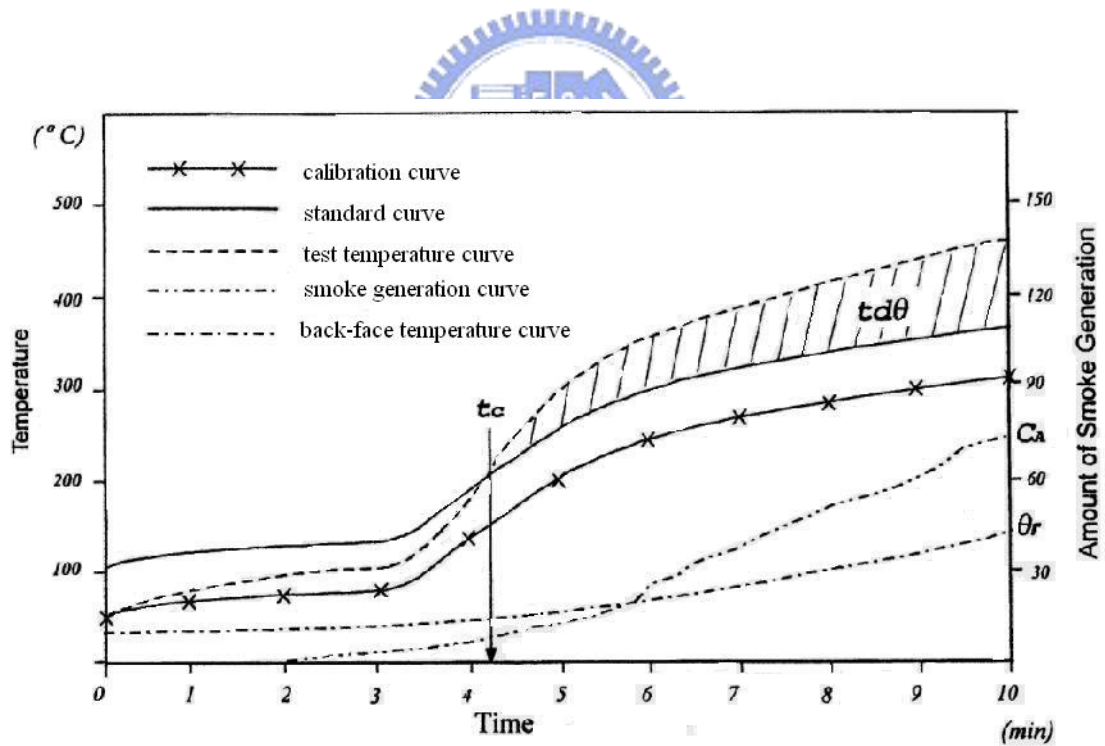


Figure 2.12: Results and specification of surface test



Figure 2.13: An elementary material test apparatus



Figure 2.14: SBI test

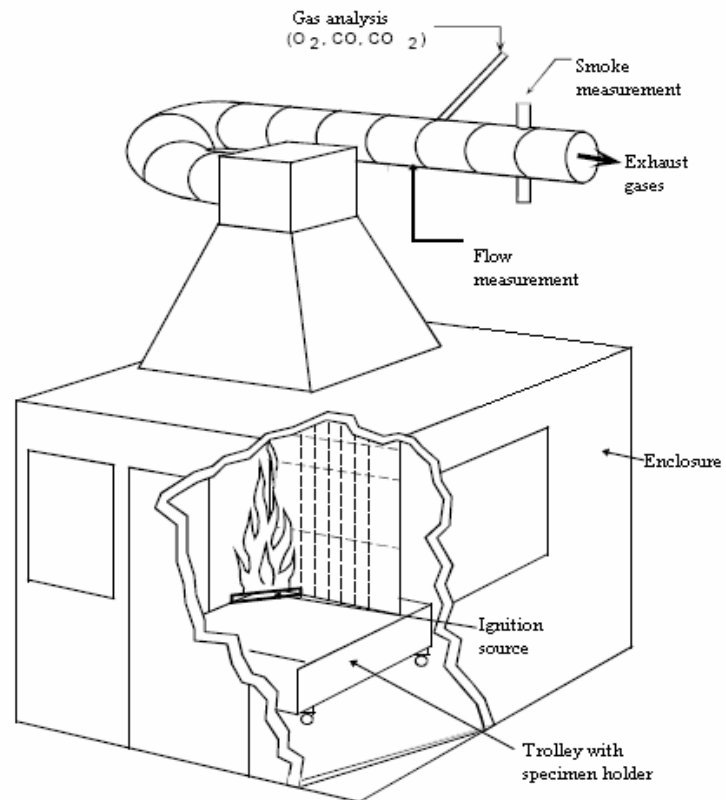


Figure 2.15: Schematic picture of SBI



Figure 2.16: Trolley of SBI

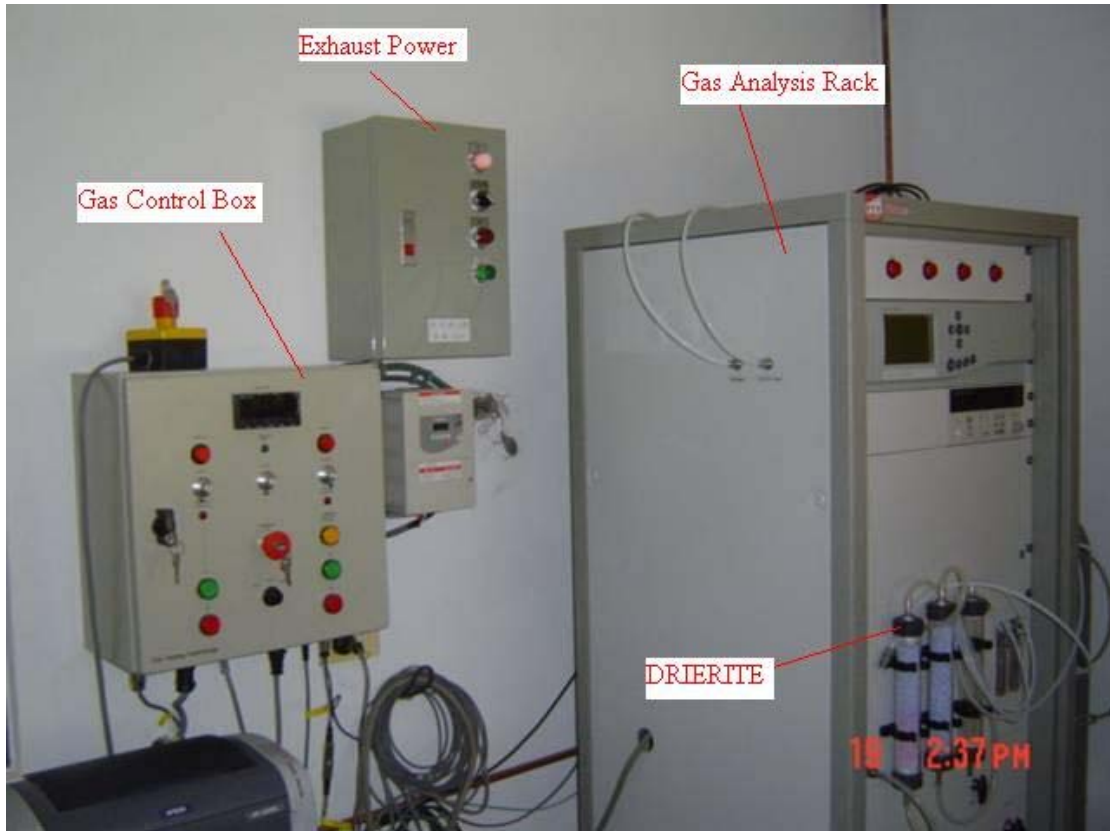


Figure 2.17: Gas Control Box and Gas Analysis Rack of SBI



Figure 2.18: Exhaust hood and Ring of SBI

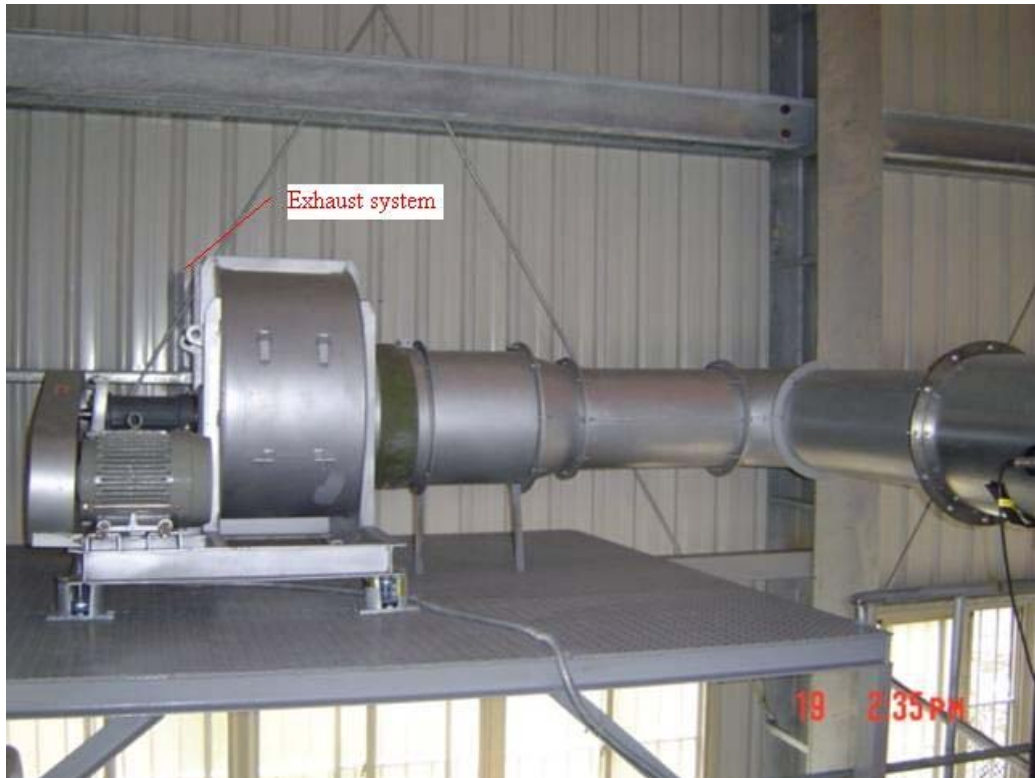


Figure 2.19: Exhaust system of SBI

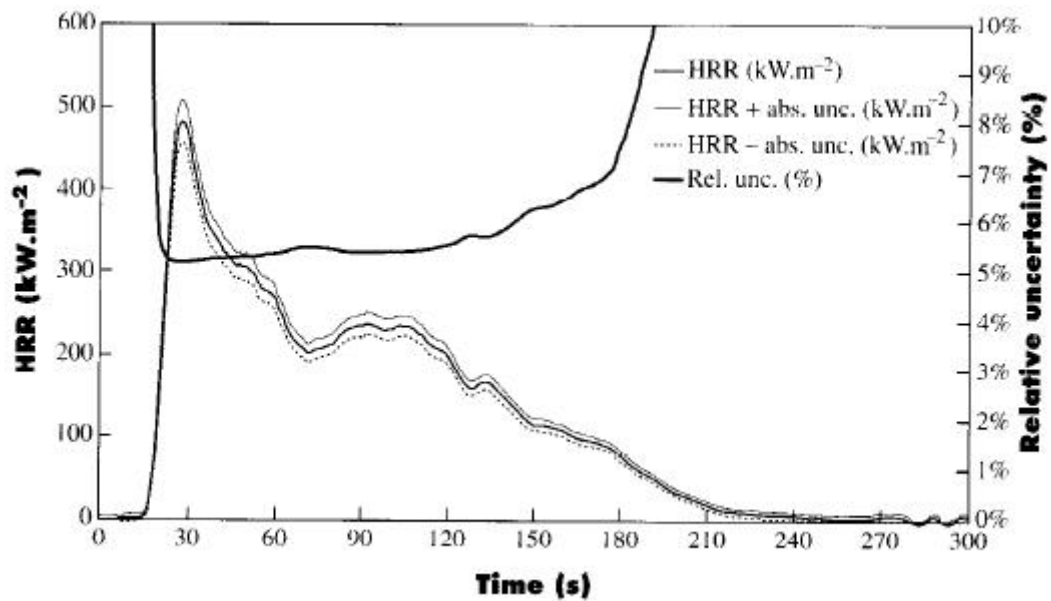


Figure 3.1: HRR \pm absolute uncertainty and relative uncertainty histories from cone calorimeter results [29]

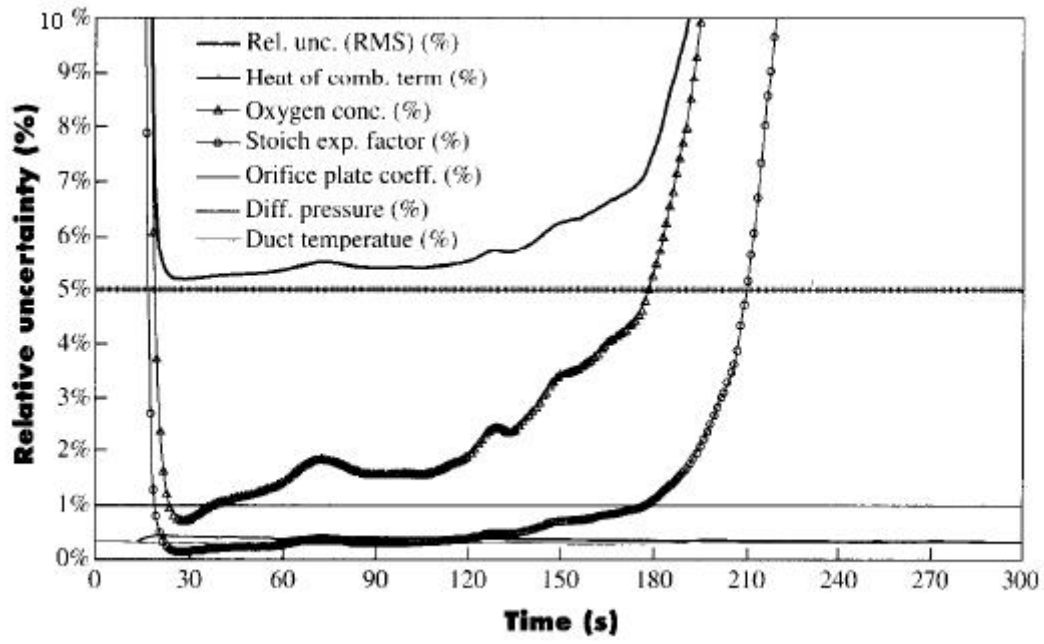


Figure 3.2: Component uncertainty histories from cone calorimeter results [29]



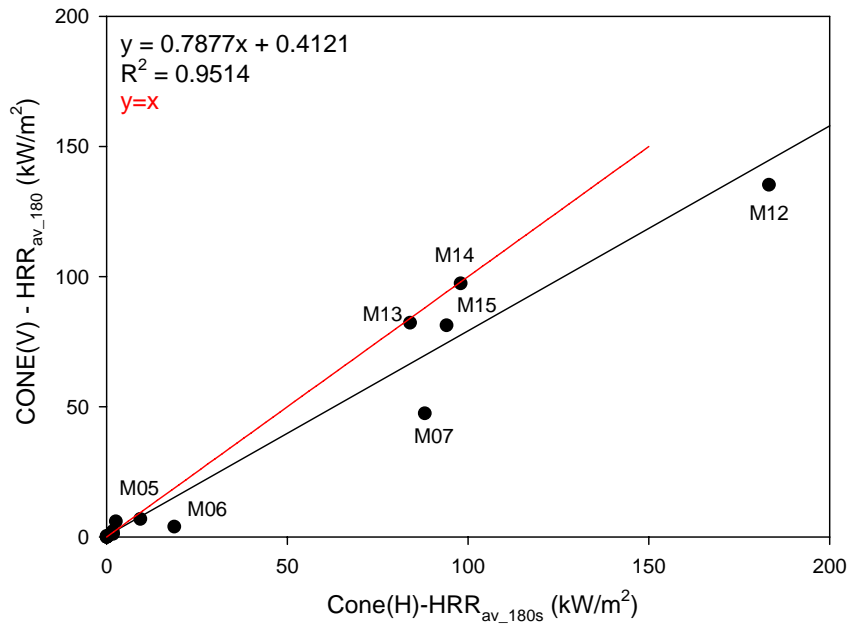
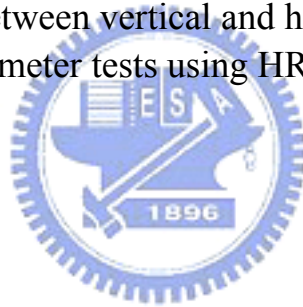


Figure 4.1: Correlation between vertical and horizontal directions of cone calorimeter tests using HRR_{av_180s}



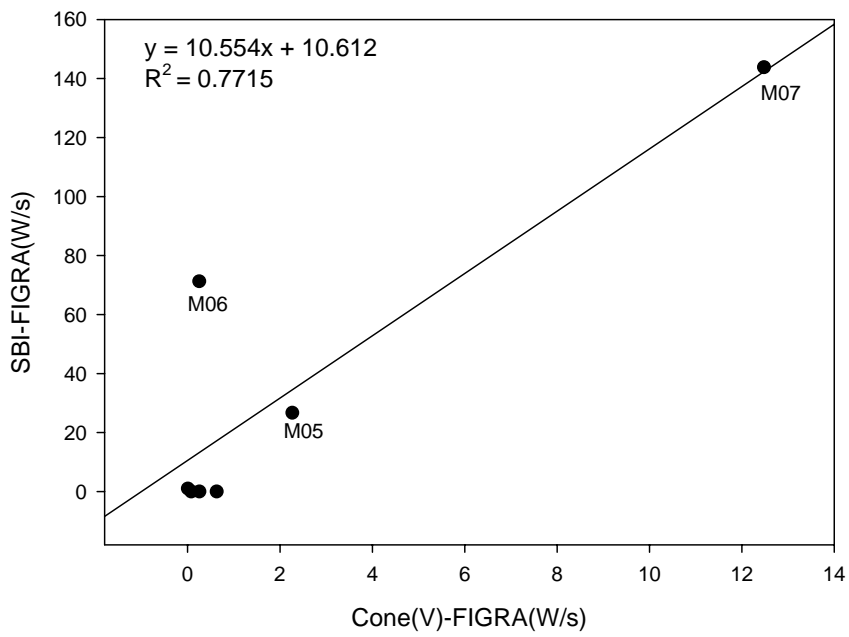


Figure 4.2: The correlation between FIGRA of cone calorimeter in vertical direction and SBI tests



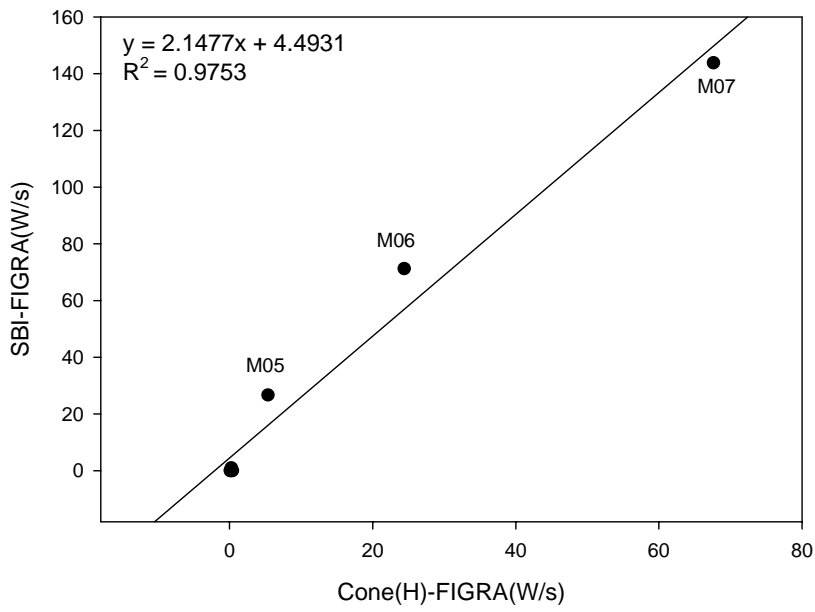


Figure 4.3: The correlation between FIGRA of cone calorimeter in horizontal direction and SBI tests



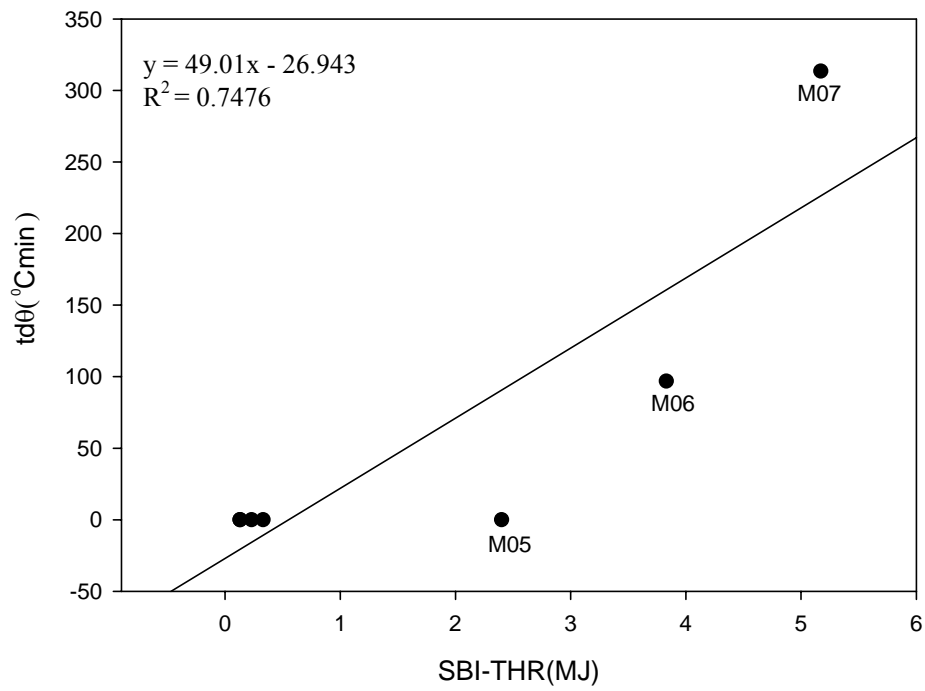


Figure 4.4: The correlation between THR_{600s} of SBI test and $td\theta$ of surface test



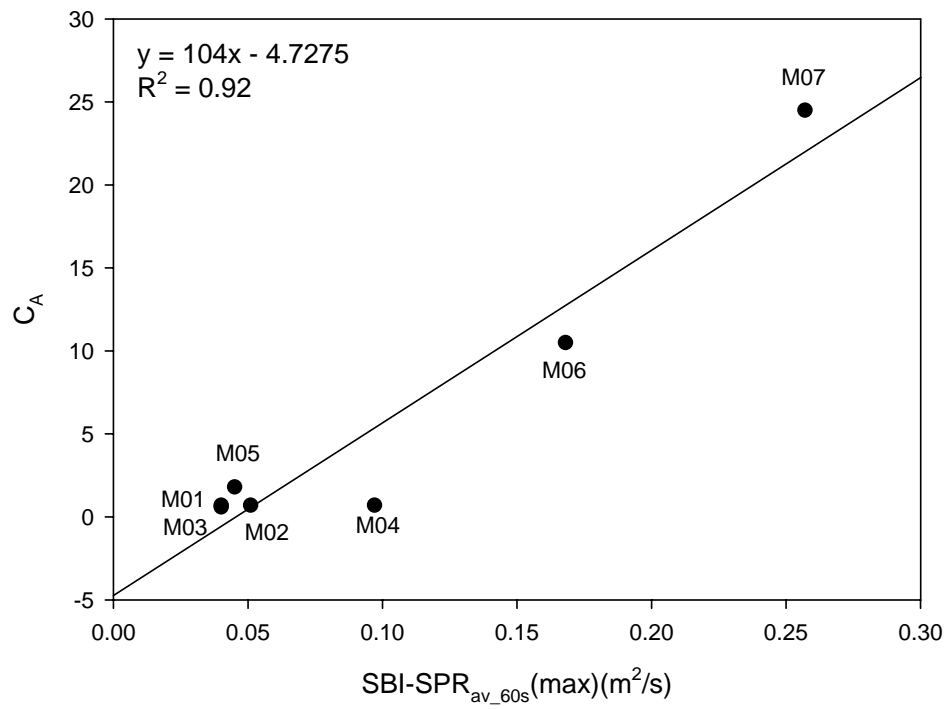


Figure 4.5: The correlation between the maximum SPR_{av_60s} of SBI test and C_A value of surface test

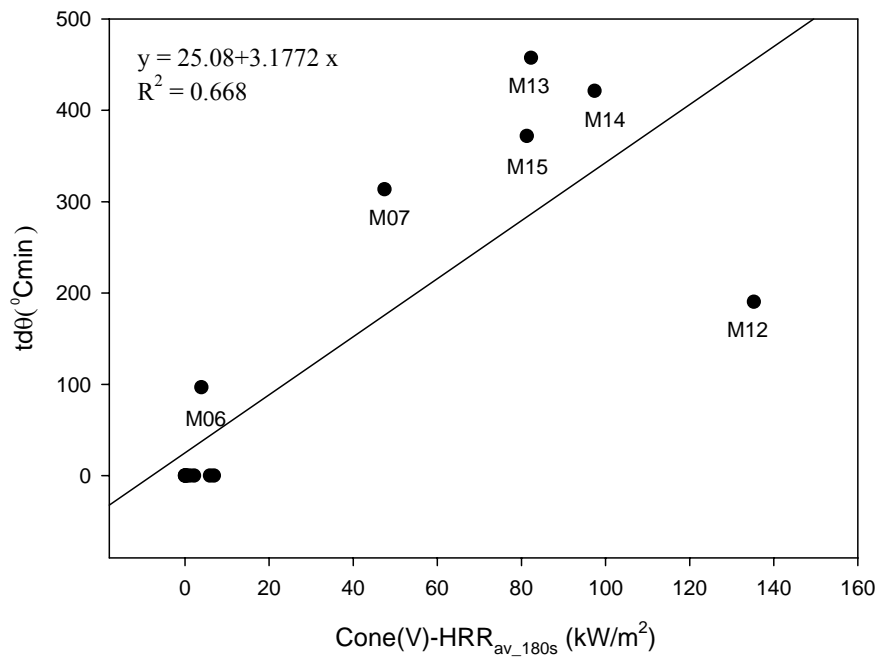


Figure 4.6: The correlation between 180s mean value of Cone Calorimeter test in vertical direction and tdθ value of surface test



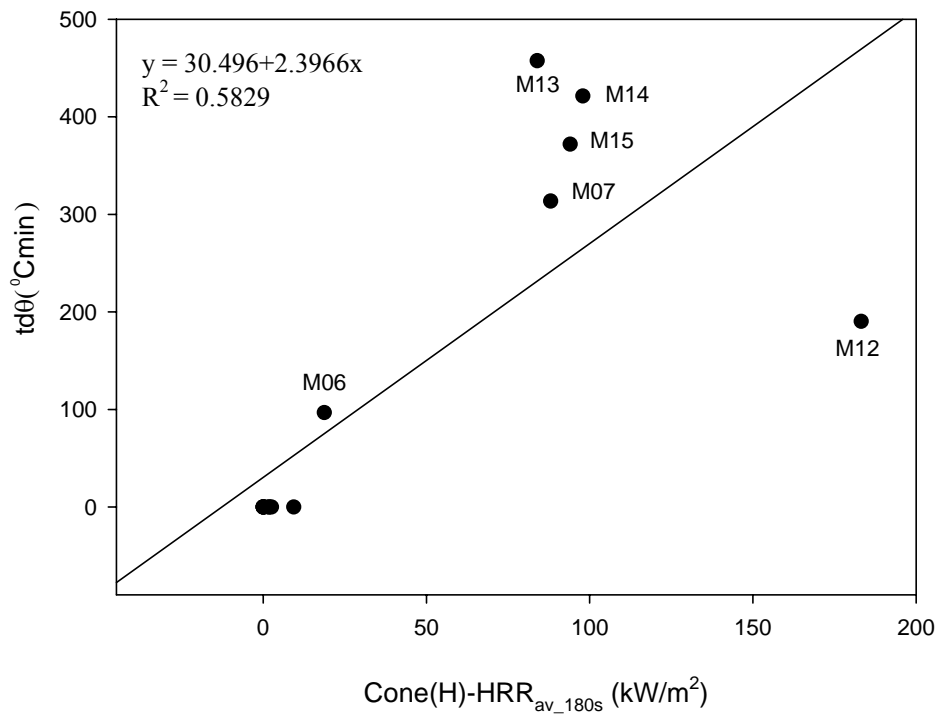
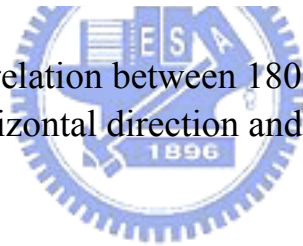


Figure 4.7: The correlation between 180s mean value of Cone Calorimeter test in horizontal direction and tdθ value of surface test



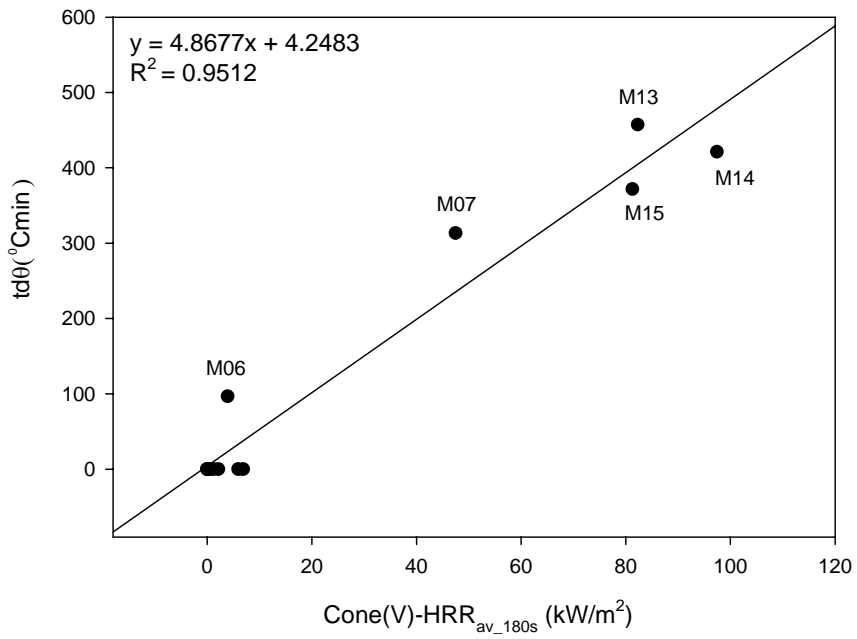


Figure 4.8: The correlation between 180s mean value of Cone Calorimeter test in vertical direction and tdθ value of surface test without M12



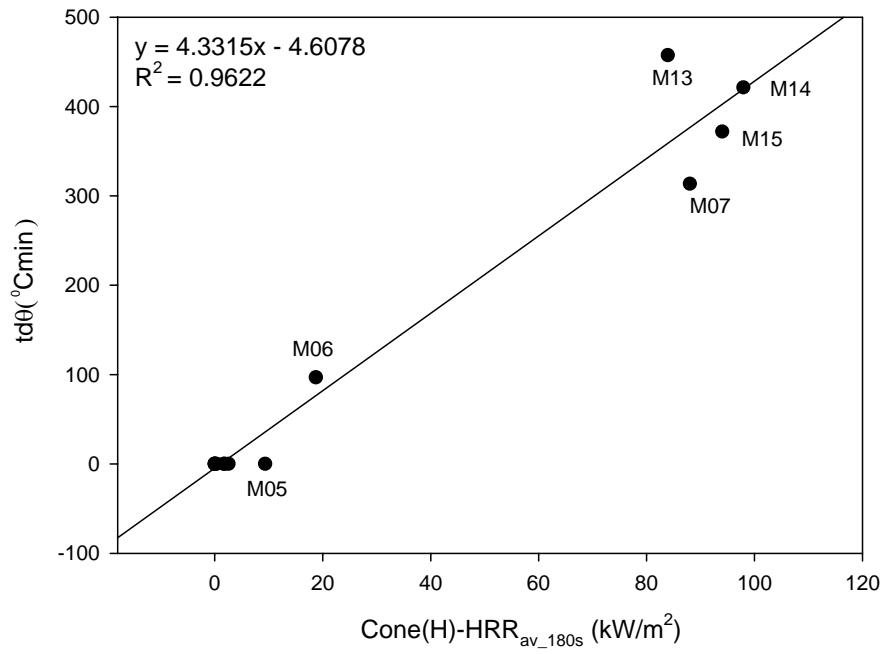


Figure 4.9: The correlation between 180s mean value of Cone Calorimeter test in horizontal direction and tdθ value of surface test without M12

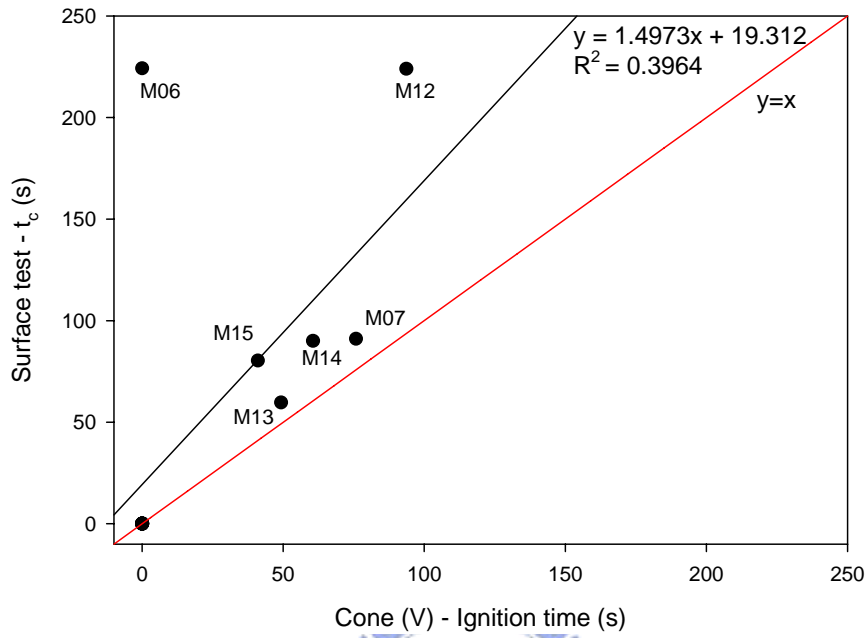


Figure 4.10: The correlation between ignition time of cone calorimeter in vertical direction and t_c value of surface test



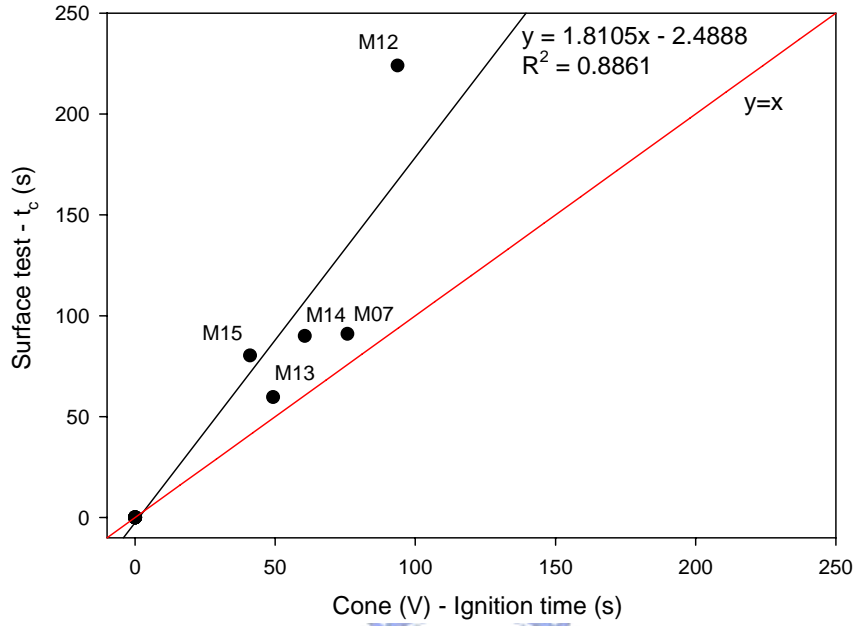


Figure 4.11: The correlation between ignition time of cone calorimeter in vertical direction and t_c value of surface test without M06

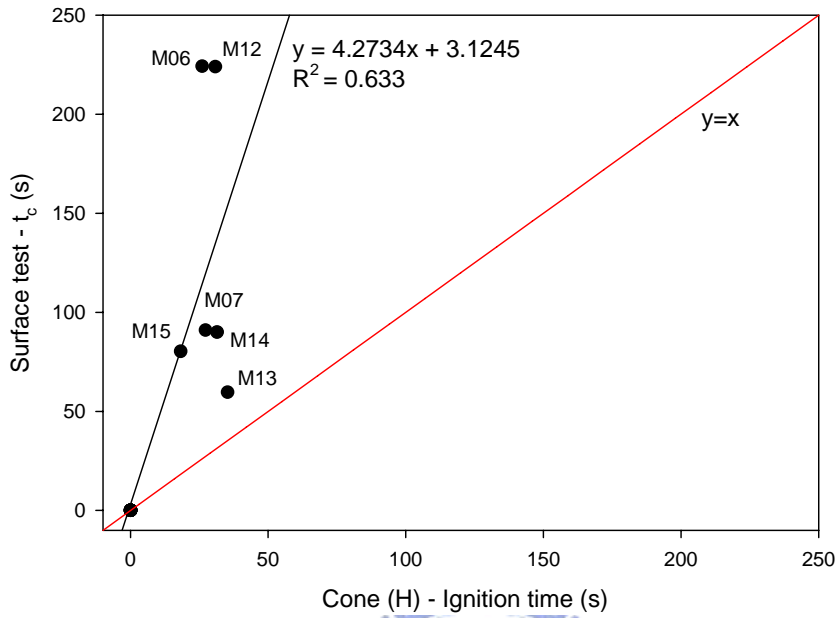
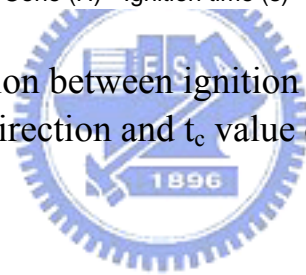


Figure 4.12: The correlation between ignition time of cone calorimeter in horizontal direction and t_c value of surface test



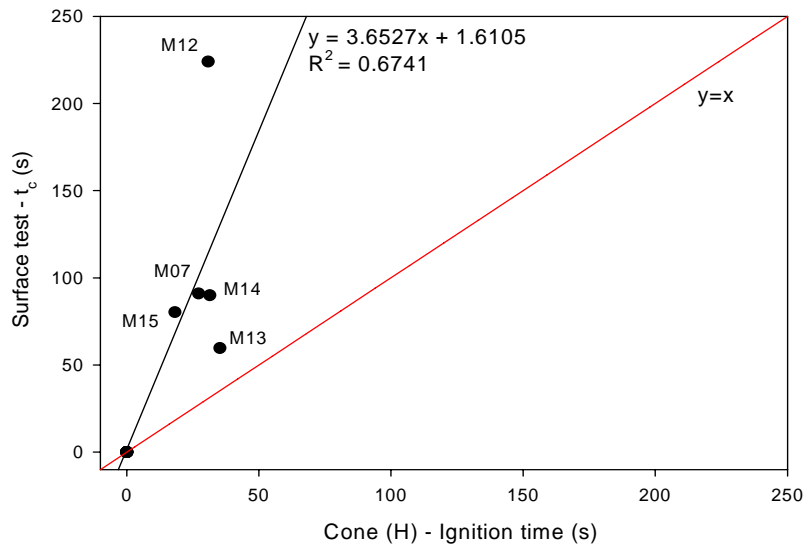
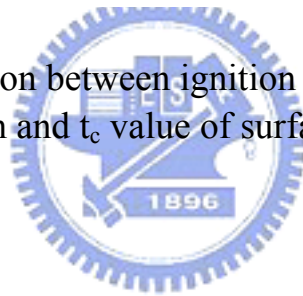


Figure 4.13: The correlation between ignition time of cone calorimeter in horizontal direction and t_c value of surface test without M06



Appendix A

The heat calculation of surface test

1. In the first 3 mins: propane burner with a flow rate of 0.35 l/min

The molecular weight of C_3H_8 : 44

The heat of combustion C_3H_8 :

$$530.5 \text{ (kcal/mol)} = 530.5 \times 4.18 = 2217.49 \text{ (kJ/mol)}$$

$$\Rightarrow \frac{2217.49}{44} = 50.3975 \text{ (kJ/kg)}$$

The specific weight of C_3H_8 : 1.56

$$\rho_{propane} = \rho_{water} \times 1.56 = 1560 \text{ (kg/m}^3\text{)}$$

$$\text{Mass} = 1560 \times 0.35 \left(\frac{\text{kg}}{\text{m}^3} \cdot \frac{\text{L}}{\text{min}} \right) = 546 \times \frac{1}{1000} = 0.546 \text{ (kg/min)}$$

$$\therefore 50.3975 \times 0.546 = 27.51 \text{ (kJ/min)}, J = W \cdot s$$

$$\frac{27.51}{60} = 0.4585 \text{ kW} = \frac{0.4585}{0.18 \times 0.18} = 14.15 \text{ (kW/m}^2\text{)}$$

2. 3mins ~ 10mins: propane burner and two quartz lamps

$$\text{The heat of two quartz lamps: } \frac{1.5}{0.18 \times 0.18} = 46.3 \text{ (kW/m}^2\text{)}$$

$$\therefore \text{Total heat of furnace: } 46.3 + 14.15 = 60.45 \text{ (kW/m}^2\text{)}$$

Appendix B1

Results of cone calorimeter tested in vertical orientation

Code	Class	Test time (s)	Ignition time (s)	Peak of HRR (kW/m ²)	Time of HRR peak(s)	HRR _{av_180s} (kW/m ²)	THR (MJ/m ²)
M01	1	1200	N.I.	9.14	840	1.72	5.53
		1200	N.I.	5.96	635	1.68	3.65
		1200	N.I.	2.47	903	0	0
M02	1	1200	N.I.	3.69	214	1.05	0
		1200	N.I.	3.85	77	1.68	0
		1200	N.I.	10.29	1180	3.67	6.95
M03	1	1200	N.I.	0	0	0	0
		1200	N.I.	1.21	1180	0	0
		1200	N.I.	0.87	1128	0	0
M04	1	1200	N.I.	3.8	592	0.08	0
		1200	N.I.	1.58	9	0	0
		1200	N.I.	5.5	791	0.69	2.99
M05	1	1200	N.I.	10.91	36	6.83	2.76
		1200	N.I.	9.25	28	6.32	4.03
		1200	N.I.	11.33	244	7.42	6.05
M06	2	600	N.I.	13.116	578	3.56	4.77
		600	N.I.	13.852	569	4.81	5.48
		600	N.I.	16.491	597	3.37	5.11
M07	F	300	66.88	124.87	191.88	46.6	10.3
		300	46.31	199.23	83.31	47.12	12.09
		300	114.32	160.89	229.32	48.7	10.478
M08	1	1200	N.I.	0.96	2	0	0
		1200	N.I.	0	0	0	0
		1200	N.I.	0.8	1180	0	0

Results of cone calorimeter tested in vertical orientation (continue)

Code	Class	Test time (s)	Ignition time(s)	Peak of HRR (kW/m ²)	Time of HRR peak(s)	HRR _{av_180s} (kW/m ²)	THR (MJ/m ²)
M09	1	1200	N.I.	3.19	1187	0	0.09
		1200	N.I.	1.1	685	0	0
		1200	N.I.	0.41	1177	0	0
M10	1	1200	N.I.	7.58	18	4.94	1.49
		1200	N.I.	8.15	52	5.97	1.6
		1200	N.I.	9.8	43	6.91	2.19
M11	1	1200	N.I.	3.21	1155	0.57	0.19
		1200	N.I.	13	122	0.44	0.1
		1200	N.I.	7.03	895	0	0.38
M12	F	300	96.83	196.43	190.83	133.91	29.21
		300	91.98	197.96	182.98	136.06	30.39
		300	92.14	200.35	183.14	135.82	30.16
M13	F	300	52.18	307.28	92.18	77.58	19.17
		300	44.23	281.75	77.23	82.76	21.03
		300	51.29	281.99	90.29	86.49	22.74
M14	F	300	57.94	215.27	107.94	96.03	25.04
		300	63.74	244.31	121.74	101.55	24.99
		300	59.98	225.77	112.98	94.62	23.59
M15	F	300	41.35	308.38	69.35	90.75	25.13
		300	39.44	301.59	68.44	77.93	22.53
		300	42.3	294.52	73.3	75.13	20.98

Appendix B2

Results of cone calorimeter tested in horizontal orientation

Code	Class	Test time (s)	Ignition time(s)	Peak of HRR (kW/m ²)	Time of HRR peak(s)	HRR _{av_180s} (kW/m ²)	THR (MJ/m ²)
M01	1	1200	N.I.	3.63	171	1.88	1.42
		1200	N.I.	3.52	132	1.49	1.05
		1200	N.I.	4.05	309	2.07	1.78
M02	1	1200	N.I.	4.03	75	2.2	0.76
		1200	N.I.	3.86	83	2.04	0.62
		1200	N.I.	2.8	137	0.8	0.18
M03	1	1200	N.I.	0.302	7	0	0
		1200	N.I.	0.638	79	0	0
		1200	N.I.	0.19	7	0	0
M04	1	1200	N.I.	3.6	594	0	0.22
		1200	N.I.	6.26	601	1.03	1.4
		1200	N.I.	3.55	287	0	0.33
M05	1	1200	N.I.	12.61	23	9.1	3.58
		1200	N.I.	14.84	214	9.82	3.48
		1200	N.I.	13.91	14	9.11	3.25
M06	3	300	39	75.52	68	16.88	5.54
		300	18	91.55	25	24.43	8.35
		300	21	81.58	32	14.86	4.44
M07	F	300	25.18	295.33	39	73.7	25.3
		300	31.03	326.16	51	99.17	24.62
		300	25.49	259.21	41	91.23	24.18
M08	1	1200	N.I.	3.25	2	0	0
		1200	N.I.	1.65	1	0	0
		1200	N.I.	2.4	1	0	0

Results of cone calorimeter tested in horizontal orientation (continue)

Code	Class	Test time (s)	Ignition time(s)	Peak of HRR (kW/m ²)	Time of HRR peak(s)	HRR _{av_180s} (kW/m ²)	THR (MJ/m ²)
M09	1	1200	N.I.	1.48	3	0	0
		1200	N.I.	2.7	1	0	0
		1200	N.I.	1.17	1	0	0
M10	1	1200	N.I.	4.32	2	1.71	0
		1200	N.I.	6.53	84	3.09	1.17
		1200	N.I.	6.07	150	2.83	1.03
M11	1	1200	N.I.	1.8	2	0	0
		1200	N.I.	0.11	420	0	0
		1200	N.I.	1.31	393	0	0
M12	F	300	33.34	332.74	66	198.24	51.74
		300	34.23	297.55	58	171.36	45.38
		300	24.87	247.15	55	180.05	45.83
M13	F	300	34.77	398.11	54	79.28	21.77
		300	32.91	348.62	52	89.87	23.88
		300	38.11	361.69	64	82.64	23.31
M14	F	300	20.91	205.19	48	97.16	25.34
		300	29.41	182.2	58	104.28	27.26
		300	44.1	274.75	80	92.35	25.14
M15	F	300	19.79	254.74	32	78.29	23.17
		300	17	429.57	24	101.28	25.3
		300	18	519.46	26	102.48	25.75

Appendix C1

Results of the surface test

Code	Class	Test time (min)	t_c (s)	$td\theta$ ($^{\circ}\text{C}\cdot\text{min}$)	C_A	t_1 (s)	C_k
M01	1	10	N.I.	0	0.9	--	+
	1	10	N.I.	0	0.5	--	+
	1	10	N.I.	0	0.8	--	+
M02	1	10	N.I.	0	0.9	--	+
	1	10	N.I.	0	0.7	--	+
	1	10	N.I.	0	0.6	--	+
M03	F	6	N.I.	0	0.4	--	-
	F	6	N.I.	0	0.9	--	-
	F	6	N.I.	0	0.6	--	-
M04	1	10	N.I.	0	0.9	--	+
	1	10	N.I.	0	0.8	--	+
	1	10	N.I.	0	0.5	--	+
M05	1	10	N.I.	0	2.3	--	+
	1	10	N.I.	0	1.8	--	+
	1	10	N.I.	0	1.5	--	+
M06	3	6	230	81.1	10.4	5	+
	F	6	229	156.9	8	43	+
	3	6	211	52.4	13	2	+
	F	6	231	117.3	6.9	45	+
	F	6	220	146.4	4.2	37	+

Results of the surface test (continue 1)

Code	Class	Test time (min)	t_c (s)	$td\theta$ ($^{\circ}\text{C}\cdot\text{min}$)	C_A	t_1 (s)	C_k
M07	F	6	79	322.4	21.7	13	–
	F	6	90	283.4	27.2	5	–
	F	6	104	334.7	24.6	12	–
M08	F	6	N.I.	0	0.5	--	–
	F	6	N.I.	0	0.5	--	–
	F	6	N.I.	0	0.5	--	–
M09	F	6	N.I.	0	0.3	--	–
	F	6	N.I.	0	0.9	--	–
	F	6	N.I.	0	0.8	--	–
M10	2	10	N.I.	0	51.4	--	+
	2	10	N.I.	0	39.1	--	+
	1	10	N.I.	0	20	--	+
M11	F	6	N.I.	0	0.5	--	+
	F	6	N.I.	0	0.6	--	+
	F	6	N.I.	0	0.6	--	+
M12	F	6	227	184.1	97.5	395	+
	F	6	231	169.8	98.3	228	+
	F	6	216	217.1	135	397	+
M13	F	6	60	414.1	82.1	94	+
	F	6	51	445.1	94.5	90	+
	F	6	68	513	124.4	472	+
M14	F	6	86	448	129.2	158	+
	F	6	85	447.3	173.2	243	+
	F	6	99	368.5	177.5	269	+

Results of the surface test (continue 2)

Code	Class	Test time (min)	t_c (s)	$td\theta$ ($^{\circ}\text{C}\cdot\text{min}$)	C_A	t_l (s)	C_k
M15	F	6	83	280.7	137.3	675	+
	F	6	68	552	101	176	+
	F	6	90	283.1	124	499	+
M12*	F	6	204	181	178.2	600	+
	F	6	197	203.4	203.6	311	+
	F	6	187	191.5	179.4	290	+
M13*	F	6	111	408.6	124.6	136	+
	F	6	67	631	148.8	318	+
	F	6	79	512.5	140.4	397	+
M14*	F	6	91	455.5	201.9	313	+
	F	6	103	399.6	202.4	320	+
	F	6	100	404.3	200.2	265	+
M15*	F	6	55	698.1	113.4	488	+
	F	6	50	735.2	132.5	405	+
	F	6	67	352.3	115.5	548	+

Appendix C2

Results of elementary material test

Code	T _{max} (°C)	T _{initial} (°C)	ΔT (°C)	Mass loss (g)	Class
M01	762.3	750	12.6	13.38	Pass
	764.8	748	16.6	18.22	Pass
	772.5	748	24.4	13.46	Pass
M02	751.1	748	2.7	13.05	Pass
	755.1	750	5.2	13	Pass
	751.1	745	6.4	12.63	Pass
M04	728.6	751	-22.1	34.7	Pass
	731.2	750	-19	32.6	Pass
	716.9	747	-30.2	30.1	Pass
M05	797.3	748	49.8	4.8	Pass
	824	751	73.2	6.9	No pass
	810.9	746	65.2	3.1	No pass

Appendix D1

The FIGRA and THR_{600s} values of SBI test

Code		FIGRA _{0.2MJ} (W/s)	FIGRA _{0.2MJ} time achieved (s)	FIGRA _{0.4MJ} (W/s)	FIGRA _{0.4MJ} time achieved (s)	THR _{600s} (MJ)
M01	1	--	--	--	--	0.1
	2	--	--	--	--	0.6
	3	--	--	--	--	0.3
M02	1	--	--	--	--	0.2
	2	--	--	--	--	0.2
	3	--	--	--	--	0.3
M03	1	--	--	--	--	0
	2	3.0	1464	3.0	1464	0.4
	3	--	--	--	--	0
M04	1	--	--	--	--	0.1
	2	--	--	--	--	0.1
	3	--	--	--	--	0.2
M05	1	11.3	582	11.3	582	1.5
	2	35.9	396	33.6	447	2.8
	3	32.9	393	22.2	522	2.9
M06	1	80.0	378	41.2	414	3.1
	2	51.8	393	48.8	453	4.4
	3	81.9	378	55.1	414	4.0
M07	1	127.7	459	127.7	459	6.4
	2	130.3	477	130.3	477	4.1
	3	173.4	447	173.4	447	5.0

--: threshold no reached

Appendix D2

The SMOGRA and TSP₆₀₀ values of SBI test

Code		SMOGRA (m ² /s ²)	Time achieved (s)	TSP ₆₀₀ (m ²)	SPR _{av_60s(max)} (m ² /s)
M01	1	--	--	12.7	0.048
	2	--	--	7.2	0.028
	3	--	--	10.2	0.044
M02	1	--	--	13.8	0.056
	2	--	--	11.6	0.04
	3	--	--	16.0	0.056
M03	1	--	--	0.4	0.04
	2	--	--	1.0	0.024
	3	--	--	0.7	0.06
M04	1	--	--	17.3	0.09
	2	--	--	9.2	0.082
	3	--	--	13.5	0.12
M05	1	--	--	14.1	0.048
	2	--	--	18.2	0.04
	3	--	--	16.8	0.048
M06	1	2.1	1038	36.9	0.23
	2	2.3	1254	35.5	0.23
	3	--	--	2.6	0.044
M07	1	7.1	639	85.6	0.24
	2	6.4	495	28.9	0.13
	3	20.2	480	106.1	0.4

--: threshold no reached